



## Review

## Protein-based inheritance

Johannes Manjrekar\*, Hiral Shah

Microbiology Department and Biotechnology Centre, The Maharaja Sayajirao University of Baroda, Vadodra, 390002, India

## ARTICLE INFO

## Keywords:

Epigenetic inheritance  
Evolution  
Prions  
Amyloid  
Intrinsically disordered proteins  
Phase separation  
Stress responses  
Bet hedging

## ABSTRACT

Epigenetic mechanisms of inheritance have come to occupy a prominent place in our understanding of living systems, primarily eukaryotes. There has been considerable and lively discussion of the possible evolutionary significance of transgenerational epigenetic inheritance. One particular type of epigenetic inheritance that has not figured much in general discussions is that based on conformational changes in proteins, where proteins with altered conformations can act as templates to propagate their own structure. An increasing number of such proteins – prions and prion-like – are being discovered. Phenotypes due to the structurally altered proteins are transmitted along with their structures. This review discusses the properties and implications of “classical” amyloid-forming prions, as well as the broader class of proteins with intrinsically disordered domains, which are proving to have fascinating properties that appear to play important roles in cell organisation and function, especially during stress responses.

## 1. Introduction

Charles Darwin never completely dismissed the possibility of some Lamarckian mechanism operating along with natural selection acting on inherited variation. Indeed, his panspermia theory of inheritance through gemmules could accommodate the idea without much difficulty, if gemmules from some part of the body were modified during the lifetime of an individual. However, with the development of classical, population and molecular genetics leading to the elaboration of Neo-Darwinian evolutionary theory, Lamarckian inheritance acquired virtual untouchability status. The past three or four decades have seen enormous development of the field of epigenetics. Epigenetics remains somewhat vaguely defined, meaning different things to different people. Interesting discussions can be found eg. in Bird [1] and Deans and Maggert [2]. The term was coined by Waddington [3], who defined it as “the branch of biology that studies the causal interactions between genes and their products which bring into being the phenotype”, primarily with reference to the unfolding of embryonic development through the interaction of genes with the cellular environment of the embryo. The first alternative definition closer to the sense in which the term is most frequently used at present was suggested by Nanney [4], who proposed that epigenetic mechanisms “allow the perpetuation of

phenotypic differences in the absence of DNA differences”, while Riggs and colleagues defined it as “the study of mitotically and/or meiotically heritable changes in gene function that cannot be explained by changes in DNA sequence” [5]. Broadly, the term epigenetics is currently most often considered to mean heritable transmission of altered traits or gene expression states not based on changes in DNA sequence. Much of epigenetic transmission is mitotic and occurs between cells of an individual (is ‘intragenerational’). This is largely based on mechanisms involving modifications to chromatin organisation and nuclear architecture – affecting patterns of gene expression – that can be transmitted fairly stably to daughter cells through many cell divisions. Epigenetic inheritance has, however, in a rapidly growing number of cases, also been found to be transgenerational, and transmitted through meiosis. Transgenerational epigenetic inheritance (TEI) has been reported in plants as well as in animals, and there are periodic reviews of the state of knowledge (and controversy), eg. [6–11]. The numerous reports of TEI with their implication of possible adaptive value – particularly when environmentally induced – have been much debated, for instance in a recent special issue of the journal *Heredity* (Aug 10 2018) on “Evolutionary consequences of epigenetic inheritance”. These developments have led to challenges to the standard Neo-Darwinian view, including calls for an “extended evolutionary synthesis” (EES),

**Abbreviations:** TEI, Transgenerational Epigenetic Inheritance; EES, Extended Evolutionary Synthesis; TSE, Transmissible Spongiform Encephalopathy; GdnHCl, Guanidine Hydrochloride; SDD-AGE, Semi-denaturing detergent-Agarose Gel Electrophoresis; GFP, Green Fluorescent Protein; IDD, Intrinsically Disordered Domain; IDP, Intrinsically Disordered Protein; PrD, Prion Domain; PFD, Prion Forming Domain; Q/N-rich, Asparagine/Glutamine-rich; GlcN, Glucosamine; NLR, NOD Like Receptor; CPEB, Cytoplasmic Polyadenylation Element Binding Protein; LTF, Long Term Facilitation; RRM, RNA Recognition Motif

\* Corresponding author.

E-mail addresses: [johannes.manjrekar@gmail.com](mailto:johannes.manjrekar@gmail.com), [jmanjrekar@yahoo.com](mailto:jmanjrekar@yahoo.com) (J. Manjrekar).

<https://doi.org/10.1016/j.semcdb.2019.07.007>

Received 7 February 2019; Accepted 8 July 2019

Available online 19 August 2019

1084-9521/ © 2019 Elsevier Ltd. All rights reserved.

incorporating epigenetic aspects of inheritance into evolutionary theory [12–16]. The case for and against the need for such a revision of evolutionary theory leading to an EES has been debated by prominent evolutionary biologists in the pages of Nature [17], and the evolutionary implications of epigenetic mechanisms discussed in Science [18].

While these developments are of immense interest, in this review we focus on one type of epigenetic inheritance, namely protein-based inheritance. Here, traits are transmitted directly by proteins through changes in their structure, rather than indirectly by modifying the expression of genes (as occurs with chromatin-based epigenetic mechanisms). Altered cellular states occur as a result of conformational changes in proteins, which are independent of any sequence changes in the encoding DNA; the conformationally altered proteins act as templates to propagate their structure by inducing “normally” folded proteins to adopt the alternate structure. Information is transmitted in these cases not through sequence, as with nucleic acids, but through protein conformation. The capacity of some proteins to do so was first observed as the culmination of decades of research into a set of then mystifying neurodegenerative diseases that occurred in some mammals, such as scrapie in sheep, “mad cow disease” in cattle, and Creutzfeldt-Jakob disease and kuru in humans – diseases now collectively referred to as Transmissible Spongiform Encephalopathies (TSEs). The etiology of these devastating diseases remained elusive, with a slow virus being suspected to be the culprit. However, no virus or other orthodox pathogenic agent was ever isolated. In 1982, Prusiner published his paradigm-changing paper [19] identifying a protein as the causative factor, work recognised with a Nobel prize. The TSE-causing agent was named a prion (proteinaceous infectious particle); the normally folded protein was named PrP<sup>C</sup> and the alternative infectious conformation PrP<sup>Sc</sup>, the superscripts standing respectively for “cellular” and “scrapie”. The scrapie form of the protein was found to adopt an amyloid structure and assemble into fibres highly resistant to harsh physical treatments such as UV irradiation and SDS, as well as proteases. The scrapie protein was shown to be highly infectious, efficiently templating the conversion of the normal PrP<sup>C</sup> into the PrP<sup>Sc</sup> form. In a mouse model TSE could be induced with PrP<sup>Sc</sup>, but only if the PrP gene was present to produce the PrP protein; PrP knockout mice developed no symptoms when infected with PrP<sup>Sc</sup>. It is beyond the scope of this review to discuss the voluminous work on the mammalian PrP prion. A good historical account is by Zabel and Reid [20].

In 1965, Cox reported in budding yeast a “cytoplasmic suppressor” –  $\psi$  – with an unusual inheritance pattern [21]. Rather than showing the characteristic Mendelian 2:2 segregation pattern of chromosomal genes in *S. cerevisiae*, when the  $\psi$  strain was mated with a normal strain, all the 4 spores resulting from meiosis inherited the  $\psi$  suppressor phenotype. The molecular basis of this inheritance remained unknown for 30 years. Another “non-Mendelian mutation” that had remained unexplained for many years was that of URE3 [22]. URE3 yeast resembled *ure2* loss-of-function mutants in their phenotype, the ability to utilise ureidosuccinate even in the presence of ammonium ions (which is under repression in the wild type). *URE2* alleles segregate in normal Mendelian fashion but, like  $\psi$ , URE3 showed non-Mendelian inheritance. In 1994 another landmark paper published by Wickner marshalled evidence that suggested the URE3 phenotype was transmitted by a protein [26]. He showed that the URE3 phenotype required the presence of the *URE2* gene, that *URE2* overexpression greatly increased the frequency with which URE3 arose, and that while cells could be cured of URE3 by Guanidine hydrochloride (GdnHCl) treatment, cured cells were able to reacquire the URE3 phenotype. (The requirement for Hsp104 is the basis for curing prions with GdnHCl, which at low millimolar concentrations acts by inhibiting Hsp104 [23–25]). Wickner proposed that URE3 was a yeast prion entirely distinct from the mammalian PrP prion, and that it converted the normal, functional Ure2 protein to the non-functional URE3 prion form [26,27]. He hypothesised that  $\psi$  too was a prion acting in a similar way to

template misfolding of the functional protein (Sup35).

The prion properties of URE3 [28–30] and PSI [31–39] were quickly established, and a standard representation of the prion vs non-prion states for yeast prions came to be used: [Prion<sup>+</sup>] vs [prion<sup>-</sup>]. Prion research in yeast took off rapidly, with the attraction of yeast as a vastly more versatile experimental system than mammalian brains. More fungal prions were discovered: the [HET-s] prion in the filamentous fungus *Podospora anserina* [40,41] and the *Saccharomyces cerevisiae* prions [PIN<sup>+</sup>]/[RNQ<sup>+</sup>] [42–44], [SWI<sup>+</sup>] [45], [OCT<sup>+</sup>] [46] and [ISP<sup>+</sup>] [47]. The normal and amyloid forms of prionogenic proteins are generally associated with distinct phenotypes. Often prions cause phenotypes resembling those of loss-of-function mutations in the gene encoding the protein, since in the prion state the normal function of the native protein is compromised, as in the case of [URE3], [PSI<sup>+</sup>], [SWI<sup>+</sup>] and [OCT<sup>+</sup>]. However, some prions have more complex phenotypes: [MOT3<sup>+</sup>] for instance, in addition to showing phenotypes associated with *MOT3* loss-of-function mutants, promotes flocculation, whereas *MOT3* deletion mutants do not [48]. [ISP<sup>+</sup>] cells show changes in phenotypes [47] and transcription profiles [49] quite different from the phenotypic effects of deletion of the encoding gene (*SFP1*). The [RNQ<sup>+</sup>] prion promotes the formation of other prions like [PSI<sup>+</sup>] and [URE3], while *RNQ* gene deletion results in lower frequencies of induction of other prions. Prion research in yeast has been central to the elucidation of many aspects of prion biology: how they arise *de novo*; their structures and what features of prion sequences determine them; the mechanisms and cellular machinery mediating their induction, maintenance and propagation; heterologous interactions among prions as well as with other macromolecules; the relation between structural variations and phenotypes; and the biological significance of prions. An excellent comprehensive review is that of Liebman and Chernoff [50].

Systematic searches for prions [51–53] led to the discovery and characterisation of a number of other prions, not only in lab strains of budding yeast, but in wild strains as well. Significantly, regulators of gene expression and nucleic acid binding proteins are strongly over-represented among prion-forming proteins. The prions described in the past decade now include not only the growing number characterised in fungi, but in prokaryotes and multicellular eukaryotes as well. Furthermore, it is emerging that the aggregation and self-templating properties of prions are not restricted to amyloid-forming proteins, but include a much wider range of proteins with so-called intrinsically disordered domains (IDDs). The dust has not yet settled on the nomenclature for proteins that can transmit information epigenetically. Amyloid-forming yeast “prions” are now generally referred to without the quotes, though the nomenclature was disputed, eg. the suggestion that they should be called prionoids to distinguish them from the mammalian PrP prions [54]. With a number of non-amyloid proteins also showing aggregation, templating and self-propagating behaviour, these recently discovered examples are generally still cautiously referred to as “prion-like”. This expanding universe of proteins with the propensity to aggregate, most frequently under stress conditions, is leading to exciting new insights into the behaviour of proteins, and some of the hitherto largely unsuspected consequences for physiological regulation and evolution.

## 2. Fungal Prion Structure(s)

As with mammalian PrP<sup>Sc</sup>, yeast prions turned out to form amyloid aggregates with a cross-beta sheet structure made up of in-register parallel beta sheets [55–59]. (The *P. anserina* [HET-s] prion is an exception, adopting a  $\beta$ -solenoid conformation with each monomer forming two turns of the helix [60–63]). The aggregates can be very large, are insoluble and resistant to proteinase and detergent treatment, characteristics harnessed in the large-scale screening of new prions using semi-denaturing-agarose gel electrophoresis (SDD-AGE). When cell lysates were centrifuged, the prion form was present in the pellet while the non-prion form remained in the supernatant [28,35,36]. If

fused to fluorescent proteins like GFP, the prion form appeared as punctate foci, while the non-prion form showed diffuse fluorescence [35,64]. Prion aggregation can proceed through multiple pathways manifested by a ribbon-like ring structure at vacuole or cell periphery, a single spot, multiple spots, or multiple long filaments [43,65–68].

Prionogenic proteins were shown to have prion-forming domains (PrDs or PFDs) [44,64,69,70] with strongly biased amino acid compositions, in most cases rich in glutamine and asparagine (Q/N-rich) [71]. Additionally, PFDs generally contain a number of hydrophobic and aromatic residues, are depleted in charged residues and sensitive to the position of prolines. Although specific residues and their spacing in PFDs may be important in nucleating the prion amyloid structure, in prions like [URE3] and [PSI<sup>+</sup>], the amino acid composition rather than specific sequences seems to be the primary determinant of prion-forming ability [69,72–75]. A search of the yeast proteome for proteins with similar composition led to the discovery of around 200 prion candidates, of which 24 formed SDS-resistant aggregates and fluorescent foci and caused altered phenotypes. Many of the proteins that formed large aggregates were more abundant in Ns than Qs [51]. While this compositional bias holds true for many prions, [HET-s] and [MOD<sup>+</sup>] lack such prion signatures [76,77]. A number of tools and algorithms have been developed for prion prediction [78–80]. A search for prion domains across phyla found an overabundance of Asn only in the *Saccharomycetes* clade (overall N-rich proteomes), while the other groups were mostly Gln-rich [81]. Human prion-like proteins FUS, TAF15 and TDP43, on the other hand, are also Ser/Gly rich. Thus Q/N-based predictions may not be optimal across all systems and not all candidates obtained by sequence-based searches form prions. Further, Q/N-rich sequences show rather weak aggregation propensities, while aromatic and non-aromatic hydrophobic amino acids tend to promote aggregate formation. Aromatic amino acids are strongly prion-promoting both for human G-rich and yeast Q/N-rich prions [74,82]. However, G-rich prions are more degradation-prone, suggesting that the presence of Q/N rich domains may prevent recognition and degradation by the cell protein quality control machinery [83]. Q and N contribute differently to prion formation. An all-N Sup35 PrD construct (Sup35<sup>N</sup>) with 44% N (compared to 15% in WT) had an increased prion induction frequency and escaped the requirement for [RNQ<sup>+</sup>], while all-Q Sup35 (Sup35<sup>Q</sup>) almost abolished prion forming ability. Sup35<sup>N</sup> was able to induce even the non-prionogenic protein Gal11 to form prions, while Sup35<sup>Q</sup> led to collapsed oligomeric intermediates that failed to form amyloids, were more toxic to neuroblastoma cells and were detected by antibodies against the toxic pre-amyloid states observed in Aβ and α-synuclein aggregation [84]. Similar amyloid promoting properties of N were also seen with the N-rich PrDs of Ure2 and Lsm4. In the Lsb2 protein, substituting 8N for 8Q increases prion-forming ability [85]. Thus Q abundance likely leads to templates with low rates of monomer addition. This may also hold true for the Q-rich proteins implicated in neurodegeneration. This “deficiency” in amyloid formation is however restricted to the short stretches of Qs as seen in Sup35, and can be overcome by much longer strings of Q [86]. Further, Q-rich amyloids induce [PSI<sup>+</sup>] more frequently than non-Q amyloids [87]. The N side chain enhances hydrogen bonding with the polypeptide backbone, increasing the formation of turns facilitating beta sheets. The difference of a single methylene group between N and Q leads to increased conformational heterogeneity and non-specific interactions. In a number of Q/N-rich nucleoporins of yeast such as Nup100, Glycine-Leucine-Phenylalanine-Glycine (GLFG) repeats promoted aggregation behaviour in proportion to the number of repeats. In the absence of [RNQ<sup>+</sup>], Nup aggregates did not adopt amyloid structures, while in the presence of [RNQ<sup>+</sup>] they did [88]. The GLFG repeats also mediated heterologous interactions between different Nup proteins: thus Nup100 aggregates could recruit other Nup proteins.

In addition to a region essential for nucleation of the amyloid structure, PFDs may contain distinct sequences required for their propagation, such as certain oligopeptide repeats in the Sup35 PFD

[89,90]. The number of these repeats is inversely related to whether the proteins form ‘off-pathway’ filaments that contain β-strands and random-coiled regions and do not proceed to form amyloid structure [91]. For Sup35, these repeats could be functionally replaced by the PrP oligonucleotide repeat region [75]. Interestingly, folding intermediates during the assembly of [PSI<sup>+</sup>] amyloid were found to be recognised by antibodies to oligomers of the amyloidogenic peptide Aβ implicated in Alzheimer’s disease, even though the primary sequences are completely unrelated [92]. These observations suggest similarities in conformations and three-dimensional structures of folding intermediates of mammalian and yeast proteins. The yeast Sup35 NM region was also shown to be able to form an amyloid aggregate in cultured mouse neuroblastoma cells, behaving as a prion inasmuch as it was transmitted to daughter cells [93].

The PFDs are frequently distinct from the functional domains of the protein, and have a disordered structure in the non-prion conformation of the protein. In Sup35, some missense mutations in the N terminal region lead to loss of prion forming ability, while the C-terminal region is sufficient for translation termination and is believed to be dispensable for prion formation [31]. Remarkably, it is the disordered N-terminal region which gives rise to the extremely stable amyloid structure in the prion. In Sup35, though the N region itself can form the prion, the charged K/E rich M domain provides solubility to the monomer as well as harbouring the Hsp104 binding site and is hence required for propagation formation. Similarly, in Rnq1 the N terminal region, which carries a PFD at its C-terminal end, modulates prion forming ability. The solubility of the C-terminal region of Sup35 may also be modulated by the NM region [94]. It has been argued that the structural flexibility of amyloid-forming proteins (as well as other proteins with intrinsically disordered domains) is essential to their cellular functions as well as their ability to undergo large conformational changes [95].

PFDs on their own can aggregate into amyloids and are able to induce prion formation of the complete protein. When fused to other proteins, PFDs cause them to form amyloid aggregates and behave as prions, a property that proved very useful in the search for novel prions. However, it is not a given that the protein from which the PFD is derived will also behave as a prion under *in vivo* conditions. The gold standard for proof that a protein forms a prion in its cellular milieu is the ability of *in vitro* aggregated amyloid to induce prion formation *in vivo* when introduced into cells, and this has been demonstrated for a number of prions [41,96–98].

Differences in primary sequence can cause prion transmission barriers between different species (or at times even within a species) [99,100]. Efficiency of [PSI<sup>+</sup>] and [URE3] transfer between *S. bayanus* or *S. paradoxus* and *S. cerevisiae* is reduced as compared to almost 100% in same-species transfers, and these barriers are not always symmetric [101–103]. The transmission efficiency is further affected by the prion variant in question [104]. Barriers can sometimes be due to even single amino acid differences. Some amyloids show great specificity in the monomers they incorporate, sequence stringency becoming a barrier in cross-species transmission. The Sup35<sup>Q</sup> and Sup35<sup>N</sup> amyloids fail to cross-seed. Sup35<sup>Q</sup> can template Sup35<sup>WT</sup> amyloids, but the opposite reaction does not occur [84]. In the case of [RNQ<sup>+</sup>], transmission is further complicated by the presence of multiple Q/N rich prion determinants and cooperativity between them [105].

A further level of complexity is the existence of prion variants, analogous to the PrP<sup>Sc</sup> “strains” that differ in incubation time and disease symptoms. PrP can adopt more than 30 self-templating conformations [106,107]. The yeast prion variants represent different amyloid aggregation forms that can arise from the same protein sequence [108–115]. “Weak” variants generally form larger aggregates with thicker fibrils, have lower seed number and mitotic transmission efficiency, recruit a lower proportion of the normal protein into the amyloid aggregate, and result in weaker prion phenotypes compared to “strong” variants [114,116–118]. Once a particular variant is established, it templates its own propagation and does not easily convert to

another variant [34,119]. A convenient read-out of nonsense suppression has been widely used for  $[PSI^+]$  variants, utilising ADE1 and ADE2 mutations containing a stop codon (*ade1-14* and *ade-2-1*). ADE loss-of-function mutants, apart from being unable to grow on media lacking adenine, develop red coloration due to accumulation of an intermediate in the adenine synthesis pathway. The ability of  $[PSI^+]$  to cause read-through of the stop codon in ADE has been exploited both as a method of selecting cells with nonsense suppressor activity on medium lacking adenine, and to estimate the strength of nonsense suppression on the basis of colony colour: strong nonsense suppression results in white colonies similar to wild type, while weaker suppression yields colonies of different shades of pink. This assay has been extensively used for testing the prionogenic capacity of potential prion-forming domains of different proteins fused to the Sup35 protein from which its own N-terminal PFD had been deleted, enabling the identification of novel prionogenic sequences not only from yeast but from other organisms as well.

Monomers maintained at different temperatures form different amyloid structures [120]. The less stable amyloids formed at 4 °C induce strong  $[PSI^+]$  prions with white colonies while the more stable amyloids formed at higher temperatures produce the pink colonies of the weak  $[PSI^+]$  phenotype. Structural analysis showed that the amyloid core of the weak fibres is larger than that of the strong ones. Random coils and beta sheets of the weak prions showed more rigid patches than the strong prions. In general, the M domain, particularly in weak variants, is highly dynamic compared to the more stable N domain. Different prion strains may thus carry variants that differ in flexibility and accessibility of chaperone binding sites [121]. Polarised light spectroscopy showed that tyrosine angles are similar within the core for weak and strong variants; however, small differences in local environments of some Tyr residues outside the amyloid core may lead to differences in fibre packing [122]. The prion variants also differ in chaperone susceptibility and requirements [123–126]. Weak  $[PSI^+]$  variants are more easily cured by Hsp104 than strong variants. Sis1 is particularly required for propagation of strong  $[PSI^+]$  variants.

The overall picture that emerges is that prionogenic proteins can exist in multiple conformational states, only some of which are self-propagating.

### 3. Prion induction and propagation

*De novo* prion emergence occurs at a low frequency, but once formed, prions can rapidly template soluble monomers to form amyloid aggregates. Prion formation is a multi-step process involving a slow lag phase where the monomeric protein may sample multiple transient conformations, leading to unfolding and formation of molten oligomers, followed by a relatively rapid assembly phase where the oligomeric seeds form large aggregates [127–132]. The lag phase can be eliminated by addition of preformed amyloid templates [37,109]. Introduction of preformed amyloid fibres is sufficient to create a prion phenotype in naive yeast cells. Prion induction frequencies vary from 1 in  $10^2$  to  $10^7$  cells, depending on the protein, background strain and environmental context. Prion states are induced at much higher frequency (eg. 1000-fold higher for  $[PSI^+]$ ) in conditions of protein overexpression [29,34]. Induction frequencies are also higher under several environmental conditions including biophysical stresses, with the increase correlating with the severity of the stress. Thermal or oxidative stress, pH, and presence of antibiotics, DMSO or ethanol can enhance yeast prion induction by triggering alternative folding. Conditions like high temperature, presence of salts like LiCl, KCl, NaCl,  $MnCl_2$ , K/Mg-acetate,  $ZnSO_4$  and compounds like DTT, increase the frequency of  $[PSI^+]$  induction 2- to 50- fold compared to that under standard growth conditions [133,134].  $[PSI^+]$  induction also increases with chronological aging in yeast. It is believed that the prion also confers a fitness advantage in aged cells by increasing autophagic flux [135]. Prolonged exposure to oxidative or salt stress also alters

induction frequency [136]. Oxidative stress causes high prion frequency, with  $H_2O_2$  leading to 300-fold higher  $[PSI^+]$  positive cells compared to normal growth conditions. Even for oxidative stress, the frequencies vary with the stress agent, with menadione showing lower frequency than  $H_2O_2$ . Oxidative stress is believed to oxidise methionine residues, which increases the prionogenicity of the proteins. Enhanced prion induction frequency is also seen in mutants of antioxidant enzymes like superoxide dismutases and catalases [137,138]. For  $[MOT3^+]$ , induction and loss of the prion are strongly related to physiological conditions:  $[MOT3^+]$  arises at very high frequency in the presence of ethanol or during growth on proline as nitrogen source, and is lost under hypoxic conditions [48].  $[LSB^+]$  is strongly induced by heat stress [139]. ER stress also leads to prion formation, especially in aggregation prone proteins, likely due to their higher hydrophobicity [140].

### 4. Prion-prion interactions

$[PIN^+]$  (for PSI Inducer) activity is required for *de novo* induction of  $[PSI^+]$  even in conditions of Sup35 overproduction [42]. The presence of the prion  $[RNQ^+]$  speeds up heterologous prion aggregation, and mere overexpression of Ure2 and New1 proteins also induces the  $[PIN^+]$  phenotype [43]. Though sequestration of the components of the cellular protein folding machinery or soluble proteins acting as inhibitors of prion formation have been proposed as mechanisms underlying this phenomenon, direct cross-seeding by providing templates for aggregation is probably the predominant cause. The  $[RNQ^+]$ - $[PSI^+]$  cross-seeding system is the most extensively studied prion-prion interaction in yeast.  $[RNQ^+]$  is a major inducer of  $[PSI^+]$  formation in  $[psi^-]$  cells,  $[PSI^+]$  rarely being observed in  $[rnq^-]$  cells [43,98,141].  $[RNQ^+]$  cross-seeding activity requires Rnq1 aggregation [142].  $[RNQ^+]$  variants with different aggregation properties differ in their ability to induce  $[PSI^+]$ , both in frequency and with regard to the  $[PSI^+]$  variants produced. In response to a range of acute (amino acid deprivation, oxidative stress, ethanol) and chronic (high salt, ER stress, incubation in stationary phase) stresses, the frequency of  $[PSI^+]$  induction and the  $[PSI^+]$  variants induced were dependent on the  $[RNQ^+]$  variant present [110,136,143,144], with stronger  $[RNQ^+]$  inducing stronger  $[PSI^+]$ . The specificity of  $[RNQ^+]$  variants was lost *in vitro*, suggesting cellular selection of particular  $[PSI^+]$  variants [144].  $[RNQ^+]$  aggregates had a wider size distribution in the stationary phase and cold stress eliminated the low molecular weight aggregates [136]. Thus the environment regulates the biophysical properties of  $[RNQ^+]$  and its  $[PSI^+]$  inducing ability, providing a link between the role of the cellular milieu and prion induction.  $[URE3]$  was initially reported to induce both  $[PSI^+]$  and  $[RNQ^+]$  [43], but later reports showed negative interactions between  $[PSI^+]$  and  $[URE3]$ , each one weakening the phenotype and *de novo* induction of the other [43,110,145].  $[LSB^+]$  aggregating at actin patches can bypass the  $[RNQ^+]$  requirement for inducing  $[PSI^+]$  [85].  $[LSB^+]$  can also promote  $[RNQ^+]$ .  $[PSI^+]$  induction is sensitive to the actin cytoskeleton and  $[LSB^+]$  aggregation is dependent on the Lsb2-actin interaction through Las17 and ubiquitination [85,139].  $[PSI^+]$  also promotes the formation of Pub1 amyloid [146]. Tia-1/Pub1 establish two-prion aggregates with Sup35 associated with the microtubule network, inhibiting *de novo*  $[PSI^+]$  induction, likely through competition [147]. An interaction of  $[PIN^+]$  and  $[SWI^+]$ , earlier described as  $[NSI^+]$ , also enhances translational read-through [148,149]. Further, the  $[SWI^+]$ ,  $[OCT^+]$  and  $[MOT3^+]$  prions individually affect multicellularity, with their soluble forms converging on the transcriptional network of the *FLO* genes that encode adhesion proteins. It will be interesting to study the interplay between these prions in modulating multicellularity.

### 5. Prions and the cellular machinery

Prion gain and loss occur spontaneously. This has stimulated work

**Table 1**  
Overview of prion proteins.

Prion <sup>a</sup>	Protein and function	Prion Phenotype(s)	Q/N rich	Hsp104 dependent	Amyloid formation	De novo frequency	Found in wild strains	Interaction with other prions
<i>S. cerevisiae</i>								
[URE3]	Ure2, N catabolite repression via Gln3 inhibition	Loss of N catabolite repression: Utilisation of poor Nitrogen sources in presence of good N sources.	Yes	Yes	Yes	10 <sup>-5</sup>	-	[PSI <sup>+</sup> ] ↓
[PSI <sup>+</sup> ]	Sup35, translation termination factor eRF3	Stop codon readthrough. Highly variable phenotypes dependent on genetic background.	Yes	Yes	Yes	10 <sup>-7</sup> - 10 <sup>-3</sup>	+	[URE3], [SWI <sup>+</sup> ] ↑
[RNQ <sup>+</sup> ]	Rnq, function unknown	Pin <sup>+</sup> factor, increases frequency of heterologous prion formation.	Yes	Yes	Yes	10 <sup>-6</sup> - ?	+	Most prions ↑
[SWI <sup>+</sup> ]	Swi1, part of SWI/SNF chromatin remodelling complex	Weak nonsense suppression. Benomyl resistance. Loss of multicellularity. Loss of induction of SWI/SNF-dependent genes.	Yes	Yes	Yes	10 <sup>-4</sup> - 10 <sup>-3</sup>	+	[RNQ <sup>+</sup> ], [PSI <sup>+</sup> ] ↑
[MOD <sup>+</sup> ]	Mod5, tRNA isopentenyl- transferase	Resistance to ergosterol synthesis inhibitors like fluconazole & clotrimazole. Nocodazole resistance	Q-rich	Yes	Yes	?	-	-
[MOT3 <sup>+</sup> ]	Mot3, transcription factor	Resistance to cell wall stressors. Induction of multicellularity.	Yes	Yes	Yes	10 <sup>-4</sup> - 10 <sup>-3</sup>	+	?
[OCT <sup>+</sup> ]	Cye8, negative transcriptional regulator with Tup1	Mating and sporulation defects. Increased flocculation. Invertase derepression. High iso-2-cytochrome c.	Yes	Yes	Yes	-	-	-
[ISP <sup>+</sup> ]	Sfp1, transcription factor	Antisuppressor of [PSI <sup>+</sup> ]. Large cells, faster growth. Resistance to aminoglycosides.	Yes	Yes	No	10 <sup>-4</sup>	-	-
[GAR <sup>+</sup> ]	Sid1, transcription regulator + Pma1, membrane proton pump	Loss of glucose repression. Decrease in HXT3 expression. Increased longevity. Higher fitness in media with mixed sugars.	No	No	No	10 <sup>-4</sup> - 10 <sup>-1</sup>	+	-
[NUP100 <sup>+</sup> ]	Nup100, nuclear pore protein	Enhanced nuclear transport	No	-	Yes	-	-	-
[LSB <sup>+</sup> ]	Lsb2, Las17-binding protein	Enhanced formation of [PSI <sup>+</sup> ] from Sup35	Yes	Yes	?	10 <sup>-3</sup>	-	[PSI <sup>+</sup> ]
[PUB]/	Pub1, RNA binding protein	Stress granule formation	Yes	+/-	Yes	-	-	[PSI <sup>+</sup> ]
<b>Mammalian</b>								
[TIA1]	TIA-1, RNA binding protein	Stress granule formation	Yes	?	Yes	-	-	[PSI <sup>+</sup> ]
<i>P. anserina</i>								
[HET-s]	Het-s	Heterokaryon incompatibility	?	+/-	Yes	-	+	-
<i>C. globosum</i>								
[HELLP]	HELLP	Heterokaryon incompatibility	No	?	Yes	-	-	-
<i>S. pombe</i>								
[CTR4 <sup>+</sup> ]	Ctr4, Copper transporter	Sensitivity to oxidative stress	N-rich	No	Yes	-	-	-
<i>C. botulinum</i>								
[Cb-Rho <sup>+</sup> ]	Rho, transcription terminator	Large-scale changes in transcriptome	N-rich	ClpB	Yes	-	-	-
<i>K. aeruginosa</i>								
Mcc1 <sup>a</sup>	Microcin, pore-forming bacteriotoxin	Inactivation of bacteriotoxin, probably reversible	-	-	Yes	-	-	-
<i>A. californica</i>								
[CPEB <sup>+</sup> ]	CPEB, cytoplasmic poly-adenylation element binding protein, translation modulator	Memory formation via long-term facilitation (LTF)	Yes	-	Yes	-	-	-
<i>D. melanogaster</i>								
[ORB2 <sup>+</sup> ]	— <sup>a</sup> —	Memory formation via (LTF)	?	-	Yes	-	-	-
<i>Mus musculus</i>								
[CPEB3 <sup>+</sup> ]	— <sup>a</sup> —	Memory formation via (LTF)	?	-	Yes	-	-	-

<sup>a</sup> For ease of presentation, a few prion-like proteins like CPEB and Rho are referred to here with the standard [PRION<sup>+</sup>] usage though it is not used in the literature for these proteins.

on cellular factors affecting formation, propagation and loss of prions. Proteins with mammalian homologues involved in clearing prions have been of particular interest with a view to countering amyloid diseases. The transmission of prions to daughter cells during cell division requires the formation of seeds or propagons [150,151]. Large  $[PSI^+]$  aggregates are resolved into new seeds by the disaggregase activity of Hsp104 and its inhibition by GdnHCl can often cure prions and their manifested phenotypes [23,33,152–155]. However, Hsp104 is not required for some prions like  $[GAR^+]$  and  $[ISP^+]$  [47,156,157]. Hsp104 is assisted by chaperones Hsp70 (Ssa1) and Hsp40 (Sis1) [158–160]. The multi-chaperone complexes break down amyloids into multiple filaments of transmissible size [161]. Hsp70 acts upstream in binding to the amyloid and targeting Hsp104 to aggregates [162].  $[PSI^+]$  (but not other prions) is also eliminated by Hsp104 overproduction, involving an Hsp90/Sti1 dependent mechanism different from the disaggregase activity [163–165]. The cytoplasmic Hsp70 s, Ssa1/2, affect  $[PSI^+]$  and  $[URE3]$  differently: overexpression of Ssa1 but not Ssa2 cures  $[URE3]$  [145]. The ribosome-associated Hsp70 s – Ssbs – affect formation and curing of  $[PSI^+]$  [166,167]. The GET pathway is involved in guiding hydrophobic proteins to membranes and preventing their aggregation. Mutations of GET pathway proteins impair curing by Hsp104 due to over-production of the co-chaperone Sgt2, which shields Sup35 from excess Hsp104 [168]. Different yeast prions show distinct Sis1 requirements, suggesting multiple roles for Sis1 [160,169,170]. In addition to Sis1, J proteins (Hsp40s) also act in a prion specific manner; thus  $[SWI^+]$  is dependent on Ydj1 while  $[URE3]$  requires Swa2 and Sse1 [125,171,172]. Sse1 overproduction also clears  $[URE3]$  [123]. Ydj1 overexpression inhibits some variants of  $[PIN^+]$  and not others. Heat shock factor Hsf1, the master regulator of chaperone expression, also modulates  $[PSI^+]$  formation. Interestingly, Hsp42, with a PrD and an intrinsically disordered domain (IDD) (which is also a component of stress granules), prevents molten oligomer formation. Hsp42 works synergistically with Hsp26 to inhibit prion formation by promoting activity of Hsp104, Hsp70 and Hsp40. Hsp26 prevents growth of newly formed fibres. Hsp31, induced during stress and diauxic shift, is involved early in inhibiting the misfolding process, reducing  $[PSI^+]$  foci [131,173]. The two homologous proteins Btn2 and Cur1 involved in endosomegolgi sorting have emerged as prion curing factors, restricting prion proteins to a single site and preventing transmission. Btn2 requires Hsp42, which in turn is dependent on Cur1 for eliminating  $[URE3]$ .

A plethora of other factors have also been shown to affect prion formation. Proteolytic cleavage of Sup35 by protease PrB1-PrA1 suppressed *de novo*  $[PSI^+]$  generation in log phase cells [174]. The ubiquitin proteasome pathway plays a role in prion clearance [175]. A genetic screen for ‘anti-prion’ factors uncovered Upf1/Nam7 and Upf3, members of the nonsense mediated mRNA decay system [176]. Siw14, a pyrophosphatase involved in the inositol polyphosphate synthesis pathway, is able to cure prions by limiting the levels of inositol poly/pyro phosphates [177]. Sla1, a Gln rich protein involved in cortical actin assembly and endocytic vesicle formation, supports  $[PSI^+]$  induction [178]. Sup35 interacts with several components of the actin cytoskeleton and disruption of actin by Latrunculin A interferes with  $[PSI^+]$  formation, particularly oxidative stress-induced  $[PSI^+]$  [65,179,180]. Alteration of the actin cytoskeleton reduces aggregation and  $[PSI^+]$  induction and increases  $[PSI^+]$  toxicity [65]. Sla2, a homologue of huntingtin interacting protein, known to modulate the actin cytoskeleton, is important for prion ring formation and is required for viability in  $[PSI^+]$   $[RNQ^+]$  cells. Mutations of Las17, involved in Lsb2-actin interaction, and Vps5 and Sac6 involved in the endocytic pathway, reduce prion induction [181]. Further, in response to heat stress, the actin-interacting protein Lsb2 attains a transient prionic state and induces  $[PSI^+]$  [85,139]. Recently,  $[PSI^+]$  aggregates and chaperones Hsp40, Hsp70 and Hsp110 were discovered in extracellular vesicles from yeast cultures at early stationary phase. Whether the cellular trafficking machinery is used as a method of cell-to-cell transfer

of prions or a way to reduce the cell load is not clear [182]. Exosomes from mammalian cells have also been shown to transfer  $[PSI^+]$  seeds to recipient cells, and interfering with exosome integrity reduces the efficiency of aggregate induction [183]. The formation and transmission of prions is thus sensitive to numerous cellular factors in prion-specific ways, and in principle cells could modulate their levels to alter frequencies of prion acquisition or loss.

## 6. Budding yeast prions

In this section we discuss the properties of the reasonably well validated yeast prions. Since general aspects of prion structure, induction and propagation have been discussed separately, the focus here is on the phenotypic, physiological, and potentially adaptive consequences of prions. Table 1 provides an overview of yeast as well as non-yeast prions.

### 6.1. $[URE3]$

URE3 was discovered as a ‘mutant’ with a similar phenotype to *ure2* mutants, but showing inheritance like a cytoplasmic element rather than the characteristic 2:2 segregation pattern of alleles of chromosomal genes [22]. In budding yeast, utilisation of poor nitrogen sources is repressed in the presence of preferred nitrogen sources like ammonia or glutamine. In the presence of these sources, the Ure2 protein sequesters the transcriptional activators Gln3 and Gat1 in the cytoplasm. Gln3 is required for expression of the allantoin uptake protein Dal5 (which can also transport ureidosuccinate). Thus, *ure2* mutants are defective in this repression and are able to utilise ureidosuccinate even in the presence of ammonia, and  $[URE3]$  shows a similar phenotype. As mentioned earlier, the unusual behaviour of URE3 was explained when Wickner proposed [26] that it was a yeast prion. He demonstrated that the  $[URE3]$  trait required the presence of an intact *URE2* gene; that although  $[URE3]$  could be cured by GdnHCl [184], such curing was reversible in that  $[URE3]$  cells could again arise among the cured cells; and that overexpression of the Ure2 protein increased the frequency at which  $[URE3]$  arose by as much as 200-fold. The Ure2 protein in  $[URE3]$  cells was shown to be proteinase K-resistant. An N-terminal Q/N-rich domain of 62 amino acids was identified as essential and sufficient for prion induction, whereas the C-terminal region lacking the N-terminal PFD was unable to convert to the prion form. Overexpression of just this N-terminal PFD was highly effective in inducing *[ure3-]* cells to become  $[URE3]$  at 2000-fold higher frequency than the spontaneous rate of  $[URE3]$  formation [28–30]. As with several other prions, different variants of  $[URE3]$  were also described [185].

### 6.2. $[PSI^+]$

$[PSI^+]$ , the prion form of the translation termination factor Sup35 [31–39], is the most intensively studied yeast prion. Initially identified as a cytoplasmically inherited suppressor that enhanced the nonsense suppressor activity of a tRNA suppressor mutation [21], it turned out to have universal nonsense suppressor activity, i.e. was able to cause read-through of all three stop codons. In its normal, active form Sup35 (also known as eRF3) functions as a translation termination factor in conjunction with Sup45 (also known as eRF1). In its aggregated, insoluble prion form the protein becomes unavailable for its role as a translation termination factor, and this depletion of the soluble protein results in leaky translation termination and read-through of stop codons. Efficient nonsense suppressors would, of course, have highly deleterious consequences, and the level of read-through in  $[PSI^+]$  cells is quite low, of the order of 1–3% [186,187].

The Sup35 protein has 3 domains: N-terminal PFD (1–123), Middle (M), and C-terminal (C, 254–685). The N domain is sufficient for prion formation [31,32,188], but propagation is more stable if the M domain

is present as well. The C domain alone is sufficient for translation termination activity, and expression of the C domain from a plasmid in  $[PSI^+]$  cells has been used to demonstrate that phenotypic effects of the prion are mainly due to translational readthrough, rather than the presence of the Sup35 amyloid aggregates *per se* [189,190]. The C terminal is, however, unstable and prone to forming non-amyloid aggregates under stress conditions [94]. Further, mutations of Thr 341 to Asp or Ala in the C domain were found to affect  $[PSI^+]$  nonsense suppression as well as amyloid formation and propagation [191], suggesting interaction of the C domain with the NM region.

As with PrP<sup>Sc</sup>,  $[PSI^+]$  too was found to be able to form variants with different properties. Weak variants tended to have lower stop codon read-through, presumably because of less efficient recruitment of the normal Sup35 protein into the amyloid prion aggregates, as reflected in the different relative amounts of insoluble Sup35 protein in lysates from different variants [109,119,192]. Genetically determined differences in the protein sequence of Sup35 also affect the kinds of  $[PSI^+]$  variants formed and consequently their phenotypes [192–195]. It may be relevant to the suppressor properties of  $[PSI^+]$  that Sup35 amyloid aggregates have been found to colocalise in cells with several chaperones and with the other termination factor, Sup45. Although Sup45 does not itself form amyloid aggregates, its colocalisation with  $[PSI^+]$  aggregates suggests that some of the pool of Sup45 may be sequestered by the  $[PSI^+]$  aggregate, thereby possibly further compromising the fidelity of translation termination.

$[PSI^+]$  strains display a large number of altered phenotypes. While the nonsense suppressor phenotypes might be expected to be generally deleterious because normal termination codons get read through (utilising near-cognate tRNAs), this is by no means always the case. Two exciting papers [189,190] compared  $[PSI^+]$ -dependent phenotypes with  $[psi^-]$  under a large number of conditions such as high temperatures, acid/base stress, hydroxyurea, oxidative stress, presence of antifungal agents, metal ions and cell wall stressors, and features such as carbon source utilisation, growth on nitrogen sources and colony morphology, in a number of different genetic backgrounds (yeast strains). Unexpectedly, in as many as about a quarter of combinations of particular yeast strain and experimental condition,  $[PSI^+]$  cells did better than  $[psi^-]$ . The differences were in almost all cases dependent on stop codon read-through. Significantly, the phenotypic effects were strongly dependent on genetic background: under the same conditions,  $[PSI^+]$  cells might survive or grow better than  $[psi^-]$  in one strain, but do more poorly in another strain. Lindquist and her co-workers interpreted these results to mean that translation past the normal termination point into the 3' UTR uncovered cryptic genetic variation that could give rise to a large number of novel phenotypes. These could arise because of the generation of extended proteins from translation of the 3'UTR region, or alternatively by the “activation” of pseudogenes with stop codons in their protein-coding regions. Attempts to identify the targets of nonsense suppression that might give rise to novel proteins have had rather limited success. Searches for plausible ORFs interrupted by stop codons which might yield functional proteins if translated through showed that a few dozen such sequences existed in the strains studied [196,197]. Readthrough of a cAMP phosphodiesterase stop codon was also demonstrated, resulting in altered cellular cAMP levels [198]. In a later transcriptomic study, some 75 genes were found to show significantly altered transcript levels in  $[PSI^+]$  cells, which included lower transcript levels of a number of genes involved in stress responses [199]. However, a recent proteomic study of over 4000 proteins failed to detect major differences between the protein profiles of  $[PSI^+]$  and  $[psi^-]$  [200], including for the proteins encoded by the genes that had been reported [199] to show altered transcript levels. It is of course possible – indeed likely – that the small amounts of extended proteins due to nonsense suppression would not be detected in a shotgun proteomics comparison, and that some of them could have large phenotypic effects even at low concentrations.

However, the effects of read-through of termination codons do not

necessarily all arise from the generation of novel proteins. mRNAs translated past the normal stop codon are also subject to quality control in the form of nonstop mRNA decay, which is triggered when a ribosome reaches the end of a 3'UTR. As a result, nonsense suppression by  $[PSI^+]$  can also result in lower levels of some proteins because of mRNA degradation triggered by read-through past the normal stop codon [201].

The kind of variation and phenotypes due to  $[PSI^+]$  strongly depend on the genetic background, which could impact  $[PSI^+]$  phenotypes in several ways. In addition to differences in the particular nonsense codons that could be read through (read-through being sequence context-dependent) and consequently the repertoire of abnormal proteins produced, there could also be differences among different strains with respect to (i) Epistatic interactions of the prion protein with other cellular components such as cytoskeletal elements, chaperones, covalently modifying enzymes etc; (ii)  $[PSI^+]$  variants produced in a given strain, due to differences in the *SUP35* gene sequence, or in the chaperone machinery, or in the conditions under which prion formation occurred (which are also known to affect the nature of the aggregates formed); and (iii) Activities of components of the protein quality control machinery, affecting the frequency of prion formation, prion stability and transmission efficiency, and the types of variants formed.

Lindquist and co-workers proposed [189,190] that, by uncovering novel (hitherto cryptic) phenotypic variation,  $[PSI^+]$  could promote survival under certain conditions. In unstable or fluctuating environments, if a population encountered conditions in which  $[PSI^+]$  conferred a growth or survival advantage, then a few cells harbouring the prion would be favoured (and the population would soon be dominated by  $[PSI^+]$ ). If conditions again changed such that  $[psi^-]$  cells were better adapted, then because of the presence of some  $[psi^-]$  cells within the population, there would be (population-level) reversion to  $[psi^-]$ . Thus, the spontaneous acquisition and loss of the prion could provide a bet-hedging mechanism for yeast populations in fluctuating environments [52,189,190,202]. Modelling of the evolutionary consequences of the ability to switch between  $[PSI^+]$  and  $[psi^-]$  states [187,203,204] suggests that switching at the known rates could be evolutionarily beneficial even for small selective advantages. Importantly, rates of  $[PSI^+]$  formation and loss are not constant but are enhanced in response to stress [48,134,139,205–207] – conditions when new selective pressures come into play, where novel phenotypes may be advantageous.

One of the arguments against  $[PSI^+]$  having any functional significance rather than merely being a ‘protein disease’, was that the persistence of the prion in lab strains was an artefact of relaxed lab conditions, and that the prion had not been found in wild populations because it would be eliminated by selection as soon as it arose. However, that argument lost force with the demonstration of the existence of  $[PSI^+]$  in a number of wild yeast isolates. In some of these,  $[PSI^+]$  produced advantageous phenotypes such as increased NaCl tolerance, resistance to acidic conditions, to fluconazole and to the DNA-damaging drug 4-nitroquinoline-1-oxide, that were lost or greatly reduced upon prion curing [53].

In addition to altered phenotypes due to stop codon read-through,  $[PSI^+]$  may have some phenotypic effects through different mechanisms. For instance, higher benomyl resistance of  $[PSI^+]$  cells in some strains was not entirely accounted for by translational readthrough. Benomyl is a microtubule depolymerising agent, and Sup35 has been reported to interact with microtubules in “two-prion” co-aggregates with Pub1 [147].

In an interesting report,  $[PSI^+]$  was shown to modulate programmed frameshifting during translation of mRNA for antizyme, which is involved in negative feedback regulation of polyamine synthesis [208]. The rate-limiting step in polyamine synthesis is Ornithine Decarboxylase (ODC) activity, and antizyme targets ODC for degradation. Antizyme translation is increased by high polyamine levels, which facilitate the +1 frameshifting event required for antizyme mRNA translation. Thus a negative feedback loop is generated for

polyamine synthesis. [*PSI*<sup>+</sup>] was shown to promote frameshifting on the antizyme mRNA even when polyamine levels are low, resulting in enhanced antizyme synthesis, inhibition of ODC, and hence lowered cellular polyamine levels. Low polyamine levels were shown to cause a number of phenotypes in the yeast strain used that resembled those observed in [*PSI*<sup>+</sup>] cells of the same strain, indicating that modification of polyamine levels may be one major way in which [*PSI*<sup>+</sup>] gives rise to altered phenotypes [208].

[*PSI*<sup>+</sup>] has recently been shown to exhibit interesting phase separation behaviour in response to pH stress, distinct from amyloid formation [209]. Cytosolic pH drops in response to starvation conditions, and this leads to large-scale phase separation behaviour in the cytosol [210], resulting in shutting down much metabolic activity – notably translation – as well as protecting proteins from damage. Some metabolic enzymes also aggregate in filamentous structures in which enzymatic activities are lost [211]. Under starvation stress or when pH is experimentally lowered, Sup35 protein undergoes liquid-liquid phase separation without amyloid formation, followed by gelation [209]. Phase separation depends on the PFD domain, but occurs only when an adjacent pH sensor domain detects a drop in pH. Franzmann et al [94] have demonstrated that the pH sensor relies on a cluster of charged residues (glutamates) that get protonated at low pH. Unlike amyloid formation, gelation is readily reversible simply by raising the pH. The ability to sequester Sup35 in such gels appears to protect it from damage, and contributes to greater fitness of cells under pH stress [94]. Similar phase separation behaviour (but not prion formation) of Sup35 has been shown in *S. pombe*.

### 6.3. [*RNQ*<sup>+</sup>]

Derkatch et al [42,43] discovered an epigenetically transmitted property with 4:0 non-Mendelian inheritance, which greatly increased the frequency of induction of [*PSI*<sup>+</sup>] and was lost upon GdnHCl treatment, named [*PIN*<sup>+</sup>] ([*PSI*] Inducer). Sondheimer and Lindquist [44] identified a prion called [*RNQ*<sup>+</sup>], and it was shown that deletion of the *RNQ* gene was sufficient to convert [*PIN*<sup>+</sup>] cells to [*pin*-] [43,212]. Variants of [*RNQ*<sup>+</sup>] differed in both the frequency at which they could induce the [*PSI*<sup>+</sup>] prion as well as in the kinds of [*PSI*<sup>+</sup>] variants obtained. While [*RNQ*<sup>+</sup>] has been thought to facilitate formation of [*PSI*<sup>+</sup>] and other prions like [*SWI*<sup>+</sup>] through heterologous cross-seeding, the nature of this interaction remains elusive. Tagged aggregates of [*RNQ*<sup>+</sup>] and [*PSI*<sup>+</sup>] show intracellular colocalisation only transiently, and once [*PSI*<sup>+</sup>] aggregates have formed, [*RNQ*<sup>+</sup>] has no effect on subsequent maintenance and propagation of [*PSI*<sup>+</sup>] [213]. Furthermore, [*RNQ*<sup>+</sup>] induces higher frequencies not only of yeast prions, but can promote amyloid formation by other aggregation-prone proteins such as mammalian huntingtin with a polyQ expansion. Thus [*RNQ*<sup>+</sup>] appears to have a broader role in facilitating aggregation of other proteins with the propensity for amyloid formation. Halfmann et al [53] detected [*RNQ*<sup>+</sup>] in 43 of 690 wild isolates they screened for the presence of prions, and all the strains which had [*PSI*<sup>+</sup>] also had [*RNQ*<sup>+</sup>]. Westergard and True [214] found naturally occurring variants of [*RNQ*<sup>+</sup>] in a number of wild yeast isolated from vineyards, breweries, and clinical samples. These variants showed differences not only in temperature sensitivity and subcellular localisation, but also in proficiency at inducing [*PSI*<sup>+</sup>] formation [110,143,215], and were distinguished even more strongly by the kinds of [*PSI*<sup>+</sup>] variants they induced, many of which displayed strong phenotypes. Intriguingly, the heterologous interaction of [*RNQ*<sup>+</sup>] with [*PSI*<sup>+</sup>] sometimes altered [*RNQ*<sup>+</sup>] structure or even led to [*RNQ*<sup>+</sup>] elimination. Direct interaction between specific sequences in [*RNQ*<sup>+</sup>] and [*PSI*<sup>+</sup>] has been demonstrated more recently [66], and crucial residues involved in this interaction have been identified [68].

### 6.4. [*SWI*<sup>+</sup>]

The Swi1 protein is a subunit of the SWI/SNF chromatin remodeling complex, which facilitates the induced expression of a number of genes required for utilisation of non-glucose sugars, as well as a variety of other genes [216,217]. Swi1 had earlier been identified as a putative Pin<sup>+</sup> element because *SWI1* overexpression caused a higher frequency of [*PSI*<sup>+</sup>] induction [43]. [*SWI*<sup>+</sup>] was subsequently shown to be a bona fide prion showing the characteristic aggregation, transmission and HSP104 dependence properties [45,51]. It arises spontaneously at high frequencies of 10<sup>-5</sup> – 10<sup>-3</sup> [218]. [*SWI*<sup>+</sup>] stability is exceptionally sensitive to alterations in activity of not only Hsp104, but other components of the chaperone machinery as well, especially members of the Hsp70 family [219]. [*SWI*<sup>+</sup>] cells had phenotypes related to impairment of SWI/SNF function, such as loss of mating type switching and sucrose utilisation. While the phenotypes so far described are largely what would be expected for partial loss of function, even for a [*SWI*<sup>+</sup>] phenotype resembling that seen in cells with a deletion of the *SWI1* gene, namely nonsense suppressor activity, the molecular basis seems to be quite different. [*SWI*<sup>+</sup>] was shown to have modest nonsense suppressor activity for the *ade1-14* mutant with a UGA stop codon, an effect greatly enhanced in a [*RNQ*<sup>+</sup>] background. Compared to [*swi*-], [*SWI*<sup>+</sup>] cells were found to have lower levels of mRNA of the translation termination factor Sup45, which acts together with Sup35 during translation termination [149]. The suppressor activity of [*SWI*<sup>+</sup>] thus appears to stem from decreased availability of the Sup45 protein, and can be abolished by expressing *SUP45* from a plasmid. *SWI1* deletion mutants expectedly showed a stronger suppressor phenotype than [*SWI*<sup>+</sup>], but surprisingly showed no decrease in Sup45 mRNA level relative to wild type [*swi*-], and the suppressor activity was not abolished by *SUP45* overexpression [220].

[*SWI*<sup>+</sup>] cells are also unable to express a number of FLO (flocculin) genes like *FLO1* and *FLO11*, resulting in complete loss of multicellularity [221]. Additional proteins required for FLO gene expression, such as Mss1, Sap30 and Msn1, also undergo conformational changes and co-aggregate with [*SWI*<sup>+</sup>], presumably rendering them inactive. An Asn-rich region of Mss1 can form prion-like aggregates in [*SWI*<sup>+</sup>] but not in [*swi*-], and these aggregates can persist even after loss of [*SWI*<sup>+</sup>].

Newby and Lindquist [222] studied cell migration and mating in a [*SWI*<sup>+</sup>] population. They observed that [*SWI*<sup>+</sup>] cells not only showed greater mobility and dispersed better under “rainfall-like” conditions than [*swi*-], but that when mixed with [*swi*-], they also caused more dispersal of small flocs of [*swi*-] cells, (which in the absence of [*SWI*<sup>+</sup>] tend to remain immobilised in large flocs). They proposed that under conditions such as nutrient depletion, where it would be advantageous to explore the environment, the greater mobility of “pioneer” [*SWI*<sup>+</sup>] cells would enable a population to adapt better. Further, they also showed that the loss of frequent mating type switching in [*SWI*<sup>+</sup>] resulted in more out-crossing, which would entail greater genetic variation within the population.

Alberti et al [51] also reported a beneficial phenotype of [*SWI*<sup>+</sup>], namely greatly enhanced resistance to benomyl. Thus, while under benign lab growth conditions [*SWI*<sup>+</sup>] cells show poorer growth than [*swi*-], it is plausible that the presence of the prion confers survival advantage in some stressful environments. Given the high frequency at which [*SWI*<sup>+</sup>] can be acquired and lost, it may represent a flexible way of responding rapidly to altered environmental conditions. Since the Swi1 protein is part of a chromatin remodelling complex required for the expression of many genes, loss of function results in pleiotropic phenotypes. Further study of the effects of [*SWI*<sup>+</sup>] are very likely to reveal additional phenotypes of this interesting prion.

### 6.5. [*MOT3*<sup>+</sup>]

Mot3 is a transcription factor that, like Swi1, is involved in regulating genes (both as a co-repressor and an activator) involved in a

range of processes such as ergosterol and cell wall biosynthesis, pheromone signalling, aerobic growth etc. [223], and consequently the [MOT3<sup>+</sup>] prion gives rise to pleiotropic phenotypes [48,51,53]. [MOT3<sup>+</sup>] was first identified in wild isolates of budding yeast [51] in a bioinformatics-based approach. Like most yeast prions it is dependent on Hsp104 for propagation, but unlike [URE3], [PSI<sup>+</sup>] and [SWI<sup>+</sup>] its formation (at high frequencies between 10<sup>-5</sup> and 10<sup>-3</sup>) is not affected by [RNQ<sup>+</sup>] [51]. [MOT3<sup>+</sup>] phenotypes related to the role of Mot3 as a repressor of genes involved in cell wall remodelling included resistance to cell wall stressors calcofluor white and congo red [51]. A subsequent study detected [MOT3<sup>+</sup>] in 6 of 96 strains tested, and found that a number of [MOT3<sup>+</sup>] phenotypes were dependent on genetic background. Thus one strain was highly resistant to calcofluor white, another strain to acidic conditions and a third to fluconazole. All these phenotypes were lost upon prion curing with GdnHCl. Remarkably, [MOT3<sup>+</sup>] formation is strongly induced by ethanol, at a high frequency of ~10<sup>-4</sup>. In the presence of high ethanol levels arising from fermentation, cells switch to respirative growth. Eventually the cellular environment becomes hypoxic due to depletion of oxygen during aerobic growth, and the prion is lost under hypoxic conditions [48].

Mot3 is a negative regulator of genes – notably FLO11 – involved in multicellularity. In [MOT3<sup>+</sup>] there is derepression of these genes, leading to various kinds of multicellular behaviours such as filament formation and invasive growth, increased flocculation, and complex colony morphology. Just as the [MOT3<sup>+</sup>]-dependent resistance to calcofluor white, fluconazole and low pH were specific to particular strains, the multicellularity phenotypes too are dependent on genetic background as well as growth and environment conditions, producing filamentation and invasive growth in some strains and altered, complex colony morphology in others.

#### 6.6. [OCT<sup>+</sup>]

Yet another transcriptional regulator, Cyc8 (aka Ssn6), which in association with Tup1 functions as a global transcription repressor involved in regulation of more than 7% of genes [224], can form a prion named [OCT<sup>+</sup>] [46]. Given the broad role of Cyc8 in transcriptional regulation, it is unsurprising that [OCT<sup>+</sup>] entails a host of altered phenotypes, largely seeming to arise from partial loss of function of Cyc8. These include defects in mating and sporulation, invertase depression, high levels of iso-2-cytochrome c and increased flocculation. [OCT<sup>+</sup>] shares the ability to modulate multicellularity with [MOT3<sup>+</sup>] and [SWI<sup>+</sup>], and it is conceivable that under stress conditions affecting rates of prion formation, an interplay of prions could contribute to the “lifestyle choice” in individual cells, possibly giving rise to a population mosaic. It has been argued in the context of [MOT3<sup>+</sup>] [48] and [SWI<sup>+</sup>] [222] that such mosaicism might benefit a population of cells under some stress conditions.

#### 6.7. [MOD<sup>+</sup>]

The [MOD<sup>+</sup>] prion was initially identified in a screen for proteins with Pin<sup>+</sup> activity, which could enhance the formation of prions with either Q/N-rich or Q-rich sequences [77]. Mod5 was the first yeast prionogenic protein found to lack a Q/N rich region, though it had a PFD domain and is dependent on Hsp104 for propagation. The non-prion form of the protein, Mod5, is a tRNA isopentenyltransferase, which modifies A<sub>37</sub> in the anticodon loop by transferring dimethylallyl pyrophosphate (DMAPP). In [MOD<sup>+</sup>] cells, levels of the modified base (<sup>16</sup>A) were found to be decreased. DMAPP is also utilised by Erg20, an enzyme involved in ergosterol biosynthesis, and since less DMAPP is utilised in [MOD<sup>+</sup>] cells for tRNA isopentenylation, more of it appears to be available for ergosterol synthesis, as reflected in higher ergosterol levels. This makes [MOD<sup>+</sup>] cells less sensitive to antifungal agents like fluconazole, which inhibit ergosterol biosynthesis. In the absence of these antifungal agents, [MOD<sup>+</sup>] cells have a growth disadvantage vis-

à-vis [mod<sup>-</sup>] cells and are gradually lost from a population, but in the presence of fluconazole, [MOD<sup>+</sup>] cells outcompete [mod<sup>-</sup>]. [MOD<sup>+</sup>] cells also showed greater tolerance for the microtubule inhibitor nocodazole. [MOD<sup>+</sup>] is unlikely to be present in most wild populations of yeast, but it would be of interest whether it can be found among clinical isolates resistant to ergosterol inhibitor antifungal agents.

#### 6.8. [ISP<sup>+</sup>]

[ISP<sup>+</sup>] (for Inversion of Suppressor Phenotype) was isolated as an “antisuppressor” that reduced nonsense suppression by [PSI<sup>+</sup>] [156]. Though curable (with rather low efficiency) by GdnHCl, [ISP<sup>+</sup>] is not dependent on Hsp104 for propagation. Sfp1, a transcription factor [225], was later shown to be the protein forming [ISP<sup>+</sup>] [47]. [ISP<sup>+</sup>] shows some features different from those of most Q/N-rich amyloid-forming yeast prions. Aside from its independence from Hsp104, aggregates are not located in the cytosol, but are nuclear. Phenotypes associated with [ISP<sup>+</sup>] are unusual in that they do not even seem to overlap with loss of function phenotypes observed for mutations in the gene. Thus, deletion of the *SFP1* gene yields no antisuppressor phenotype. Other phenotypes of [ISP<sup>+</sup>] too are absent in *SFP1* deletion mutants: higher growth rate, larger cells and resistance to drugs that affect translation, such as cycloheximide and paromomycin. Indeed, with respect to all these traits, *SFP1* deletion mutants showed an opposite phenotype: slower growth than wild type [*isp*<sup>-</sup>], smaller cells and greater sensitivity to aminoglycosides. The effect of [ISP<sup>+</sup>] on transcription has also been investigated. Intriguingly, although there were no striking changes in expression of known targets of Sfp1 regulation, [ISP<sup>+</sup>] altered the transcript levels of a number of genes that are not direct targets of Sfp1. The [ISP<sup>+</sup>] prion thus elicits phenotypes and altered gene expression that are reminiscent of gain of function and neomorphic mutations. The cellular basis of these properties so far remains in the realm of speculation.

#### 6.9. [GAR<sup>+</sup>]

[GAR<sup>+</sup>] was investigated as a possible prion [157] because of earlier reports in the literature of non-Mendelian inheritance of loss of glucose repression in a “mutant” [226] that showed cytoplasmic transmission not attributable to a plasmid or mitochondrial defect [227]. As with [PSI<sup>+</sup>] and [URE3], the basis of this inheritance remained unexplained for decades. Brown and Lindquist [157] demonstrated that the trait was due to a prion, which they named [GAR<sup>+</sup>] (for “resistant to glucose-associated repression,”): it arose at much higher frequencies than mutations in DNA, showed dominance in crosses and non-Mendelian 4:0 meiotic transmission, and could be transferred through cytoduction (cytoplasmic transfer without nuclear transfer). However, [GAR<sup>+</sup>] turned out to be unorthodox in a number of respects. In the first place, it is not an altered structural form of a single protein, but requires two entirely dissimilar proteins for its formation: Std1 and Pma1. Std1 is involved in the glucose signalling pathway, and Pma1 is a plasma membrane proton pump. Transient overexpression of *STD1* increased the frequency of [GAR<sup>+</sup>] formation nearly 1000-fold, but once [GAR<sup>+</sup>] had been induced, not only was *STD1* overexpression no longer required, but even  $\Delta$ *std1* (*STD1* gene deletion) cells derived from a [GAR<sup>+</sup>] background continued to propagate the [GAR<sup>+</sup>] state. [GAR<sup>+</sup>] thus requires the Std1 protein for its formation but not propagation. [GAR<sup>+</sup>] cells showed association of Std1 and Pma1 at the plasma membrane (while [*gar*<sup>-</sup>] did not), but neither protein was found to relocalise into the kinds of large foci observed with amyloid-forming prions, nor were any insoluble SDS-resistant forms of the two proteins observed. While, unlike most other yeast amyloid-forming prions, [GAR<sup>+</sup>] propagation does not require Hsp104, it is dependent on the chaperone machinery, and transient inhibition of Hsp70 cures cells of [GAR<sup>+</sup>].

*Saccharomyces* species are highly specialised to utilise glucose

efficiently, converting it fermentatively into alcohol, which is then catabolised aerobically. *Saccharomyces* have evolved very stringent catabolite repression for alternate carbon sources in the presence of even trace amounts of glucose. [GAR<sup>+</sup>] cells bypass this catabolite repression and are able to utilise alternate carbon sources even in the presence of glucose or the non-metabolisable glucose mimetic glucosamine (GlcN). [GAR<sup>+</sup>] was found to arise at high but different frequencies (roughly in the range 10<sup>-4</sup> to 10<sup>-3</sup>) in different strains of *S. cerevisiae*, the frequency being constant for any given strain [157]. Further, the [GAR<sup>+</sup>] trait is present not only in *S. cerevisiae*, but also in *S. paradoxus* and *S. bayanus* [157], in which a similar prionic state dependent on Std1 and Pma1 was shown to arise at high frequencies.

Two exciting follow-up papers [228,229] looked at [GAR<sup>+</sup>] in an ecological and evolutionary context. About 100 ecologically and genetically diverse strains were tested for ability to grow on glycerol medium containing GlcN. Some cells that could bypass glucose repression arose in all strains, but at different frequencies ranging from 1 in 50000 to as high as 1 in 5. The frequencies were characteristic of the strains. Tellingly, they were not correlated with genetic relatedness between the strains, but correlated strongly with their ecological niche. The frequency at which [GAR<sup>+</sup>] appeared was 1/50000 – 1/10000 in most lab strains and in 14 brewery strains; 1/500 – 1/50 in 21 fruit strains; and as high as 1/10 – 1/5 in wine strains. Two yeast species that diverged from *S. cerevisiae* ~100 million years ago – *Candida glabrata* and *Naumovozya castelli*, which too have glucose repression operating through similar mechanisms – were also investigated for the ability to acquire [GAR<sup>+</sup>]. Both species when plated on medium with glycerol + GlcN gave rise to grower colonies at frequencies of ~10<sup>-4</sup> and ~5 × 10<sup>-3</sup> respectively. A more distantly related species thought to have diverged ~250 million years ago, *Dekkera bruxellensis*, also shows glucose repression. Though the underlying biochemical basis of glucose repression is different from that in Saccharomycetes, *D. bruxellensis* too could give rise to cells with [GAR<sup>+</sup>] properties able to bypass glucose repression, at a frequency of ~4 × 10<sup>-4</sup>. Jarosz et al conclude that “organisms separated by hundreds of millions of years of evolution possess a protein-based epigenetic mechanism that heritably converts cells from metabolic specialists to generalists”.

A further twist to the story of [GAR<sup>+</sup>] is the discovery that it could be induced by certain bacteria, initially serendipitously observed because of bacterial contamination on yeast culture plates. The contaminant (*Staphylococcus hominis*) colonies induced growth on glycerol + GlcN of yeast in their vicinity, and it was shown that this was due to a secreted diffusible signal [228,229]. This induction was not specific to the strain of *S. cerevisiae* (W303) in which it was first observed: 15 genetically diverse yeast strains were tested, and all responded to the bacterial signal. Various phylogenetically diverse species of bacteria were also tested for ability to induce [GAR<sup>+</sup>], and 31 (about 30% of the species tested) were able to do so, to different extents. Strong inducers increased *de novo* [GAR<sup>+</sup>] formation frequency 10000-fold. Further, a number of these species were also able to induce [GAR<sup>+</sup>] (or a very similar heritable epigenetic mechanism) in *N. castellii*, *C. glabrata* and *D. brucei* as well. The benefit of this inter-kingdom communication for the bacteria is that it results in lower ethanol production by the yeast, creating a less hostile environment for the bacteria to grow. The yeast appear to benefit by better growth of [GAR<sup>+</sup>] cells on mixed sugar media and the ability to utilise alternate sugars even in the presence of glucose, as well as increased cell longevity. [GAR<sup>+</sup>] cells also show better uptake than [gar<sup>-</sup>] of otherwise less preferred nutrients, which may be abundant in some environments, such as proline in grape must. The signal was subsequently identified to be lactic acid (LA), a common metabolic product secreted by many bacteria [230]. LA applied directly to [gar<sup>-</sup>] cultures induces [GAR<sup>+</sup>] in about 5/100 cells at 0.015% LA; at 1% LA, almost all cells become [GAR<sup>+</sup>].

Much remains to be learned about the physical and biochemical basis of this intriguing prion and its role in physiological and ecological

contexts, but it has already provided fascinating new insights into prion biology as well as microbial communities and the interactions within them.

#### 6.10. [CTR4<sup>+</sup>] of *Schizosaccharomyces pombe*

For a long time after the discovery of the first prions in *S. cerevisiae*, the only other demonstrated fungal prion was [HET-s] of *P. anserina* [40]. While the [GAR<sup>+</sup>] prion was shown to form not only in *S. cerevisiae*, but also in *S. paradoxus* and *S. bayanus* [157] and the more distantly related yeasts *N. castellii*, *C. glabrata* and *D. bruxellensis*, searches for prions in the fission yeast *S. pombe* had not proven very encouraging. The *S. pombe* Hsp104 had been reported to be unable to support prion propagation in *S. cerevisiae*, and *in silico* analysis of potentially prionogenic proteins in *S. pombe* had suggested that their proportion was comparatively low (0.4% as against 2.7% in *S. cerevisiae*) [231]. There had been one report of epigenetic inheritance where a “prion-like state” conferred by an extrachromosomal element, designated [Cin<sup>+</sup>] for Calnexin independent, enabled cells to survive without calnexin [232], but a prion was not rigorously shown to be responsible. However, in 2017 Sideri et al demonstrated first that *S. pombe* could maintain and propagate the *S. cerevisiae* [PSI<sup>+</sup>] prion in an Hsp104-dependent manner, suggesting that *S. pombe* had the cellular machinery for prion propagation. They then showed that a protein with an Asn-rich predicted PFD domain of 55 residues, Ctr4, could indeed form prion-like aggregates [233]. Ctr4 is a subunit of the copper transporter. Overexpression of the *ctr4*<sup>+</sup> gene caused the formation of large Ctr4 aggregates that showed SDS, proteinase K and heat resistance typical of amyloids. Cells which formed the [CTR4<sup>+</sup>] aggregates became sensitive to H<sub>2</sub>O<sub>2</sub> stress, a phenotype also shown by *ctr4* deletion mutants. The [CTR4<sup>+</sup>] phenotype is inherited in non-Mendelian fashion, and [ctr4<sup>-</sup>] cells can be transformed to [CTR4<sup>+</sup>] with protein extracts from [CTR4<sup>+</sup>] cells. However, [CTR4<sup>+</sup>] propagation is not dependent on Hsp104. It is highly likely that it requires Hsp70 or some other components of the chaperone system, but this remains to be elucidated. *S. pombe* has a number of other proteins with strong PFD-like domains, including at least 3 homologues of prion-forming proteins of *S. cerevisiae*. It will be interesting to see whether more prions will turn up now that the “ice has been broken”.

#### 6.11. [HET-s] of *Podospora anserina*

[HET-s] was one of the first fungal prions to be described [40,41]. However, it was different from yeast prions in several ways. It is the only prion for which high-resolution structure has been elucidated. The [HET-s] amyloid structure is quite distinct from that of all yeast prions (reviewed in Riek and Saupé) [234]. Recent findings suggest it is a member of a distinct group of potentially prion-forming proteins in filamentous fungi [235–237] as well as metazoans. It is the only fungal prion to which a clear-cut function has long been ascribed (and generally accepted), namely that of heterokaryon incompatibility between different strains. Further, unlike other prions, [HET-s] does not show structural variants, and the prion form is encoded by a specific allele of the gene. There are two alleles, *het-S* and *het-s*, coding for proteins with 95% amino acids identity. Het-s can exist in a soluble Het-s\* form (compatible with Het-S) or in the insoluble [HET-s] prion form (incompatible with Het-S). The C-terminal region of Het-s (residues 218–289) constitutes the PFD and can independently form amyloid aggregates as well as template prion formation by the entire protein. If hyphae of a strain with Het-S encounter hyphae with the prionic [HET-s] form, hyphal fusion to form heterokaryons is “forbidden” (whereas homokaryon fusions are “allowed”.) [HET-s]-Het-S interaction (through the PFD region present in both) leads to cell death by converting Het-S to an aggregated prion-like membrane form. The structural change in Het-S exposes its N-terminal region, termed HeLo, which is required for it to form pores in the plasma membrane [238]. Het-s is unable to form

this membrane-spanning pore structure responsible for killing of heterokaryons. Het-s is thus like a Het-S allele which has lost pore-forming ability, but in its aggregated prion form induces pore formation by Het-S. Sequences very similar to two imperfect 21-amino acid repeats in the Het-S/s protein that are critical for aggregation, are present in a number of NOD-like receptors (NLRs) in various filamentous fungi. The gene encoding one of these NLRs, NWD2, is adjacent to the het-S/s gene in *P. anserina* [235], and when bound to a ligand, NWD2 can also trigger membrane localisation and pore formation by Het-S [236]. Remarkably, this mechanism appears to have been conserved and is used in animals too, as described in the section on MAVS and ASC, and the Het-s PFD can functionally substitute the ACS PYRIN domain.

Another cell death-inducing protein, HELLP, was recently identified in the filamentous fungus *Chaetomium globosum*, which also has an N-terminal HeLo-like domain and a C-terminal PFD (named PP) [230]. Like *het-S/s*, the *hellp* gene is adjacent to an NLR gene in a gene cluster, along with a lipase-encoding gene (*sbp*), and both the *Sbp* and NLR protein have a PP domain similar to that in HELLP. *Sbp* can exist in soluble as well as aggregated states, and when a strain with fluorescently tagged prion-like aggregated *Sbp* is grown together with a strain with tagged HELLP, at sites of “confrontation” of the two kinds of hyphae, there is membrane relocalisation of *Sbp* and HELLP, together with membrane disruption by HELLP. *C. globosum* thus seems to employ a very similar mechanism of cell death effectors as *P. anserina*, and it appears that this mechanism is used in animal cells too for necroptosis, where the MLKL protein acts like HELLP and Het-S when triggered by proteins with the RHIM amyloid-forming motif similar to the fungal PP motif.

## 7. Bacterial Prions

### 7.1. Cb-Rho of *Clostridium botulinum*

The *S. cerevisiae* Sup35 protein was shown to be transmitted as a prion in *Escherichia coli* [239,240], but demonstration of an endogenous bacterial prion only came more recently. In a computational analysis of the *C. botulinum* proteome, 54 proteins were predicted to have prion-forming potential. The transcription termination factor Rho was found to have a PFD-like region with a highly polar, Asn-rich sequence that could assemble into amyloid-like structures [241]. Cb-Rho was subsequently characterised as a prion [242]. Its 68 amino acid PFD could functionally replace that of *S. cerevisiae* Sup35. The complete Cb-Rho protein formed aggregates *in vivo*, and cells were cured by overexpression of ClpB, the *C. botulinum* homologue of Hsp104. Transcription termination was compromised in the prion form, resulting in large-scale changes in the transcriptome. A number of distantly related bacteria contain similar PFD-like sequences in the Rho protein. It remains to be seen whether any of them turn out to be prionogenic.

### 7.2. Microcin of *Klebsiella aeruginosa*

A second bacterial protein with prion properties has been described in *Klebsiella aeruginosa*. Many bacteria produce bacteriotoxins to inhibit growth of other bacteria. One class of these toxins are the pore-forming microcins. In *K. aeruginosa* RY492, Microcin E492 – a 7.8 kDa peptide – was found to exist in an active soluble form, *Mcc<sup>a</sup>*, and an inactive  $\beta$ -sheet-rich, protease-resistant, aggregated form, *Mcc<sup>ia</sup>*. The active *Mcc<sup>a</sup>* is produced only during exponential growth, getting converted to amyloid *Mcc<sup>ia</sup>* during stationary phase. Once generated, *Mcc<sup>ia</sup>* can act in prion-like fashion. *Mcc<sup>ia</sup>* can be induced in *Mcc<sup>a</sup>* cells by culture medium from *Mcc<sup>ia</sup>* cells as well as by *in vitro* generated *Mcc<sup>ia</sup>*. The *Mcc* protein fused to Sup35 MC could also bring about its prionisation. A short stretch of *Mcc*, 16-37, has considerable sequence similarity to the mammalian PrP amyloid-promoting sequence 111-133, and a 25-amino acid peptide of *Mcc* from this region can form aggregates and seed prion formation.

## 8. *Aplysia* CPEB, *Drosophila* Orb2 and mammalian CPEB3

A neuronal CPEB (Cytoplasmic Polyadenylation Element Binding) protein (CPEB in *Aplysia californica*, Orb2 in *Drosophila melanogaster* and CPEB3 in mammals) is present in synapses, where it has been shown to regulate translation in a highly synapse-specific manner. Though present at multiple synapses of a single neuron, CPEB is activated only at synapses that have been stimulated by signalling, where it regulates translation of mRNAs to allow synthesis of proteins essential for long-term facilitation (LTF), an essential aspect of memory formation. While the specifics of the signalling leading to activation of this CPEB isoform are not identical in *Aplysia*, *Drosophila* and mammalian neurons, the broader scheme is the same. CPEB of *Aplysia* was the first to be shown to have properties of a prion [243]. The Q/N-rich 160 amino acid N-terminal region, when fused to a reporter in yeast, conferred on it characteristic prion properties. The full-length protein also behaved as a prion when expressed in yeast. Its translation regulation was tested on an mRNA containing a CPE. Surprisingly, the reporter mRNA was not translated in cells containing the soluble CPEB protein, but only in cells with the aggregated form, providing the first example (apart from the somewhat unusual [HET-s] prion) of a protein whose function was dependent on prionisation.

CPEB in all three organisms has subsequently been amply demonstrated to endogenously promote translation of target mRNAs at neuronal synapses [244–249]; for a good overview see Si and Kandel [242]. Of particular note is that activation of CPEB through aggregation is triggered by synaptic stimulation by a neurotransmitter; that this activation is highly specific to the stimulated synapse alone and does not occur in other synapses of the same neuron that have not been stimulated; and that the resulting local translation of synaptic mRNAs is essential for LTF and memory formation but not for short term memory.

## 9. MAVS and ASC of mammals

Two mammalian activators of antiviral immune responses were reported to have prion-like properties – MAVS [250,251] and ASC [251]. A sensor of viral infection, RIG-1, interacts via its CARD domain with the CARD domain of MAVS, causing MAVS to form very large aggregates which activate the transcription factor IRF3 to induce interferon expression. *In vitro* generated MAVS fibrils can promote aggregation of MAVS in a prion-like manner [250]. The CARD domain functions as a PFD in yeast, inducible by RIG-1. Conversely, the yeast Sup35 NM region can functionally substitute the CARD domain of MAVS in mammalian cells. Mutations in MAVS eliminating its ability to form a prion in yeast also cause loss of its ability to activate IRF3 [251]. A nearly identical story holds for ASC, where NLRP3 is the upstream activator and the PYRIN domain of ASC plays a similar role to the MAVS CARD domain. However, prion properties of endogenous MAVS and ASC such as cell to cell transmission and chaperone dependence have not been described thus far.

## 10. Tia-1 and Pub1

Tia-1 (T-cell inducer antigen 1) involved in the formation of stress granules (SGs) has been shown to have prion-like properties. It carries a C-terminal intrinsically disordered Q/N rich PFD, forms SDS resistant amyloid aggregates on overexpression and is visible as fluorescent foci under cellular stress [147,252]. Tia-1 is an RNA binding protein with three N-terminal RNA recognition motifs (RRMs), and both domains are required for SG formation. Its N-terminal domain interacts with stalled translation pre-initiation complexes, followed by aggregation of these multi-protein complexes through the C terminus to form SGs that temporarily sequester RNAs. Tia-1 foci also colocalise with P bodies, likely transferring certain mRNAs for degradation. The SG forming activity of the C-terminus can be replaced by the yeast Sup35 PrD [147] and Tia-1 aggregation is dependent on Hsp104. Pub1, the yeast

homolog of Tia-1, also carries a C-terminal PFD [51]. Tia-1 and Pub1 form homo-oligomers, and can also form hetero-oligomers with Sup35 [147]. The two-prion Tia-1/Pub1–Sup35 complexes are visible as line structures associated with microtubules, distinct from pure Tia-1 foci and  $[PSI^+]$  rings, regulating microtubule integrity and cell morphology. Tia-1/Pub1 aggregation is enhanced in late log phase in response to glucose starvation-induced cytoplasmic acidification. The Tia-1/Pub1–Sup35 complex is able to recruit translational machinery including ribosomal subunits, initiation factor and Poly-A binding protein1 (Pab1) to microtubules, carries tubulin mRNA, and its disruption leads to sensitivity to the anti-microtubule drug benomyl [147]. Further, Pub1 undergoes distinct patterns of phase separation, forming reversible gel-like condensates at low pH, while partitioning into more solid condensates in response to temperature stress that require Hsp104 for dissolution [253].

## 11. Prion candidates in other systems

### 11.1. *Plasmodium falciparum* prions?

Approximately 30% of the proteins of *P. falciparum* have long Q/N-rich stretches. Computational analysis suggests that ~10% of proteins (503) have potentially prionogenic sequences, and this set of proteins is enriched in transcriptional regulators and RNA binding proteins. Putative prion-forming peptides from Sec2, IF2 and protein kinase PK4 were experimentally shown to be able to form amyloid. However, *in vivo* prion formation by the entire proteins has not so far been demonstrated [254].

### 11.2. *Luminidependens* $[LD^+]$ of *Arabidopsis thaliana*

A computational search in *A. thaliana* for proteins with potential PFDs threw up nearly 500 candidates. Putative PFDs of three of them were tested and found to form higher-order oligomers in yeast, and the *Luminidependens* PFD could functionally replace the Sup35 PFD [255]. Prion behaviour of endogenous *Luminidependens* has not, however, been demonstrated *in vivo*.

### 11.3. Prion-like domains in eukaryotic viruses

Analysis of nearly 3 million viral protein sequences identified 2769 prion-like domains in viruses of plants, mammals and insects [256]. To date there has been no experimental validation of any viral prions.

## 12. Non-Amyloid prion-like proteins, IDPs and phase separation

Earlier studies identifying prions relied on shared features of known prions [51]. A recent search for protein driven heritable changes, using transient overexpression of ~5300 (almost all) ORFs in budding yeast, discovered 46 new proteins (~1% of the proteome) showing prion-like behaviour to confer molecular memory [257]. This study adds Azf1(-Transcription Factor), Psp1(Polymerase1 suppressor), Vts1(post-transcriptional regulator), Ash1(component of histone deacetylase complex), Kap95(karyopherin-nuclear import), Mrs3(Mitochondrial iron transporter), Pbp2(RNA binding protein), Haa1(transcriptional activator), Scd5(Protein phosphatase targeting subunit), Slm1(phosphoinositide binding protein), Heh2(Inner nuclear membrane protein), Pbp1(stress granule, P body component), Mph1(3'-5' DNA helicase), Rlm1(MADS box Transcription Factor), Pol32 (subunit of DNA Polymerase  $\delta$ ) and many others to the growing list of proteins conferring heritable traits persisting for many (at least 100) generations after the protein levels had returned to normal, indicating that protein-based inheritance mechanisms are much more widespread than previously thought. Most of these proteins in their prion-like state did not affect growth on rich medium, but almost all caused better survival and growth under most stress conditions tested – oxidative stress, osmotic

stress, temperature shock, acid stress and presence of metal ions – compared to naïve cells in which the protein had not been over-expressed. Only one protein, Haa1, previously known to be involved in acid tolerance, was mostly detrimental in its prion-like form. The heritable phenotype was also induced by protein transformation using nucleic acid-free preparations from prion-containing cells, for 5 proteins so tested. The phenotypic traits were driven by loss of function in some cases (7 of 15 tested), resembling phenocopies of deletion mutants, while in others they showed gain of function. Half of these (Azf1, Heh2, Pbp2 and Vts1) were qualitatively similar but stronger than the phenotypes of deletion mutants, while the others showed entirely distinct phenotypes not observed in loss of function mutants. For instance,  $[RLM1^+]$  showed strongly improved growth on  $MnCl_2$ , while  $\Delta rlm1$  did not.

The list of prion-like proteins is enriched for transcriptional and post-transcriptional regulators (DNA and RNA binding), including both activators and repressors, suggesting that changes in gene expression may be a common feature underlying these acquired traits. Most of these new prion candidates are not Q/N rich (except for Rbs1 and Scd5), do not form amyloid, and many are not dependent on Hsp104. While they lack any striking compositional bias, they have intrinsically disordered regions (a feature shared with Q/N rich prions), interspersed with ordered regions. Nevertheless, even in the absence of amyloid formation (lack of high molecular weight aggregates and large fluorescent foci characteristic of prions), the alternate protein conformations display altered fluorescence signals and localisation. They showed different chaperone requirements, with Kap95 and Snt1 requiring Hsp90, 19 others dependent on Hsp70 and 11 on Hsp104. Some did not require Hsp70, Hsp90 or Hsp104 and may require other chaperones like Hsp40. Curing of these prionic aggregates resulted in loss of the associated phenotypes. Around 25 wild strains isolated from different environments were also subjected to curing by transient chaperone inhibition and showed altered phenotypes after curing, with the phenotype being specific both to the chaperone inhibited and the yeast strain. Three fluorescently tagged human homologues of yeast prion-like proteins – Ipo11, Pold3 and Mef2d (respective homologues of Kap120, Pol32 and Rlm1) were also tested in yeast for prion-like behavior. All 3 formed fluorescent foci after transient overexpression; while Mef2d returned to a diffuse pattern after subculture, Ipo11 and Pold3 retained the prion-like fluorescence pattern.

Intrinsically disordered proteins (IDPs) are abundant across all taxa, and several examples have been studied since the late 1990s in cellular signalling [258]. IDPs have multiple equivalent low energy conformational states that are involved in transient and dynamic molecular interactions with multiple partners. Many IDPs fold into a stable conformation upon ligand binding or environmental change, which may affect protein activation and alter accessibility of interaction motifs or sites of post-translational modifications [259]. The binding is often based on a small number of residues, permitting high specificity along with reasonable affinity to allow spontaneous dissociation [259]. In recent years, the role of IDPs in stress response proteins and DNA/RNA binding proteins has come to the forefront. IDPs are involved in abiotic stress resistance, particularly desiccation, in tardigrades and plants [260]. A number of IDPs undergo liquid-liquid phase separation and reorganise cellular components into membrane-less organelles like stress granules and P bodies to sequester proteins and RNA that are protected and released upon restoration of favourable conditions to carry out their normal function [261].

Phase separation of proteins is said to occur when “a well-mixed solution of proteins demixes into two coexisting phases, one that is enriched for the protein and the other depleted of it” [262]. It involves the formation of liquid-like condensates of proteins, a state different from the fibrillar aggregation of prions. Recently, the N-terminal prion domain of Sup35 has been shown to act as a pH sensor directing phase separation of Sup35 in response to pH changes, avoiding irreversible aggregation of the GTPase domain [209] (discussed in the section on

[ $PSI^+$ ]). A trend that emerged from earlier prion studies is the overabundance of proteins involved in RNA binding (4 in 10). IDPs that undergo phase separation also show an abundance of RNA recognition motifs (RRMs). ~1% of the human proteome is made up of potentially prionogenic proteins; disproportionately, 12% of them have motifs involved in RNA binding. Prion-like proteins implicated in neurodegenerative diseases also show an abundance of RNA binding proteins like TDP43, FUS and TAF15. In intrinsically disordered FUS family proteins, interactions between Tyr residues of the PFD and Arg in the RNA binding domains regulate the saturation concentration of the protein, suggesting a synergistic role for both domains in phase separation [263]. PFDs by themselves show phase separation properties distinct from the full proteins, likely governed by Tyr-Tyr interactions. With neighbouring glycines favouring fluidity and Gln and Ser tipping the balance towards phase separation, Wang et al suggest that the Tyr-Arg interaction is sensitive to the local electrostatic environment and discuss the possibility of predicting phase transition thresholds based on amino acid composition [263]. This may explain earlier findings that phosphorylation of serine modulates FUS phase separation. The sub-cellular localisation of RNA binding proteins is also known to affect their probability of aggregation. FUS and TAF15 for instance are present in soluble form within the nucleus but form aggregates in the cytoplasm. RNA keeps the prion-like RNA binding proteins FUS, TDP43 and TAF15 soluble within the nucleus, while lower RNA/protein ratios in the cytoplasm are unfavourable for protein solubility, leading to phase separation [209]. During stress, FUS proteins are transported out into the cytoplasm, tipping them towards forming aggregates. Prolonged periods of stress lock these proteins in the aggregation state. Phosphorylation or mutation of Tau leads to liquid-liquid phase separation, forming droplets which are likely intermediates in Tau aggregation. Acetylation, phosphorylation, methylation and ubiquitination affect liquid-liquid phase separation of FUS proteins [264–266]. Due to the presence of multiple S/Y/R residues, proteins can be modified to different degrees, allowing them to follow distinct folding and phase separation paths which may be responsible for the different prion strains (or non-prionic aggregates). Pab1 forms colloidal clusters in response to different stresses. Mutations that affect the hydrophobicity of the proline rich P domain of Pab1 also tune the stress sensitivity of the protein. It seems likely that selection has acted to “adjust” protein solubility to strike a balance between growth and efficient stress sensing [262,267]. Pub1 too undergoes distinct patterns of phase separation, forming reversible gel-like condensates at low pH, while in response to temperature stress partitioning into more solid condensates that require Hsp104 for dissolution [253]. pH dependent Pub1 separation is mediated by the RRM and is reduced in presence of RNA binding [253,267]. Pub1 and many other proteins carry P domain-like sequences [51]. In the case of Tia-1, Zn modulates reversible phase separation into spherical droplets that grow in size with time and later transform into more irregular fibrillar shapes [268]. This phase separation is facilitated by molecular crowding and eliminated by a reducing environment. A broader cellular stress response leads to formation of stress granules under thermal and nutritional stress [269]. In contrast to the buffering role of RNA discussed above, stress granule formation sequesters silenced mRNAs and RNA binding proteins regulating translation and protein stability. Proteins with IDDs and RBDs are abundant in stress granules.

It is an exciting time, and the flurry of new findings in the past few years about protein behaviour, and the ability of altered protein conformations to profoundly alter cell physiology in metastable, heritable ways (especially under conditions of stress), has already begun to change our understanding of how cells and organisms manage their affairs, challenging the hegemony of long-standing conceptions of how nucleic acid-encoded information and its differential regulation “stands above” other modes of information flow in living systems. Now, with technologies available to monitor single molecule conformations and perturbations, it will be possible to study the mechanistic details of how

different stresses and local protein environments trigger distinct conformational pathways in proteins prone to disorder. Much remains to be learnt about the biophysical basis of protein structural changes, the ways in which they are modulated by environmental and physiological conditions, the cellular machinery involved, and the functional roles and evolutionary significance of these structural transitions. How, eventually, do all these protein behaviours contribute to cell survival? Franzmann and Alberti discuss a decade of exciting work in their recent review on how many of these aspects of protein structure and function converge on cellular stress responses, suggesting a more universal phenomenon [261]. Better understanding of these behaviours also holds the promise of more effective interventions in neurodegenerative diseases linked to protein misfolding, such as TSE, Alzheimer’s disease, Huntington’s disease etc.

### 13. Why are there prions?

Why do prions and prion-like proteins exist? It is becoming clear that a very large number of proteins have IDDs, a good number of which have been shown to, and many are more likely to be able to, seed alternate protein structures under at least some intracellular conditions. Did evolution favour such sequences for their ability to form prions and act as epigenetic elements? Or do prion-like aggregates have other roles that were selected for, such as protective functions through sequestration of proteins, RNAs and perhaps other associated molecules under stress conditions? This could include different aspects like temporary, reversible sequestration during periods of stress, and irreversible aggregation of toxic alternately folded forms into relatively non-toxic aggregates. Or are IDDs common simply because they confer conformational flexibility and versatility on proteins in their interactions with other macromolecules, and is the propensity to form aggregates an incidental “by-product”? Whatever the primary selective forces may have been that led to the wide-spread prevalence of IDDs and PFDs, it is becoming clear that the biophysical properties arising from them have been exploited extensively and in hitherto little-appreciated ways. Protein aggregation and phase separation behaviour have attracted intense attention in recent years and appear to play a crucial role particularly in physiological stress responses, but likely also in other phenomena such as immune responses, cell killing pathways and memory formation. The emerging picture is beginning to suggest that evolution may have favoured the capacity of many proteins to adopt drastically different conformational and aggregation states that enable them to alter cellular states in stable but mostly reversible ways, and that prion formation may have “come with the territory”. This does not, of course, preclude the possibility that some prions may give rise to beneficial phenotypes that can confer selective advantage or play physiological roles as reversible switches. “Bet-hedging” strategies as suggested for prions [52,190], (see section above on [ $PSI^+$ ]) have been mathematically modelled [187,203,204,270], with the broad conclusion that, with the assumed rates of *de novo* generation and loss of prions, even modest selective advantages conferred by prions would make prion-based bet-hedging strategies viable. Bet hedging through TEI has also been discussed more generally [271–273], and the viability of bet-hedging strategies depends on a number of variables. One important factor is the environment – its level of heterogeneity (both spatial and temporal), the frequency and duration of environmental changes and oscillations, and the magnitude of selection pressure imposed by it. The nature of the epigenetic variation is also crucial – the frequency at which it can arise and be lost, the degree of its “linkage” to environmental conditions (eg. to what extent it can be induced in specific environments), its stability, and the possible costs of the epigenetic phenotype (eg. slower growth rate), as well as the long-term costs of maintaining the epigenetic mechanism. TEI is thus likely to be adaptive for some combination of variables and not for others. Beaumont et al [274] in an experimental study demonstrated the evolution of bet hedging (through stochastic phenotypic switching) in a lab

population of the bacterium *Pseudomonas fluorescens* subjected to fluctuating environmental conditions.

An additional interesting aspect concerns prebiotic evolution. The RNA world hypothesis has lost much of its sheen and has for some years occupied something of a TINA (There Is No Alternative) position. However, one interesting alternative hypothesis has been that of an early amyloid, rather than RNA, world [275,276]. Short peptides are known to form fairly readily, with no improbably difficult energy barriers to surmount, under presumed prebiotic conditions, and amyloid formation does not require large proteins, but can occur even with short, low complexity peptides. Amyloids formed from small peptides not only have the important virtue (under harsh physico-chemical conditions) of great stability (unlike RNA), but also the crucial ability to template their own propagation. Fascinatingly, structures based on the amyloid fold can also have a variety of catalytic activities [277–279]. The amyloid hypothesis of the origin of life posits that these properties of amyloids formed from short, low-complexity peptides could have given rise to the earliest self-replicating assemblages of macromolecules. The realisation that such simple amyloids can have catalytic activity has already prompted attempts to engineer novel amyloid-based enzymes with useful catalytic properties. Whether the prevalence in modern proteins of low-complexity peptide domains with amyloid-forming potential is because of their importance in prebiotic evolution remains a moot question. Beyond amyloid formation, it will also be interesting to see whether the catalytic activities of such aggregates are based on and therefore restricted to only amyloid structures, or whether IDD or peptides which can form other kinds of non-amyloid aggregates might also turn out to have unexpected catalytic properties. The ability of proteins with IDDs to undergo phase separation provides an additional dimension, reminiscent of Oparin's coacervate hypothesis of the origin of life. The not too distant future may well bring surprising new insights.

## Funding

This research did not receive any specific grant from funding agencies in the public, commercial, or not-for-profit sectors.

## Declaration of Competing Interest

None.

## References

- [1] A. Bird, Perceptions of epigenetics, *Nature* 447 (7143) (2007) 396–398.
- [2] C. Deans, K.A. Maggert, What do you mean, "epigenetic"? *Genetics* 199 (4) (2015) 887–896.
- [3] C.H. Waddington, The epigenotype, *Endeavour* 18 (1942).
- [4] D.L. Nanney, Epigenetic Control Systems, *Proc. Natl. Acad. Sci. U. S. A.* 44 (7) (1958) 712–717.
- [5] V.E.A. Russo, R.A. Martienssen, A.D. Riggs, *Epigenetic Mechanisms of Gene Regulation*, Cold Spring Harbor Lab Press, Woodbury, 1996.
- [6] E. Heard, R.A. Martienssen, Transgenerational epigenetic inheritance: myths and mechanisms, *Cell* 157 (1) (2014) 95–109.
- [7] E. Whitelaw, Disputing Lamarckian epigenetic inheritance in mammals, *Genome Biol* 16 (2015) 60.
- [8] A.V. Probst, O. Mittelsten Scheid, Stress-induced structural changes in plant chromatin, *Curr Opin Plant Biol* 27 (2015) 8–16.
- [9] W. Burggren, Epigenetic Inheritance and Its Role in Evolutionary Biology: Re-Evaluation and New Perspectives, *Biology (Basel)* 5 (2) (2016).
- [10] K.J. Verhoeven, B.M. von Holdt, V.L. Sork, Epigenetics in ecology and evolution: what we know and what we need to know, *Mol Ecol* 25 (8) (2016) 1631–1638.
- [11] A. Boskovic, O.J. Rando, Transgenerational Epigenetic Inheritance, *Annu Rev Genet* 52 (2018) 21–41.
- [12] M. Pigliucci, Do we need an extended evolutionary synthesis? *Evolution* 61 (12) (2007) 2743–2749.
- [13] E. Danchin, A. Charmantier, F.A. Champagne, A. Mesoudi, B. Pujol, S. Blanchet, Beyond DNA: integrating inclusive inheritance into an extended theory of evolution, *Nat Rev Genet* 12 (7) (2011) 475–486.
- [14] E. Jablonka, Epigenetic variations in heredity and evolution, *Clin Pharmacol Ther* 92 (6) (2012) 683–688.
- [15] E.V. Koonin, Does the central dogma still stand? *Biol Direct* 7 (2012) 27.
- [16] M.K. Skinner, Environmental epigenetics and a unified theory of the molecular aspects of evolution: a neo-Lamarckian concept that facilitates neo-Darwinian evolution, *Genome Biol Evol* 7 (5) (2015) 1296–1302.
- [17] K. Laland, T. Uller, M. Feldman, K. Sterelny, G.B. Müller, A. Moczek, E. Jablonka, J. Odling-Smee, G.A. Wray, H.E. Hoekstra, D.J. Futuyma, R.E. Lenski, T.F. Mackay, D. Schluter, J.E. Strassmann, Does evolutionary theory need a rethink? *Nature* 514 (7521) (2014) 161–164.
- [18] U. Grossniklaus, W.G. Kelly, B. Kelly, A.C. Ferguson-Smith, M. Pembrey, S. Lindquist, Transgenerational epigenetic inheritance: how important is it? *Nat Rev Genet* 14 (3) (2013) 228–235.
- [19] S.B. Prusiner, Novel proteinaceous infectious particles cause scrapie, *Science* 216 (4542) (1982) 136–144.
- [20] M.D. Zabel, C. Reid, A brief history of prions, *Pathog Dis* 73 (9) (2015) ftv087.
- [21] B.S. Cox, [PSI], a cytoplasmic suppressor of super-suppression in yeast, *Heredity* 20 (1965) 505–521.
- [22] F. Lacroute, Non-Mendelian mutation allowing ureidosuccinic acid uptake in yeast, *J Bacteriol* 106 (2) (1971) 519–522.
- [23] P.C. Ferreira, F. Ness, S.R. Edwards, B.S. Cox, M.F. Tuite, The elimination of the yeast [PSI<sup>+</sup>] prion by guanidine hydrochloride is the result of Hsp104 inactivation, *Mol Microbiol* 40 (6) (2001) 1357–1369.
- [24] G. Jung, D.C. Masison, Guanidine hydrochloride inhibits Hsp104 activity in vivo: a possible explanation for its effect in curing yeast prions, *Curr Microbiol* 43 (1) (2001) 7–10.
- [25] V. Grimminger, K. Richter, A. Imhof, J. Buchner, S. Walter, The prion curing agent guanidinium chloride specifically inhibits ATP hydrolysis by Hsp104, *J Biol Chem* 279 (9) (2004) 7378–7383.
- [26] R.B. Wickner, [URE3] as an altered URE2 protein: evidence for a prion analog in *Saccharomyces cerevisiae*, *Science* 264 (5158) (1994) 566–569.
- [27] B. Cox, Cytoplasmic inheritance. Prion-like factors in yeast, *Curr Biol* 4 (8) (1994) 744–748.
- [28] D.C. Masison, R.B. Wickner, Prion-inducing domain of yeast Ure2p and protease resistance of Ure2p in prion-containing cells, *Science* 270 (5233) (1995) 93–95.
- [29] D.C. Masison, M.L. Maddelein, R.B. Wickner, The prion model for [URE3] of yeast: spontaneous generation and requirements for propagation, *Proc. Natl. Acad. Sci. U. S. A.* 94 (23) (1997) 12503–12508.
- [30] D.C. Masison, H.K. Edskes, M.L. Maddelein, K.L. Taylor, R.B. Wickner, [URE3] and [PSI] are prions of yeast and evidence for new fungal prions, *Curr Issues Mol Biol* 2 (2) (2000) 51–59.
- [31] S.M. Doel, S.J. McCreedy, C.R. Nierras, B.S. Cox, The dominant PNM2- mutation which eliminates the psi factor of *Saccharomyces cerevisiae* is the result of a missense mutation in the SUP35 gene, *Genetics* 137 (3) (1994) 659–670.
- [32] M.D. Ter-Avanesyan, A.R. Dagkesamanskaya, V.V. Kushnirov, V.N. Smirnov, The SUP35 omnipotent suppressor gene is involved in the maintenance of the non-Mendelian determinant [psi<sup>+</sup>] in the yeast *Saccharomyces cerevisiae*, *Genetics* 137 (3) (1994) 671–676.
- [33] Y.O. Chernoff, S.L. Lindquist, B. Ono, S.G. Inge-Vechtomo, S.W. Liebman, Role of the chaperone protein Hsp104 in propagation of the yeast prion-like factor [psi<sup>+</sup>], *Science* 268 (5212) (1995) 880–884.
- [34] I.L. Derkatch, Y.O. Chernoff, V.V. Kushnirov, S.G. Inge-Vechtomo, S.W. Liebman, Genesis and variability of [PSI] prion factors in *Saccharomyces cerevisiae*, *Genetics* 144 (4) (1996) 1375–1386.
- [35] M.M. Patino, J.J. Liu, J.R. Glover, S. Lindquist, Support for the prion hypothesis for inheritance of a phenotypic trait in yeast, *Science* 273 (5275) (1996) 622–626.
- [36] S.V. Paushkin, V.V. Kushnirov, V.N. Smirnov, M.D. Ter-Avanesyan, Propagation of the yeast prion-like [psi<sup>+</sup>] determinant is mediated by oligomerization of the SUP35-encoded polypeptide chain release factor, *EMBO J* 15 (12) (1996) 3127–3134.
- [37] J.R. Glover, A.S. Kowal, E.C. Schirmer, M.M. Patino, J.J. Liu, S. Lindquist, Self-seeded fibers formed by Sup35, the protein determinant of [PSI<sup>+</sup>], a heritable prion-like factor of *S. cerevisiae*, *Cell* 89 (5) (1997) 811–819.
- [38] C.Y. King, P. Tittmann, H. Gross, R. Gebert, M. Aebi, K. Wuthrich, Prion-inducing domain 2-114 of yeast Sup35 protein transforms in vitro into amyloid-like filaments, *Proc. Natl. Acad. Sci. U. S. A.* 94 (13) (1997) 6618–6622.
- [39] S.V. Paushkin, V.V. Kushnirov, V.N. Smirnov, M.D. Ter-Avanesyan, In vitro propagation of the prion-like state of yeast Sup35 protein, *Science* 277 (5324) (1997) 381–383.
- [40] V. Coustou, C. Deleu, S. Saube, J. Begueret, The protein product of the het-s heterokaryon incompatibility gene of the fungus *Podospora anserina* behaves as a prion analog, *Proc. Natl. Acad. Sci. U. S. A.* 94 (18) (1997) 9773–9778.
- [41] M.L. Maddelein, S. Dos Reis, S. Duvezin-Caubet, B. Couly-Salin, S.J. Saube, Amyloid aggregates of the HET-s prion protein are infectious, *Proc. Natl. Acad. Sci. U. S. A.* 99 (11) (2002) 7402–7407.
- [42] I.L. Derkatch, M.E. Bradley, P. Zhou, Y.O. Chernoff, S.W. Liebman, Genetic and environmental factors affecting the de novo appearance of the [PSI<sup>+</sup>] prion in *Saccharomyces cerevisiae*, *Genetics* 147 (2) (1997) 507–519.
- [43] I.L. Derkatch, M.E. Bradley, J.Y. Hong, S.W. Liebman, Prions affect the appearance of other prions: the story of [PIN<sup>+</sup>], *Cell* 106 (2) (2001) 171–182.
- [44] N. Sondheimer, S. Lindquist, Rnq1: an epigenetic modifier of protein function in yeast, *Mol Cell* 5 (1) (2000) 163–172.
- [45] Z. Du, K.W. Park, H. Yu, Q. Fan, L. Li, Newly identified prion linked to the chromatin-remodeling factor Swi1 in *Saccharomyces cerevisiae*, *Nat Genet* 40 (4) (2008) 460–465.
- [46] B.K. Patel, J. Gavin-Smyth, S.W. Liebman, The yeast global transcriptional co-repressor protein Cyc8 can propagate as a prion, *Nat Cell Biol* 11 (3) (2009) 344–349.
- [47] T. Rogoza, A. Goginashvili, S. Rodionova, M. Ivanov, O. Viktorovskaya, A. Rubel,

- K. Volkov, L. Mironova, Non-Mendelian determinant [ISP+] in yeast is a nuclear-residing prion form of the global transcriptional regulator Sfp1, *Proc. Natl. Acad. Sci. U. S. A.* 107 (23) (2010) 10573–10577.
- [48] D.L. Holmes, A.K. Lancaster, S. Lindquist, R. Halfmann, Heritable remodeling of yeast multicellularity by an environmentally responsive prion, *Cell* 153 (1) (2013) 153–165.
- [49] P. Drozdova, T. Rogoza, E. Radchenko, P. Lipaeva, L. Mironova, Transcriptional response to the [ISP+] prion of *Saccharomyces cerevisiae* differs from that induced by the deletion of its structural gene, *SFP1*, *FEMS Yeast Res* 14 (8) (2014) 1160–1170.
- [50] S.W. Liebman, Y.O. Chernoff, Prions in yeast, *Genetics* 191 (4) (2012) 1041–1072.
- [51] S. Alberti, R. Halfmann, O. King, A. Kapila, S. Lindquist, A systematic survey identifies prions and illuminates sequence features of prionogenic proteins, *Cell* 137 (1) (2009) 146–158.
- [52] R. Halfmann, S. Alberti, S. Lindquist, Prions, protein homeostasis, and phenotypic diversity, *Trends Cell Biol* 20 (3) (2010) 125–133.
- [53] R. Halfmann, D.F. Jarosz, S.K. Jones, A. Chang, A.K. Lancaster, S. Lindquist, Prions are a common mechanism for phenotypic inheritance in wild yeasts, *Nature* 482 (7385) (2012) 363–368.
- [54] A. Aguzzi, Cell biology: Beyond the prion principle, *Nature* 459 (7249) (2009) 924–925.
- [55] U. Baxa, N. Cheng, D.C. Winkler, T.K. Chiu, D.R. Davies, D. Sharma, H. Inouye, D.A. Kirschner, R.B. Wickner, A.C. Steven, Filaments of the Ure2p prion protein have a cross-beta core structure, *J Struct Biol* 150 (2) (2005) 170–179.
- [56] F. Shewmaker, R.B. Wickner, Ageing in yeast does not enhance prion generation, *Yeast* 23 (16) (2006) 1123–1128.
- [57] U. Baxa, R.B. Wickner, A.C. Steven, D.E. Anderson, L.N. Marekov, W.M. Yau, R. Tycko, Characterization of beta-sheet structure in Ure2p1-89 yeast prion fibrils by solid-state nuclear magnetic resonance, *Biochemistry* 46 (45) (2007) 13149–13162.
- [58] F. Shewmaker, E.D. Ross, R. Tycko, R.B. Wickner, Amyloids of shuffled prion domains that form prions have a parallel in-register beta-sheet structure, *Biochemistry* 47 (13) (2008) 4000–4007.
- [59] F. Shewmaker, D. Kryndushkin, B. Chen, R. Tycko, R.B. Wickner, Two prion variants of Sup35p have in-register parallel beta-sheet structures, independent of hydration, *Biochemistry* 48 (23) (2009) 5074–5082.
- [60] C. Ritter, M.L. Maddelein, A.B. Siemer, T. Luhrs, M. Ernst, B.H. Meier, S.J. Saupé, R. Riek, Correlation of structural elements and infectivity of the HET-s prion, *Nature* 435 (7043) (2005) 844–848.
- [61] A.B. Siemer, C. Ritter, M.O. Steinmetz, M. Ernst, R. Riek, B.H. Meier, 13C, 15N resonance assignment of parts of the HET-s prion protein in its amyloid form, *J Biomol NMR* 34 (2) (2006) 75–87.
- [62] C. Wasmer, A. Lange, H. Van Melckebeke, A.B. Siemer, R. Riek, B.H. Meier, Amyloid fibrils of the HET-s(218-289) prion form a beta solenoid with a triangular hydrophobic core, *Science* 319 (5869) (2008) 1523–1526.
- [63] H. Van Melckebeke, C. Wasmer, A. Lange, E. Ab, A. Loquet, A. Bockmann, B.H. Meier, Atomic-resolution three-dimensional structure of HET-s(218-289) amyloid fibrils by solid-state NMR spectroscopy, *J Am Chem Soc* 132 (39) (2010) 13765–13775.
- [64] H.K. Edskes, V.T. Gray, R.B. Wickner, The [URE3] prion is an aggregated form of Ure2p that can be cured by overexpression of Ure2p fragments, *Proc. Natl. Acad. Sci. U. S. A.* 96 (4) (1999) 1498–1503.
- [65] E.E. Ganusova, L.N. Ozolins, S. Bhagat, G.P. Newnam, R.D. Wegrzyn, M.Y. Sherman, Y.O. Chernoff, Modulation of prion formation, aggregation, and toxicity by the actin cytoskeleton in yeast, *Mol Cell Biol* 26 (2) (2006) 617–629.
- [66] F. Arslan, J.Y. Hong, V. Kanneganti, S.K. Park, S.W. Liebman, Heterologous aggregates promote de novo prion appearance via more than one mechanism, *PLoS Genet* 11 (1) (2015) e1004814.
- [67] J. Sharma, B.T. Wisniewski, E. Paulson, J.O. Obayoe, S.J. Merrill, A.L. Manogaran, De novo [PSI+] prion formation involves multiple pathways to form infectious oligomers, *Sci Rep* 7 (1) (2017) 76.
- [68] K.M. Keefer, K.C. Stein, H.L. True, Heterologous prion-forming proteins interact to cross-seed aggregation in *Saccharomyces cerevisiae*, *Sci Rep* 7 (1) (2017) 5853.
- [69] L. Li, S. Lindquist, Creating a protein-based element of inheritance, *Science* 287 (5453) (2000) 661–664.
- [70] A. Santoso, P. Chien, L.Z. Osherovich, J.S. Weissman, Molecular basis of a yeast prion species barrier, *Cell* 100 (2) (2000) 277–288.
- [71] A.H. DePace, A. Santoso, P. Hillner, J.S. Weissman, A critical role for amino-terminal glutamine/asparagine repeats in the formation and propagation of a yeast prion, *Cell* 93 (7) (1998) 1241–1252.
- [72] E.D. Ross, U. Baxa, R.B. Wickner, Scrambled prion domains form prions and amyloid, *Mol Cell Biol* 24 (16) (2004) 7206–7213.
- [73] E.D. Ross, H.K. Edskes, M.J. Terry, R.B. Wickner, Primary sequence independence for prion formation, *Proc. Natl. Acad. Sci. U. S. A.* 102 (36) (2005) 12825–12830.
- [74] J.A. Toombs, B.R. McCarty, E.D. Ross, Compositional determinants of prion formation in yeast, *Mol Cell Biol* 30 (1) (2010) 319–332.
- [75] J.A. Toombs, N.M. Liss, K.R. Cobble, Z. Ben-Musa, E.D. Ross, [PSI+] maintenance is dependent on the composition, not primary sequence, of the oligopeptide repeat domain, *PLoS One* 6 (7) (2011) e21953.
- [76] V. Taneja, M.L. Maddelein, N. Talarek, S.J. Saupé, S.W. Liebman, A non-Q/N-rich prion domain of a foreign prion, [Het-s], can propagate as a prion in yeast, *Mol Cell* 27 (1) (2007) 67–77.
- [77] G. Suzuki, N. Shimazu, M. Tanaka, A yeast prion, Mod5, promotes acquired drug resistance and cell survival under environmental stress, *Science* 336 (6079) (2012) 355–359.
- [78] E.D. Ross, K.S. Maclean, C. Anderson, A. Ben-Hur, A bioinformatics method for identifying Q/N-rich prion-like domains in proteins, *Methods Mol Biol* 1017 (2013) 219–228.
- [79] A.K. Lancaster, A. Nutter-Upham, S. Lindquist, O.D. King, PLAAC: a web and command-line application to identify proteins with prion-like amino acid composition, *Bioinformatics* 30 (17) (2014) 2501–2502.
- [80] V. Espinosa Angarica, S. Ventura, J. Sancho, Discovering putative prion sequences in complete proteomes using probabilistic representations of Q/N-rich domains, *BMC Genomics* 14 (2013) 316.
- [81] L. An, D. Fitzpatrick, P.M. Harrison, Emergence and evolution of yeast prion and prion-like proteins, *BMC Evol Biol* 16 (2016) 24.
- [82] J.A. Toombs, M. Petri, K.R. Paul, G.Y. Kan, A. Ben-Hur, E.D. Ross, De novo design of synthetic prion domains, *Proc. Natl. Acad. Sci. U. S. A.* 109 (17) (2012) 6519–6524.
- [83] S.M. Casarina, K.R. Paul, S. Machihara, E.D. Ross, Sequence features governing aggregation or degradation of prion-like proteins, *PLoS Genet* 14 (7) (2018) e1007517.
- [84] R. Halfmann, S. Alberti, R. Krishnan, N. Lyle, C.W. O'Donnell, O.D. King, B. Berger, R.V. Pappu, S. Lindquist, Opposing effects of glutamine and asparagine govern prion formation by intrinsically disordered proteins, *Mol Cell* 43 (1) (2011) 72–84.
- [85] T.A. Chernova, D.A. Kiktev, A.V. Romanyuk, J.R. Shanks, O. Laur, M. Ali, A. Ghosh, D. Kim, Z. Yang, M. Mang, Y.O. Chernoff, K.D. Wilkinson, Yeast short-lived actin-associated protein forms a metastable prion in response to thermal stress, *Cell Rep* 18 (3) (2017) 751–761.
- [86] L.Z. Osherovich, B.S. Cox, M.F. Tuite, J.S. Weissman, Dissection and design of yeast prions, *PLoS Biol* 2 (4) (2004) E86.
- [87] I.L. Derkatch, S.M. Uptain, T.F. Outeiro, R. Krishnan, S.L. Lindquist, S.W. Liebman, Effects of Q/N-rich, polyQ, and non-polyQ amyloids on the de novo formation of the [PSI+] prion in yeast and aggregation of Sup35 in vitro, *Proc. Natl. Acad. Sci. U. S. A.* 101 (35) (2004) 12934–12939.
- [88] R. Halfmann, J.R. Wright, S. Alberti, S. Lindquist, M. Rexach, Prion formation by a yeast GLFG nucleoporin, *Prion* 6 (4) (2012) 391–399.
- [89] J.J. Liu, S. Lindquist, Oligopeptide-repeat expansions modulate 'protein-only' inheritance in yeast, *Nature* 400 (6744) (1999) 573–576.
- [90] S.N. Parham, C.G. Resende, M.F. Tuite, Oligopeptide repeats in the yeast protein Sup35p stabilize intermolecular prion interactions, *EMBO J* 20 (9) (2001) 2111–2119.
- [91] S. Hess, S.L. Lindquist, T. Scheibel, Alternative assembly pathways of the amyloidogenic yeast prion determinant Sup35-NM, *EMBO Rep* 8 (12) (2007) 1196–1201.
- [92] R. Krishnan, J.L. Goodman, S. Mukhopadhyay, C.D. Pacheco, E.A. Lemke, A.A. Deniz, S. Lindquist, Conserved features of intermediates in amyloid assembly determine their benign or toxic states, *Proc. Natl. Acad. Sci. U. S. A.* 109 (28) (2012) 11172–11177.
- [93] C. Krammer, D. Kryndushkin, M.H. Suhre, E. Kremmer, A. Hofmann, A. Pfeifer, T. Scheibel, R.B. Wickner, H.M. Schatzl, I. Vorberg, The yeast Sup35NM domain propagates as a prion in mammalian cells, *Proc. Natl. Acad. Sci. U. S. A.* 106 (2) (2009) 462–467.
- [94] T.M. Franzmann, M. Jahnel, A. Pozniakovskiy, J. Mahamid, A.S. Holehouse, E. Nuske, D. Richter, W. Baumeister, S.W. Grill, R.V. Pappu, A.A. Hyman, S. Alberti, Phase separation of a yeast prion promotes cellular fitness, *Science* 359 (6371) (2018).
- [95] T. Scheibel, S.L. Lindquist, The role of conformational flexibility in prion propagation and maintenance for Sup35p, *Nat Struct Biol* 8 (11) (2001) 958–962.
- [96] H.E. Sparrer, A. Santoso, F.C. Szoka Jr., J.S. Weissman, Evidence for the prion hypothesis: induction of the yeast [PSI+] factor by in vitro-converted Sup35 protein, *Science* 289 (5479) (2000) 595–599.
- [97] A. Brachmann, U. Baxa, R.B. Wickner, Prion generation in vitro: amyloid of Ure2p is infectious, *EMBO J* 24 (17) (2005) 3082–3092.
- [98] B.K. Patel, S.W. Liebman, Prion-proof for [PIN+] : infection with in vitro-made amyloid aggregates of Rnq1p-(132-405) induces [PIN+], *J Mol Biol* 365 (3) (2007) 773–782.
- [99] P.M. Tessier, S. Lindquist, Prion recognition elements govern nucleation, strain specificity and species barriers, *Nature* 447 (7144) (2007) 556–561.
- [100] K.L. Bruce, Y.O. Chernoff, Sequence specificity and fidelity of prion transmission in yeast, *Semin Cell Dev Biol* 22 (5) (2011) 444–451.
- [101] B. Chen, G.P. Newnam, Y.O. Chernoff, Prion species barrier between the closely related yeast proteins is detected despite coaggregation, *Proc. Natl. Acad. Sci. U. S. A.* 104 (8) (2007) 2791–2796.
- [102] H.K. Edskes, L.M. McCann, A.M. Hebert, R.B. Wickner, Prion variants and species barriers among *Saccharomyces Ure2* proteins, *Genetics* 181 (3) (2009) 1159–1167.
- [103] E.G. Afanasieva, V.V. Kushnirov, M.F. Tuite, M.D. Ter-Avanesyan, Molecular basis for transmission barrier and interference between closely related prion proteins in yeast, *J Biol Chem* 286 (18) (2011) 15773–15780.
- [104] B. Chen, K.L. Bruce, G.P. Newnam, S. Gyoenova, A.V. Romanyuk, Y.O. Chernoff, Genetic and epigenetic control of the efficiency and fidelity of cross-species prion transmission, *Mol Microbiol* 76 (6) (2010) 1483–1499.
- [105] M.L. Kadnar, G. Artico, I.L. Derkatch, Distinct type of transmission barrier revealed by study of multiple prion determinants of Rnq1, *PLoS Genet* 6 (1) (2010) e1000824.
- [106] C. Kim, T. Haldiman, Y. Cohen, W. Chen, J. Blevins, M.S. Sy, M. Cohen, J.G. Safar, Protease-sensitive conformers in broad spectrum of distinct PrPSc structures in sporadic Creutzfeldt-Jakob disease are indicator of progression rate, *PLoS Pathog* 7 (9) (2011) e1002242.
- [107] J.G. Safar, Molecular pathogenesis of sporadic prion diseases in man, *Prion* 6 (2) (2012) 108–115.

- [108] P. Zhou, L.L. Derkatch, S.M. Uptain, M.M. Patino, S.W. Liebman, The yeast non-Mendelian factor [ETA+] is a variant of [PSI+], a prion-like form of release factor eRF3, *EMBO J* 18 (5) (1999) 1182–1191.
- [109] S.M. Uptain, G.J. Sawicki, B. Caughey, S. Lindquist, Strains of [PSI+] are distinguished by their efficiencies of prion-mediated conformational conversion, *EMBO J* 20 (22) (2001) 6236–6245.
- [110] M.E. Bradley, H.K. Edskes, J.Y. Hong, R.B. Wickner, S.W. Liebman, Interactions among prions and prion "strains" in yeast, *Proc. Natl. Acad. Sci. U. S. A.* 99 (Suppl. 4) (2002) 16392–16399.
- [111] D.S. Kryndushkin, I.M. Alexandrov, M.D. Ter-Avanesyan, V.V. Kushnirov, Yeast [PSI+] prion aggregates are formed by small Sup35 polymers fragmented by Hsp104, *J Biol Chem* 278 (49) (2003) 49636–49643.
- [112] S.N. Bagriantsev, V.V. Kushnirov, S.W. Liebman, Analysis of amyloid aggregates using agarose gel electrophoresis, *Methods Enzymol* 412 (2006) 33–48.
- [113] S.W. Liebman, S.N. Bagriantsev, I.L. Derkatch, Biochemical and genetic methods for characterization of [PIN+] prions in yeast, *Methods* 39 (1) (2006) 23–34.
- [114] M. Tanaka, S.R. Collins, B.H. Toyama, J.S. Weissman, The physical basis of how prion conformations determine strain phenotypes, *Nature* 442 (7102) (2006) 585–589.
- [115] B.H. Toyama, M.J. Kelly, J.D. Gross, J.S. Weissman, The structural basis of yeast prion strain variants, *Nature* 449 (7159) (2007) 233–237.
- [116] A. Derdowski, S.S. Sindi, C.L. Klaips, S. DiSalvo, T.R. Serio, A size threshold limits prion transmission and establishes phenotypic diversity, *Science* 330 (6004) (2010) 680–683.
- [117] R. Marchante, D.M. Beal, N. Koloteva-Levine, T.J. Purton, M.F. Tuite, W.F. Xue, The physical dimensions of amyloid aggregates control their infective potential as prion particles, *Elife* 6 (2017).
- [118] R. Ghosh, J. Dong, J. Wall, K.K. Frederick, Amyloid fibrils embodying distinctive yeast prion phenotypes exhibit diverse morphologies, *FEMS Yeast Res* 18 (6) (2018).
- [119] N.V. Kochneva-Pervukhova, M.B. Chechenova, I.A. Valouev, V.V. Kushnirov, V.N. Smirnov, M.D. Ter-Avanesyan, [Psi(+)] prion generation in yeast: characterization of the 'strain' difference, *Yeast* 18 (6) (2001) 489–497.
- [120] M. Tanaka, P. Chien, N. Naber, R. Cooke, J.S. Weissman, Conformational variations in an infectious protein determine prion strain differences, *Nature* 428 (6980) (2004) 323–328.
- [121] K.K. Frederick, G.T. Debelouchina, C. Kayatekin, T. Dorminy, A.C. Jacavone, R.G. Griffin, S. Lindquist, Distinct prion strains are defined by amyloid core structure and chaperone binding site dynamics, *Chem Biol* 21 (2) (2014) 295–305.
- [122] A. Reymer, K.K. Frederick, S. Rocha, T. Beke-Somfai, C.C. Kitts, S. Lindquist, B. Norden, Orientation of aromatic residues in amyloid cores: structural insights into prion fiber diversity, *Proc. Natl. Acad. Sci. U. S. A.* 111 (48) (2014) 17158–17163.
- [123] D. Kryndushkin, R.B. Wickner, Nucleotide exchange factors for Hsp70s are required for [URE3] prion propagation in *Saccharomyces cerevisiae*, *Mol Biol Cell* 18 (6) (2007) 2149–2154.
- [124] Q. Fan, K.W. Park, Z. Du, K.A. Morano, L. Li, The role of Sse1 in the de novo formation and variant determination of the [PSI+] prion, *Genetics* 177 (3) (2007) 1583–1593.
- [125] J.K. Hines, T. Higurashi, M. Srinivasan, E.A. Craig, Influence of prion variant and yeast strain variation on prion-molecular chaperone requirements, *Prion* 5 (4) (2011) 238–244.
- [126] M.T. Astor, E. Kamiya, Z.A. Sporn, S.E. Berger, J.K. Hines, Variant-specific and reciprocal Hsp40 functions in Hsp104-mediated prion elimination, *Mol Microbiol* (2018).
- [127] T.R. Serio, A.G. Cashikar, A.S. Kowal, G.J. Sawicki, J.J. Moslehi, L. Serpell, M.F. Arnsdorf, S.L. Lindquist, Nucleated conformational conversion and the replication of conformational information by a prion determinant, *Science* 289 (5483) (2000) 1317–1321.
- [128] T. Scheibel, A.S. Kowal, J.D. Bloom, S.L. Lindquist, Bidirectional amyloid fiber growth for a yeast prion determinant, *Curr Biol* 11 (5) (2001) 366–369.
- [129] T. Scheibel, J. Bloom, S.L. Lindquist, The elongation of yeast prion fibers involves separable steps of association and conversion, *Proc. Natl. Acad. Sci. U. S. A.* 101 (8) (2004) 2287–2292.
- [130] R. Krishnan, S.L. Lindquist, Structural insights into a yeast prion illuminate nucleation and strain diversity, *Nature* 435 (7043) (2005) 765–772.
- [131] M.L. Duennwald, A. Echeverria, J. Shorter, Small heat shock proteins potentiate amyloid dissolution by protein disaggregases from yeast and humans, *PLoS Biol* 10 (6) (2012) e1001346.
- [132] J. Yang, A.J. Dear, T.C.T. Michaels, C.M. Dobson, T.P.J. Knowles, S. Wu, S. Perrett, Direct observation of oligomerization by single molecule fluorescence reveals a multistep aggregation mechanism for the yeast prion protein Ure2, *J Am Chem Soc* 140 (7) (2018) 2493–2503.
- [133] Y.O. Chernoff, Stress and prions: lessons from the yeast model, *FEBS Lett* 581 (19) (2007) 3695–3701.
- [134] J. Tyedmers, M.L. Madariaga, S. Lindquist, Prion switching in response to environmental stress, *PLoS Biol* 6 (11) (2008) e294.
- [135] S.H. Speldewinde, C.M. Grant, The frequency of yeast [PSI+] prion formation is increased during chronological ageing, *Microb Cell* 4 (4) (2017) 127–132.
- [136] L. Westergaard, H.L. True, Extracellular environment modulates the formation and propagation of particular amyloid structures, *Mol Microbiol* 92 (4) (2014) 698–715.
- [137] T.C. Sideri, N. Koloteva-Levine, M.F. Tuite, C.M. Grant, Methionine oxidation of Sup35 protein induces formation of the [PSI+] prion in a yeast peroxiredoxin mutant, *J Biol Chem* 286 (45) (2011) 38924–38931.
- [138] V.A. Doronina, G.L. Staniforth, S.H. Speldewinde, M.F. Tuite, C.M. Grant, Oxidative stress conditions increase the frequency of de novo formation of the yeast [PSI+] prion, *Mol Microbiol* 96 (1) (2015) 163–174.
- [139] T.A. Chernova, A.V. Romanyuk, T.S. Karpova, J.R. Shanks, M. Ali, N. Moffatt, R.L. Howie, A. O'Dell, J.G. McNally, S.W. Liebman, Y.O. Chernoff, K.D. Wilkinson, Prion induction by the short-lived, stress-induced protein Lsb2 is regulated by ubiquitination and association with the actin cytoskeleton, *Mol Cell* 43 (2) (2011) 242–252.
- [140] N. Hamdan, P. Kritsiligkou, C.M. Grant, ER stress causes widespread protein aggregation and prion formation, *J Cell Biol* 216 (8) (2017) 2295–2304.
- [141] J. Sharma, S.W. Liebman, Exploring the basis of [PIN(+)] variant differences in [PSI+] induction, *J Mol Biol* 425 (17) (2013) 3046–3059.
- [142] K.C. Stein, H.L. True, The [RNQ+] prion: a model of both functional and pathological amyloid, *Prion* 5 (4) (2011) 291–298.
- [143] T. Kalastavadi, H.L. True, Analysis of the [RNQ+] prion reveals stability of amyloid fibers as the key determinant of yeast prion variant propagation, *J Biol Chem* 285 (27) (2010) 20748–20755.
- [144] J. Sharma, S.W. Liebman, Variant-specific prion interactions: Complicating factors, *Cell Logist* 3 (1) (2013) e25698.
- [145] C. Schwimmer, D.C. Masion, Antagonistic interactions between yeast [PSI+] and [URE3] prions and curing of [URE3] by Hsp70 protein chaperone Ssa1p but not by Ssa2p, *Mol Cell Biol* 22 (11) (2002) 3590–3598.
- [146] V.N. Urakov, A.B. Vishnevskaya, I.M. Alexandrov, V.V. Kushnirov, V.N. Smirnov, M.D. Ter-Avanesyan, Interdependence of amyloid formation in yeast: implications for polyglutamine disorders and biological functions, *Prion* 4 (1) (2010) 45–52.
- [147] X. Li, J.B. Rayman, E.R. Kandel, I.L. Derkatch, Functional role of Tia1/Pub1 and Sup35 prion domains: directing protein synthesis machinery to the tubulin cytoskeleton, *Mol Cell* 55 (2) (2014) 305–318.
- [148] A.A. Nizhnikov, Z.M. Magomedova, A.A. Rubel, A.M. Kondrashkina, S.G. Inge-Vechtomo, A.P. Galkin, [NSI+] is a determinant has a pleiotropic phenotypic manifestation that is modulated by SUP35, SUP45, and VTS1 genes, *Curr Genet* 58 (1) (2012) 35–47.
- [149] A.A. Nizhnikov, T.A. Ryzhova, K.V. Volkov, S.P. Zadorsky, J.V. Sopova, S.G. Inge-Vechtomo, A.P. Galkin, Interaction of Prions Causes Heritable Traits in *Saccharomyces cerevisiae*, *PLoS Genet* 12 (12) (2016) e1006504.
- [150] B. Cox, F. Ness, M. Tuite, Analysis of the generation and segregation of propagons: entities that propagate the [PSI+] prion in yeast, *Genetics* 165 (1) (2003) 23–33.
- [151] R. Aron, T. Higurashi, C. Sahi, E.A. Craig, J-protein co-chaperone Sis1 required for generation of [RNQ+] seeds necessary for prion propagation, *EMBO J* 26 (16) (2007) 3794–3803.
- [152] S.S. Eaglestone, L.W. Ruddock, B.S. Cox, M.F. Tuite, Guanidine hydrochloride blocks a critical step in the propagation of the prion-like determinant [PSI+] of *Saccharomyces cerevisiae*, *Proc. Natl. Acad. Sci. U. S. A.* 97 (1) (2000) 240–244.
- [153] G. Jung, G. Jones, R.D. Wegrzyn, D.C. Masion, A role for cytosolic hsp70 in yeast [PSI+] prion propagation and [PSI+] as a cellular stress, *Genetics* 156 (2) (2000) 559–570.
- [154] G. Jung, G. Jones, D.C. Masion, Amino acid residue 184 of yeast Hsp104 chaperone is critical for prion-curing by guanidine, prion propagation, and thermotolerance, *Proc. Natl. Acad. Sci. U. S. A.* 99 (15) (2002) 9936–9941.
- [155] N.V. Romanova, Y.O. Chernoff, Hsp104 and prion propagation, *Protein Pept Lett* 16 (6) (2009) 598–605.
- [156] K.V. Volkov, A.Y. Aksenova, M.J. Soom, K.V. Osipov, A.V. Svitin, C. Kurischko, I.S. Shkundina, M.D. Ter-Avanesyan, S.G. Inge-Vechtomo, L.N. Mironova, Novel non-Mendelian determinant involved in the control of translation accuracy in *Saccharomyces cerevisiae*, *Genetics* 160 (1) (2002) 25–36.
- [157] J.C. Brown, S. Lindquist, A heritable switch in carbon source utilization driven by an unusual yeast prion, *Genes Dev* 23 (19) (2009) 2320–2332.
- [158] N. Sondheimer, N. Lopez, E.A. Craig, S. Lindquist, The role of Sis1 in the maintenance of the [RNQ+] prion, *EMBO J* 20 (10) (2001) 2435–2442.
- [159] Y. Song, Y.X. Wu, G. Jung, Y. Tutar, E. Eisenberg, L.E. Greene, D.C. Masion, Role for Hsp70 chaperone in *Saccharomyces cerevisiae* prion seed replication, *Eukaryot Cell* 4 (2) (2005) 289–297.
- [160] T. Higurashi, J.K. Hines, C. Sahi, R. Aron, E.A. Craig, Specificity of the J-protein Sis1 in the propagation of 3 yeast prions, *Proc. Natl. Acad. Sci. U. S. A.* 105 (43) (2008) 16596–16601.
- [161] D.C. Masion, P.A. Kirkland, D. Sharma, Influence of Hsp70s and their regulators on yeast prion propagation, *Prion* 3 (2) (2009) 65–73.
- [162] J. Winkler, J. Tyedmers, B. Bukau, A. Mogk, Hsp70 targets Hsp100 chaperones to substrates for protein disaggregation and prion fragmentation, *J Cell Biol* 198 (3) (2012) 387–404.
- [163] G.C. Hung, D.C. Masion, N-terminal domain of yeast Hsp104 chaperone is dispensable for thermotolerance and prion propagation but necessary for curing prions by Hsp104 overexpression, *Genetics* 173 (2) (2006) 611–620.
- [164] B. Moosavi, J. Wongwigkarn, M.F. Tuite, Hsp70/Hsp90 co-chaperones are required for efficient Hsp104-mediated elimination of the yeast [PSI+] prion but not for prion propagation, *Yeast* 27 (3) (2010) 167–179.
- [165] M. Reidy, D.C. Masion, Stl1 regulation of Hsp70 and Hsp90 is critical for curing of *Saccharomyces cerevisiae* [PSI+] prions by Hsp104, *Mol Cell Biol* 30 (14) (2010) 3542–3552.
- [166] Y.O. Chernoff, G.P. Newnam, J. Kumar, K. Allen, A.D. Zink, Evidence for a protein mutator in yeast: role of the Hsp70-related chaperone ssb in formation, stability, and toxicity of the [PSI] prion, *Mol Cell Biol* 19 (12) (1999) 8103–8112.
- [167] K.D. Allen, R.D. Wegrzyn, T.A. Chernova, S. Muller, G.P. Newnam, P.A. Winslett, K.B. Wittich, K.D. Wilkinson, Y.O. Chernoff, Hsp70 chaperones as modulators of prion life cycle: novel effects of Ssa and Ssb on the *Saccharomyces cerevisiae* prion [PSI+], *Genetics* 169 (3) (2005) 1227–1242.
- [168] D.A. Kiktev, J.C. Patterson, S. Muller, B. Bariar, T. Pan, Y.O. Chernoff, Regulation

- of chaperone effects on a yeast prion by cochaperone Sgt2, *Mol Cell Biol* 32 (24) (2012) 4960–4970.
- [169] P.A. Kirkland, M. Reidy, D.C. Masison, Functions of yeast Hsp40 chaperone Sis1p dispensable for prion propagation but important for prion curing and protection from prion toxicity, *Genetics* 188 (3) (2011) 565–577.
- [170] J.M. Harris, P.P. Nguyen, M.J. Patel, Z.A. Sporn, J.K. Hines, Functional diversification of hsp40: distinct j-protein functional requirements for two prions allow for chaperone-dependent prion selection, *PLoS Genet* 10 (7) (2014) e1004510.
- [171] E.M. Troisi, M.E. Rockman, P.P. Nguyen, E.E. Oliver, J.K. Hines, Swa2, the yeast homolog of mammalian auxilin, is specifically required for the propagation of the prion variant [URE3-1], *Mol Microbiol* 97 (5) (2015) 926–941.
- [172] E.E. Oliver, E.M. Troisi, J.K. Hines, Prion-specific Hsp40 function: The role of the auxilin homolog Swa2, *Prion* 11 (3) (2017) 174–185.
- [173] T. Grousl, S. Ungelenk, S. Miller, C.T. Ho, M. Khokhrina, M.P. Mayer, B. Bukau, A. Mogk, A prion-like domain in Hsp42 drives chaperone-facilitated aggregation of misfolded proteins, *J Cell Biol* 217 (4) (2018) 1269–1285.
- [174] A. Okamoto, N. Hosoda, A. Tanaka, G.P. Newnam, Y.O. Chernoff, S.I. Hoshino, Proteolysis suppresses spontaneous prion generation in yeast, *J Biol Chem* 292 (49) (2017) 20113–20124.
- [175] K.D. Allen, T.A. Chernova, E.P. Tennant, K.D. Wilkinson, Y.O. Chernoff, Effects of ubiquitin system alterations on the formation and loss of a yeast prion, *J Biol Chem* 282 (5) (2007) 3004–3013.
- [176] M. Son, R.B. Wickner, Nonsense-mediated mRNA decay factors cure most [PSI+] prion variants, *Proc. Natl. Acad. Sci. U. S. A.* 115 (6) (2018) E1184–E1193.
- [177] R.B. Wickner, A.C. Kelly, E.E. Bezsonov, H.K. Edskes, [PSI+] prion propagation is controlled by inositol polyphosphates, *Proc. Natl. Acad. Sci. U. S. A.* 114 (40) (2017) E8402–E8410.
- [178] P.A. Bailleul, G.P. Newnam, J.N. Steenberg, Y.O. Chernoff, Genetic study of interactions between the cytoskeletal assembly protein sla1 and prion-forming domain of the release factor Sup35 (eRF3) in *Saccharomyces cerevisiae*, *Genetics* 153 (1) (1999) 81–94.
- [179] P.A. Bailleul-Winslett, G.P. Newnam, R.D. Wegrzyn, Y.O. Chernoff, An antiprion effect of the anticytoskeletal drug latrunculin A in yeast, *Gene Expr* 9 (3) (2000) 145–156.
- [180] S.H. Speldewinde, V.A. Doronina, M.F. Tuite, C.M. Grant, Disrupting the cortical actin cytoskeleton points to two distinct mechanisms of yeast [PSI+] prion formation, *PLoS Genet* 13 (4) (2017) e1006708.
- [181] A.L. Manogaran, J.Y. Hong, J. Hufana, J. Tyedmers, S. Lindquist, S.W. Liebman, Prion formation and polyglutamine aggregation are controlled by two classes of genes, *PLoS Genet* 7 (5) (2011) e1001386.
- [182] M. Kabani, R. Melki, Sup35p in Its Soluble and Prion States Is Packaged inside Extracellular Vesicles, *MBio* 6 (4) (2015).
- [183] S. Liu, A. Hossinger, J.P. Hofmann, P. Denner, I.M. Vorberg, Horizontal Transmission of Cytosolic Sup35 Prions by Extracellular Vesicles, *MBio* 7 (4) (2016).
- [184] M. Aigle, F. Lacroute, Genetical aspects of [URE3], a non-mitochondrial, cytoplasmically inherited mutation in yeast, *Mol Gen Genet* 136 (4) (1975) 327–335.
- [185] M. Schlumpberger, S.B. Prusiner, I. Herskowitz, Induction of distinct [URE3] yeast prion strains, *Mol Cell Biol* 21 (20) (2001) 7035–7046.
- [186] M. Firoozan, C.M. Grant, J.A. Duarte, M.F. Tuite, Quantitation of readthrough of termination codons in yeast using a novel gene fusion assay, *Yeast* 7 (2) (1991) 173–183.
- [187] A.K. Lancaster, J.P. Bardill, H.L. True, J. Masel, The spontaneous appearance rate of the yeast prion [PSI+] and its implications for the evolution of the evolvability properties of the [PSI+] system, *Genetics* 184 (2) (2010) 393–400.
- [188] M.D. Ter-Avanesyan, V.V. Kushnir, A.R. Dagkesamanskaya, S.A. Didichenko, Y.O. Chernoff, S.G. Inge-Vechtov, V.N. Smirnov, Deletion analysis of the SUP35 gene of the yeast *Saccharomyces cerevisiae* reveals two non-overlapping functional regions in the encoded protein, *Mol Microbiol* 7 (5) (1993) 683–692.
- [189] H.L. True, S.L. Lindquist, A yeast prion provides a mechanism for genetic variation and phenotypic diversity, *Nature* 407 (6803) (2000) 477–483.
- [190] H.L. True, I. Berlin, S.L. Lindquist, Epigenetic regulation of translation reveals hidden genetic variation to produce complex traits, *Nature* 431 (7005) (2004) 184–187.
- [191] M. Kabani, B. Cosnier, L. Bousset, J.P. Rousset, R. Melki, C. Fabret, A mutation within the C-terminal domain of Sup35p that affects [PSI+] prion propagation, *Mol Microbiol* 81 (3) (2011) 640–658.
- [192] I.L. Derkatch, M.E. Bradley, P. Zhou, S.W. Liebman, The PNM2 mutation in the prion protein domain of SUP35 has distinct effects on different variants of the [PSI+] prion in yeast, *Curr Genet* 35 (2) (1999) 59–67.
- [193] C.Y. King, Supporting the structural basis of prion strains: induction and identification of [PSI] variants, *J Mol Biol* 307 (5) (2001) 1247–1260.
- [194] S. DiSalvo, A. Derdowski, J.A. Pezza, T.R. Serio, Dominant prion mutants induce curing through pathways that promote chaperone-mediated disaggregation, *Nat Struct Mol Biol* 18 (4) (2011) 486–492.
- [195] K.J. Verges, M.H. Smith, B.H. Toyama, J.S. Weissman, Strain conformation, primary structure and the propagation of the yeast prion [PSI+], *Nat Struct Mol Biol* 18 (4) (2011) 493–499.
- [196] P. Harrison, A. Kumar, N. Lan, N. Echols, M. Snyder, M. Gerstein, A small reservoir of disabled ORFs in the yeast genome and its implications for the dynamics of proteome evolution, *J Mol Biol* 316 (3) (2002) 409–419.
- [197] O. Namy, G. Duchateau-Nguyen, I. Hatin, S. Hermann-Le Denmat, M. Termier, J.P. Rousset, Identification of stop codon readthrough genes in *Saccharomyces cerevisiae*, *Nucleic Acids Res* 31 (9) (2003) 2289–2296.
- [198] O. Namy, G. Duchateau-Nguyen, J.P. Rousset, Translational readthrough of the PDE2 stop codon modulates cAMP levels in *Saccharomyces cerevisiae*, *Mol Microbiol* 43 (3) (2002) 641–652.
- [199] A. Baudin-Baillieu, R. Legendre, C. Kuchly, I. Hatin, S. Demais, C. Mestdagh, D. Gautheret, O. Namy, Genome-wide translational changes induced by the prion [PSI+], *Cell Rep* 8 (2) (2014) 439–448.
- [200] P.H.W. Chan, L. Lee, E. Kim, T. Hui, N. Stoynov, R. Nassar, M. Moksa, D.M. Cameron, M. Hirst, J. Gsponer, T. Mayor, The [PSI+] yeast prion does not wildly affect proteome composition whereas selective pressure exerted on [PSI+] cells can promote aneuploidy, *Sci Rep* 7 (1) (2017) 8442.
- [201] M.A. Wilson, S. Meaux, R. Parker, A. van Hoof, Genetic interactions between [PSI+] and nonstop mRNA decay affect phenotypic variation, *Proc. Natl. Acad. Sci. U. S. A.* 102 (29) (2005) 10244–10249.
- [202] J. Shorter, S. Lindquist, Hsp104, Hsp70 and Hsp40 interplay regulates formation, growth and elimination of Sup35 prions, *EMBO J* 27 (20) (2008) 2712–2724.
- [203] O.D. King, J. Masel, The evolution of bet-hedging adaptations to rare scenarios, *Theor Popul Biol* 72 (4) (2007) 560–575.
- [204] C.K. Griswold, J. Masel, Complex adaptations can drive the evolution of the capacitor [PSI], even with realistic rates of yeast sex, *PLoS Genet* 5 (6) (2009) e1000517.
- [205] M.F. Tuite, C.R. Mundy, B.S. Cox, Agents that cause a high frequency of genetic change from [psi+] to [psi-] in *Saccharomyces cerevisiae*, *Genetics* 98 (4) (1981) 691–711.
- [206] B.S. Cox, M.F. Tuite, C.S. McLaughlin, The psi factor of yeast: a problem in inheritance, *Yeast* 4 (3) (1988) 159–178.
- [207] G.P. Newnam, J.L. Birchmore, Y.O. Chernoff, Destabilization and recovery of a yeast prion after mild heat shock, *J Mol Biol* 408 (3) (2011) 432–448.
- [208] O. Namy, A. Galopier, C. Martini, S. Matsufuji, C. Fabret, J.P. Rousset, Epigenetic control of polyamines by the prion [PSI+], *Nat Cell Biol* 10 (9) (2008) 1069–1075.
- [209] S. Maharana, J. Wang, D.K. Papadopoulos, D. Richter, A. Pozniakovskiy, I. Poser, M. Bickle, S. Rizk, J. Guillen-Boixet, T.M. Franzmann, M. Jahnel, L. Marrone, Y.T. Chang, J. Sternecker, P. Tomancak, A.A. Hyman, S. Alberti, RNA buffers the phase separation behavior of prion-like RNA binding proteins, *Science* 360 (6391) (2018) 918–921.
- [210] M.C. Munder, D. Midtvedt, T. Franzmann, E. Nuske, O. Otto, M. Herbig, E. Ulbricht, P. Muller, A. Taubenberger, S. Maharana, L. Malinowska, D. Richter, J. Guck, V. Zaburdaev, S. Alberti, A pH-driven transition of the cytoplasm from a fluid- to a solid-like state promotes entry into dormancy, *Elife* 5 (2016).
- [211] I. Petrovska, E. Nuske, M.C. Munder, G. Kulasegaran, L. Malinowska, S. Kroschwald, D. Richter, K. Fahmy, K. Gibson, J.M. Verbavatz, S. Alberti, Filament formation by metabolic enzymes is a specific adaptation to an advanced state of cellular starvation, *Elife* (2014).
- [212] L.Z. Osherovich, J.S. Weissman, Multiple Gln/Asn-rich prion domains confer susceptibility to induction of the yeast [PSI(+)] prion, *Cell* 106 (2) (2001) 183–194.
- [213] Z. Du, S. Valtierra, L. Li, An insight into the complex prion-prion interaction network in the budding yeast *Saccharomyces cerevisiae*, *Prion* 8 (6) (2014) 387–392.
- [214] L. Westergard, H.L. True, Wild yeast harbour a variety of distinct amyloid structures with strong prion-inducing capabilities, *Mol Microbiol* 92 (1) (2014) 183–193.
- [215] V.J. Huang, K.C. Stein, H.L. True, Spontaneous variants of the [RNQ+] prion in yeast demonstrate the extensive conformational diversity possible with prion proteins, *PLoS One* 8 (10) (2013) e79582.
- [216] C.L. Peterson, I. Herskowitz, Characterization of the yeast SWI1, SWI2, and SWI3 genes, which encode a global activator of transcription, *Cell* 68 (3) (1992) 573–583.
- [217] L.G. Burns, C.L. Peterson, The yeast SWI-SNF complex facilitates binding of a transcriptional activator to nucleosomal sites in vivo, *Mol Cell Biol* 17 (8) (1997) 4811–4819.
- [218] Z. Du, D.K. Goncharoff, X. Cheng, L. Li, Analysis of [SWI(+)] formation and propagation events, *Mol Microbiol* 104 (1) (2017) 105–124.
- [219] J.K. Hines, X. Li, Z. Du, T. Higurashi, L. Li, E.A. Craig, [SWI], the prion formed by the chromatin remodeling factor Swi1, is highly sensitive to alterations in Hsp70 chaperone system activity, *PLoS Genet* 7 (2) (2011) e1001309.
- [220] K.S. Antonets, S.F. Kliver, D.E. Plev, A.R. Shuvalova, E.A. Andreeva, S.G. Inge-Vechtov, A.A. Nizhnikov, Distinct mechanisms of phenotypic effects of inactivation and prionization of Swi1 protein in *Saccharomyces cerevisiae*, *Biochemistry (Mosc)* 82 (10) (2017) 1147–1157.
- [221] Z. Du, Y. Zhang, L. Li, The yeast prion [SWI(+)] abolishes multicellular growth by triggering conformational changes of multiple regulators required for Flocculin gene expression, *Cell Rep* 13 (12) (2015) 2865–2878.
- [222] G.A. Newby, S. Lindquist, Pioneer cells established by the [SWI+] prion can promote dispersal and out-crossing in yeast, *PLoS Biol* 15 (11) (2017) e2003476.
- [223] A.V. Grishin, M. Rothenberg, M.A. Downs, K.J. Blumer, Mot3, a Zn finger transcription factor that modulates gene expression and attenuates mating pheromone signaling in *Saccharomyces cerevisiae*, *Genetics* 149 (2) (1998) 879–892.
- [224] R.L. Smith, A.D. Johnson, Turning genes off by Ssn6-Tup1: a conserved system of transcriptional repression in eukaryotes, *Trends Biochem Sci* 25 (7) (2000) 325–330.
- [225] Z. Xu, D. Norris, The SFP1 gene product of *Saccharomyces cerevisiae* regulates G2/M transitions during the mitotic cell cycle and DNA-damage response, *Genetics* 150 (4) (1998) 1419–1428.
- [226] A.J. Ball, D.K. Wong, J.J. Elliott, Glucosamine resistance in yeast. I. A preliminary genetic analysis, *Genetics* 84 (2) (1976) 311–317.
- [227] B.A. Kunz, A.J. Ball, Glucosamine resistance in yeast. II. Cytoplasmic determinants conferring resistance, *Mol Gen Genet* 153 (2) (1977) 169–177.

- [228] D.F. Jarosz, J.C.S. Brown, G.A. Walker, M.S. Datta, W.L. Ung, A.K. Lancaster, A. Rotem, A. Chang, G.A. Newby, D.A. Weitz, L.F. Bisson, S. Lindquist, Cross-kingdom chemical communication drives a heritable, mutually beneficial prion-based transformation of metabolism, *Cell* 158 (5) (2014) 1083–1093.
- [229] D.F. Jarosz, A.K. Lancaster, J.C.S. Brown, S. Lindquist, An evolutionarily conserved prion-like element converts wild fungi from metabolic specialists to generalists, *Cell* 158 (5) (2014) 1072–1082.
- [230] D.M. Garcia, D. Dietrich, J. Clardy, D.F. Jarosz, A common bacterial metabolite elicits prion-based bypass of glucose repression, *Elife* 5 (2016).
- [231] P.M. Harrison, M. Gerstein, A method to assess compositional bias in biological sequences and its application to prion-like glutamine/asparagine-rich domains in eukaryotic proteomes, *Genome Biol* 4 (6) (2003) R40.
- [232] R. Guerin, C. Turcotte, A. Leroux, L.A. Rokeach, The epigenetic calnexin-independent state is induced in response to environmental changes, *FEMS Yeast Res* 9 (8) (2009) 1250–1259.
- [233] T. Sideri, Y. Yashiroda, D.A. Ellis, M. Rodriguez-Lopez, M. Yoshida, M.F. Tuite, J. Bahler, The copper transport-associated protein Ctr4 can form prion-like epigenetic determinants in *Schizosaccharomyces pombe*, *Microb Cell* 4 (1) (2017) 16–28.
- [234] R. Riek, S.J. Saube, The HET-S/s prion motif in the control of programmed cell death, *Cold Spring Harb Perspect Biol* 8 (9) (2016).
- [235] A. Daskalov, M. Paoletti, F. Ness, S.J. Saube, Genomic clustering and homology between HET-S and the NWD2 STAND protein in various fungal genomes, *PLoS One* 7 (4) (2012) e34854.
- [236] A. Daskalov, B. Habenstein, D. Martinez, A.J. Debets, R. Sabate, A. Loquet, S.J. Saube, Signal transduction by a fungal NOD-like receptor based on propagation of a prion amyloid fold, *PLoS Biol* 13 (2) (2015) e1002059.
- [237] A. Daskalov, B. Habenstein, R. Sabate, M. Berbon, D. Martinez, S. Chaignepain, B. Couлары-Salin, K. Hofmann, A. Loquet, S.J. Saube, Identification of a novel cell death-inducing domain reveals that fungal amyloid-controlled programmed cell death is related to necroptosis, *Proc. Natl. Acad. Sci. U. S. A.* 113 (10) (2016) 2720–2725.
- [238] C. Seuring, J. Greenwald, C. Wasmer, R. Wepf, S.J. Saube, B.H. Meier, R. Riek, The mechanism of toxicity in HET-S/HET-s prion incompatibility, *PLoS Biol* 10 (12) (2012) e1001451.
- [239] S.J. Garrity, V. Sivanathan, J. Dong, S. Lindquist, A. Hochschild, Conversion of a yeast prion protein to an infectious form in bacteria, *Proc. Natl. Acad. Sci. U. S. A.* 107 (23) (2010) 10596–10601.
- [240] A.H. Yuan, S.J. Garrity, E. Nako, A. Hochschild, Prion propagation can occur in a prokaryote and requires the ClpB chaperone, *Elife* 3 (2014) e02949.
- [241] I. Pallares, V. Iglesias, S. Ventura, The Rho termination factor of *Clostridium botulinum* contains a prion-like domain with a highly amyloidogenic core, *Front Microbiol* 6 (2015) 1516.
- [242] A.H. Yuan, A. Hochschild, A bacterial global regulator forms a prion, *Science* 355 (6321) (2017) 198–201.
- [243] K. Si, S. Lindquist, E.R. Kandel, A neuronal isoform of the aplysia CPEB has prion-like properties, *Cell* 115 (7) (2003) 879–891.
- [244] K. Si, Y.B. Choi, E. White-Grindley, A. Majumdar, E.R. Kandel, Aplysia CPEB can form prion-like multimers in sensory neurons that contribute to long-term facilitation, *Cell* 140 (3) (2010) 421–435.
- [245] S.U. Heinrich, S. Lindquist, Protein-only mechanism induces self-perpetuating changes in the activity of neuronal Aplysia cytoplasmic polyadenylation element binding protein (CPEB), *Proc. Natl. Acad. Sci. U. S. A.* 108 (7) (2011) 2999–3004.
- [246] A. Majumdar, W.C. Cesario, E. White-Grindley, H. Jiang, F. Ren, M.R. Khan, L. Li, E.M. Choi, K. Kannan, F. Guo, J. Unruh, B. Slaughter, K. Si, Critical role of amyloid-like oligomers of *Drosophila* Orb2 in the persistence of memory, *Cell* 148 (3) (2012) 515–529.
- [247] J.S. Stephan, L. Fioriti, N. Lamba, L. Colnaghi, K. Karl, I.L. Derkatch, E.R. Kandel, The CPEB3 protein is a functional prion that interacts with the actin cytoskeleton, *Cell Rep* 11 (11) (2015) 1772–1785.
- [248] R. Hervas, L. Li, A. Majumdar, C. Fernandez-Ramirez Mdel, J.R. Unruh, B.D. Slaughter, A. Galera-Prat, E. Santana, M. Suzuki, Y. Nagai, M. Bruix, S. Casas-Tinto, M. Menendez, D.V. Laurents, K. Si, M. Carrion-Vazquez, Molecular basis of Orb2 amyloidogenesis and blockade of memory consolidation, *PLoS Biol* 14 (1) (2016) e1002361.
- [249] K. Si, E.R. Kandel, The role of functional prion-like proteins in the persistence of memory, *Cold Spring Harb Perspect Biol* 8 (4) (2016) a021774.
- [250] F. Hou, L. Sun, H. Zheng, B. Skaug, Q.X. Jiang, Z.J. Chen, MAVS forms functional prion-like aggregates to activate and propagate antiviral innate immune response, *Cell* 146 (3) (2011) 448–461.
- [251] X. Cai, J. Chen, H. Xu, S. Liu, Q.X. Jiang, R. Halfmann, Z.J. Chen, Prion-like polymerization underlies signal transduction in antiviral immune defense and inflammasome activation, *Cell* 156 (6) (2014) 1207–1222.
- [252] N. Gilks, N. Kedersha, M. Ayodele, L. Shen, G. Stoecklin, L.M. Dember, P. Anderson, Stress granule assembly is mediated by prion-like aggregation of TIA-1, *Mol Biol Cell* 15 (12) (2004) 5383–5398.
- [253] S. Kroschwald, M.C. Munder, S. Maharana, T.M. Franzmann, D. Richter, M. Ruer, A.A. Hyman, S. Alberti, Different material states of Pub1 condensates define distinct modes of stress adaptation and recovery, *Cell Rep* 23 (11) (2018) 3327–3339.
- [254] I. Pallares, N.S. de Groot, V. Iglesias, R. Sant'Anna, A. Biosca, X. Fernandez-Busquets, S. Ventura, Discovering putative prion-like proteins in *Plasmodium falciparum*: a computational and experimental analysis, *Front Microbiol* 9 (2018) 1737.
- [255] S. Chakrabortee, C. Kayatekin, G.A. Newby, M.L. Mendillo, A. Lancaster, S. Lindquist, Luminidependens (LD) is an Arabidopsis protein with prion behavior, *Proc Natl Acad Sci U S A* 113 (21) (2016) 6065–6070.
- [256] G. Tetz, V. Tetz, Prion-like domains in eukaryotic viruses, *Sci Rep* 8 (1) (2018) 8931.
- [257] S. Chakrabortee, J.S. Byers, S. Jones, D.M. Garcia, B. Bhullar, A. Chang, R. She, L. Lee, B. Fremin, S. Lindquist, D.F. Jarosz, Intrinsically disordered proteins drive emergence and inheritance of biological traits, *Cell* 167 (2) (2016) 369–381 e12.
- [258] R. van der Lee, M. Buljan, B. Lang, R.J. Weatheritt, G.W. Daughdrill, A.K. Dunker, M. Fuxreiter, J. Gough, J. Gsponer, D.T. Jones, P.M. Kim, R.W. Kriwacki, C.J. Oldfield, R.V. Pappu, P. Tompa, V.N. Uversky, P.E. Wright, M.M. Babu, Classification of intrinsically disordered regions and proteins, *Chem Rev* 114 (13) (2014) 6589–6631.
- [259] M.M. Babu, The contribution of intrinsically disordered regions to protein function, cellular complexity, and human disease, *Biochem Soc Trans* 44 (5) (2016) 1185–1200.
- [260] T.C. Boothby, G.J. Pielak, Intrinsically disordered proteins and desiccation tolerance: elucidating functional and mechanistic underpinnings of anhydrobiosis, *Bioessays* 39 (11) (2017).
- [261] T.M. Franzmann, S. Alberti, Protein phase separation as a stress survival strategy, *Cold Spring Harb Perspect Biol* (2019).
- [262] T. Franzmann, S. Alberti, Prion-like low-complexity sequences: Key regulators of protein solubility and phase behavior, *J Biol Chem* (2018).
- [263] J. Wang, J.M. Choi, A.S. Holehouse, H.O. Lee, X. Zhang, M. Jahnel, S. Maharana, R. Lemaitre, A. Pozniakovskiy, D. Drechsel, I. Poser, R.V. Pappu, S. Alberti, A.A. Hyman, A molecular grammar governing the driving forces for phase separation of prion-like RNA binding proteins, *Cell* 174 (3) (2018) 688–699 e16.
- [264] Z. Monahan, V.H. Ryan, A.M. Janke, K.A. Burke, S.N. Rhoads, G.H. Zerze, R. O'Meally, G.L. Dignon, A.E. Conicella, W. Zheng, R.B. Best, R.N. Cole, J. Mittal, F. Shewmaker, N.L. Fawzi, Phosphorylation of the FUS low-complexity domain disrupts phase separation, aggregation, and toxicity, *EMBO J* 36 (20) (2017) 2951–2967.
- [265] S.N. Rhoads, Z.T. Monahan, D.S. Yee, F.P. Shewmaker, The role of post-translational modifications on prion-like aggregation and liquid-phase separation of FUS, *Int J Mol Sci* 19 (3) (2018).
- [266] S. Qamar, G. Wang, S.J. Randle, F.S. Ruggeri, J.A. Varela, J.Q. Lin, E.C. Phillips, A. Miyashita, D. Williams, F. Strohl, W. Meadows, R. Ferry, V.J. Dardov, G.G. Tartaglia, L.A. Farrer, G.S. Kaminski Schierle, C.F. Kaminski, C.E. Holt, P.E. Fraser, G. Schmitt-Ulms, D. Klenerman, T. Knowles, M. Vendruscolo, P. St George-Hyslop, FUS phase separation is modulated by a molecular chaperone and methylation of arginine cation- $\pi$  interactions, *Cell* 173 (3) (2018) 720–734 e15.
- [267] J.A. Riback, C.D. Katanski, J.L. Kear-Scott, E.V. Pilipenko, A.E. Rojek, T.R. Sosnick, D.A. Drummond, Stress-triggered phase separation is an adaptive, evolutionarily tuned response, *Cell* 168 (6) (2017) 1028–1040 e19.
- [268] J.B. Rayman, K.A. Karl, E.R. Kandel, TIA-1 self-multimerization, phase separation, and recruitment into stress granules are dynamically regulated by Zn(2), *Cell Rep* 22 (1) (2018) 59–71.
- [269] D.S.W. Protter, R. Parker, Principles and properties of stress granules, *Trends Cell Biol* 26 (9) (2016) 668–679.
- [270] J. Masel, C.K. Griswold, The strength of selection against the yeast prion [PSI<sup>+</sup>], *Genetics* 181 (3) (2009) 1057–1063.
- [271] I. Kronholm, S. Collins, Epigenetic mutations can both help and hinder adaptive evolution, *Mol Ecol* 25 (8) (2016) 1856–1868.
- [272] R.E. O'Dea, D.W.A. Noble, S.L. Johnson, D. Hesselton, S. Nakagawa, The role of non-genetic inheritance in evolutionary rescue: epigenetic buffering, heritable bet hedging and epigenetic traps, *Environ Epigenet* 2 (1) (2016) dvv014.
- [273] M.I. Lind, F. Spagopoulou, Evolutionary consequences of epigenetic inheritance, *Heredity* (Edinb) 121 (3) (2018) 205–209.
- [274] H.J. Beaumont, J. Gallie, C. Kost, G.C. Ferguson, P.B. Rainey, Experimental evolution of bet hedging, *Nature* 462 (7269) (2009) 90–93.
- [275] C.P.J. Maury, Self-propagating  $\beta$ -sheet polypeptide structures as prebiotic informational molecular entities: the amyloid world, *Origins Life Evol Biosphere* 39 (2008) 141–150.
- [276] C.P.J. Maury, Amyloid and the origin of life: self-replicating catalytic amyloids as prebiotic informational and prometallic entities, *Cell Mol Life Sci* (2018), <https://doi.org/10.1007/s00018-018-2797-9>.
- [277] C.M. Rufo, Y.S. Moroz, O.V. Moroz, J. Stör, T.A. Smith, X. Hu, W.F. DeGrado, I.V. Korendovych, Short peptides self-assemble to produce catalytic amyloids, *Nat Chem* 6 (2014) 303–309.
- [278] R. Riek, D.S. Eisenberg, The activities of amyloids from a structural perspective, *Nature* 539 (2016) 227–235.
- [279] S.K. Rout, M.P. Friedmann, R. Riek, J. Greenwald, A prebiotic template-directed peptide synthesis based on amyloids, *Nat Commun* 9 (1) (2018) 234–242.

## RESEARCH ARTICLE

# Dual role for fungal-specific outer kinetochore proteins during cell cycle and development in *Magnaporthe oryzae*

Hiral Shah<sup>1</sup>, Kanika Rawat<sup>1,\*;§</sup>, Harsh Ashar<sup>1,†;§</sup>, Rajesh Patkar<sup>1,¶</sup> and Johannes Manjrekar<sup>2,¶</sup>

## ABSTRACT

The outer kinetochore DASH complex (also known as the Dam1 complex) ensures proper spindle structure and chromosome segregation. While DASH complex protein requirement diverges among different yeasts, its role in filamentous fungi has not yet been investigated. We studied the dynamics and role of middle (Mis12) and outer (Dam1 and Ask1) kinetochore proteins in the filamentous fungal pathogen, *Magnaporthe oryzae*, which undergoes multiple cell cycle-linked developmental transitions. While Mis12 was constitutively present in the nucleus, Dam1 and Ask1 were recruited only during mitosis. Although Dam1 was not required for viability, loss of its function (*dam1Δ*) delayed mitotic progression, resulting in impaired conidial and hyphal development. Both Dam1 and Ask1 also localised to the hyphal tips, in the form of punctae oscillating back and forth from the growing ends, suggesting that *Magnaporthe* DASH complex proteins may play a non-canonical role in polarised growth during interphase, in addition to their function in nuclear segregation during mitosis. Impaired appressorial (infection structure) development and host penetration in the *dam1Δ* mutant suggest that fungus-specific Dam1 complex proteins could be an attractive target for a novel anti-fungal strategy.

This article has an associated First Person interview with the first author of the paper.

**KEY WORDS:** Kinetochore, Dam1 complex, DASH complex, Filamentous fungus, *Magnaporthe*, Rice blast fungus

## INTRODUCTION

Chromosome segregation is a determining step in cell division. During mitosis, the kinetochore (KT) brings about precise chromosome segregation at anaphase and anomalies in chromosome separation are associated with malfunction and disease in multicellular organisms. In unicellular yeasts, such aberrant chromosomal segregation often leads to loss of viability. The kinetochore differs in structure and composition among eukaryotes (Van Hooff et al., 2017).

The microtubule (MT)-associated DASH complex (also known as the Dam1 complex) is a fungus-specific component of the outer kinetochore. This complex has varying roles in the yeasts *Saccharomyces cerevisiae*, *Schizosaccharomyces pombe* and *Candida albicans*, where it has been studied extensively; however, very little is known about its function in filamentous fungi.

The DASH complex is made up of 10 subunits, namely Dam1, Ask1, Spc34, Hsk3, Dad1–Dad4, Duo1 and Spc19, all of which are essential for viability in *S. cerevisiae* and *C. albicans*. By contrast, none of these subunits are individually essential for survival in *S. pombe*. In *S. cerevisiae*, Dam1 is required for proper spindle assembly and elongation (Hofmann et al., 1998; Cheeseman et al., 2001a), while Ask1 is required for bipolar attachment (Janke et al., 2002). Dam1 directly interacts with MTs and other DASH members to form DASH complex oligomers (Legal et al., 2016). The yeast DASH complex members are MT plus-end-interacting proteins (TIPs). The *S. pombe dam1Δ* mutant displays chromosome segregation delay and ectopic septation (Sanchez-Perez et al., 2005). Further, *S. pombe* DASH complex mutants are sensitive to the MT poison thiabendazole, low temperature and high osmolarity – all phenotypes shared by genes involved in MT stability and dynamics (Sanchez-Perez et al., 2005; Gao et al., 2010). Dam1 was also discovered to be a multicopy suppressor of mutations in the spindle regulator Cdc13, and MT plus-end-binding protein Mal3 (Ebf1 in mammalian cells) (Sanchez-Perez et al., 2005). Further, in *S. pombe*, retrieval of unclustered kinetochores is dependent on Dam1 (Franco et al., 2007).

In *S. pombe*, Dam1 is recruited to the kinetochore in early mitosis, where it is observed as a single spot that resolves into several spots at metaphase, while Dad1 remains associated with the kinetochore throughout the cell cycle (Liu et al., 2005; Sanchez-Perez et al., 2005). The DASH complex spots co-localise with other kinetochore proteins such as Mtw1 (in *S. cerevisiae*; Mis12 in *S. pombe*) and Ndc80 (Sanchez-Perez et al., 2005). In *S. cerevisiae*, Dam1 is present at the kinetochore throughout the cell cycle, clustered as a single nucleus-associated spot during interphase, which divides into two spots closely associated with the spindle pole bodies at mitosis. Dam1 has also been observed all along the spindle in *S. cerevisiae*. Association of Ask1 with the kinetochore is dependent on Ndc10 (also known as Cbf2 in *S. cerevisiae*) and the MT spindle in budding yeast. *In vitro* MT-binding studies using *S. cerevisiae* proteins have shown 16-member oligomeric rings that encircle the MT. However, rings are not essential for MT attachment. Recently, electron cryotomography studies in *S. cerevisiae* cells have shown the presence of one or two, partial or complete rings with 17-fold symmetry associated with spindle MTs (Ng et al., 2019).

With respect to nuclear envelope continuity, fungi exhibit a spectrum of types of mitosis. While *S. cerevisiae* and *S. pombe* both undergo closed mitosis, filamentous fungi show differences; semi-open in *Aspergillus nidulans*, open in *Ustilago maydis* and semi-closed in *Magnaporthe oryzae*. Further, in *S. cerevisiae* mitosis lasts around 50 min while in *S. pombe* and many filamentous fungi it

<sup>1</sup>Bharat Chattoo Genome Research Centre, Department of Microbiology and Biotechnology Centre, The Maharaja Sayajirao University of Baroda, Vadodara 390002, Gujarat, India. <sup>2</sup>Biotechnology Programme, Department of Microbiology and Biotechnology Centre, The Maharaja Sayajirao University of Baroda, Vadodara 390002, Gujarat, India.

\*Present address: Centre for Ecological Sciences, Indian Institute of Science, Bengaluru-560012, Karnataka, India. †Present address: Stem Cell Biology Group, Advanced Centre for Treatment, Research and Education in Cancer, Tata Memorial Centre, Kharghar, Navi Mumbai 410210, Maharashtra, India.

§These authors contributed equally to this work

¶Authors for correspondence (jmanjrekar@yahoo.com; rajeshpatkar-biotech@msubaroda.ac.in)

© H.S., 0000-0002-8143-8244; K.R., 0000-0002-8309-7754; H.A., 0000-0003-2140-8542; R.P., 0000-0001-7266-2394; J.M., 0000-0001-8760-2028

is completed in less than 5 min. In addition, mitosis in filamentous fungi is often associated with distinct morphological differentiation not observed in most yeasts, setting different requirements and constraints on spindle assembly and elongation. Thus, owing to these differences, it is likely that KT–spindle structure and assembly differ in filamentous fungi. Unlike yeasts, the filamentous fungal pathogen *M. oryzae* undergoes several morphologically distinct developmental transitions during its life cycle.

During the *M. oryzae* pathogenic life cycle, the three-celled conidium germinates on the leaf surface to extend a polarised germ tube. While entry of the germinating cell nucleus into S phase is required for the swelling of the germ tube tip (switching from polarised to isotropic growth to form the incipient appressorium), entry into mitosis is necessary for the further development of the appressorium (Saunders et al., 2010a). The diploid nucleus of the germinating cell undergoes the first round of infection-related mitosis in the germ tube. Nuclear division is followed by migration, during which one daughter nucleus returns to the germinated cell in the conidium and the other travels into the appressorium. Subsequently, exit from mitosis is required for appressorium maturation and function (Saunders et al., 2010b). Interestingly, the appressorium then switches back to polarised growth to form the penetration peg that breaches the host epidermis and elaborates into the primary infection hypha (IH). This developmental transition is again dependent on the S phase checkpoint. At this point, the second round of infection-related mitosis in the mature appressorium contributes a nucleus to the IH. The IH nuclei undergo semi-closed mitosis lasting roughly 3 min (Jones et al., 2016). Thus, the crucial morphological transitions during *M. oryzae* infection are tightly coupled to different stages of the cell cycle. Secondary hyphae then develop from the primary IH and spread to the neighbouring host cells, resulting in typical disease lesions in a few days. These secondary hyphae later give rise to the aerial hyphae, some of which eventually form conidiophores bearing 3–5 sympodial conidia. A single lesion can produce a new generation of thousands of conidia that can initiate a new infection cycle.

*M. oryzae* infects rice and several other cereal crops across the world, and is a serious threat to global food security (Dean et al., 2012). Investigating the role of fungus-specific components in the development of this fungus would provide new targets for novel anti-fungal strategies. DASH complex proteins are not found in rice or other plant hosts making them potential candidates; however, within filamentous fungi, only the Duo1 subunit of *Magnaporthe* has been studied so far. The *M. oryzae* protein Duo1 plays a role in conidiation and full virulence in rice, but not much information is available regarding its function as a kinetochore protein in mitosis or its localisation during the cell cycle (Peng et al., 2011). In this study, we focused on the role of DASH complex proteins in chromosome segregation, especially during the cell cycle-regulated morphological transitions in *M. oryzae*. Using deletion mutants and GFP-tagged strains, we studied the behaviour of Dam1 and Ask1 during nuclear division, spindle dynamics and nuclear migration, and its effect on *M. oryzae* development. We show that in addition to its role in proper chromosome segregation, Dam1 – through its localisation in the hyphal tip compartment during interphase – is involved in polarised growth.

## RESULTS

### DASH complex protein Dam1 is recruited to the nucleus during mitosis

We identified the orthologue of *S. cerevisiae* and *S. pombe* Dam1 in *M. oryzae* (MGG\_00874) using BLASTP. Although the overall

protein sequence similarity was ~30–40%, the DASH complex domain of *M. oryzae* Dam1 showed significant homology (~60%) with that of yeasts. The Dam1 proteins show considerable size variation across organisms, ranging from 343 amino acids in *S. cerevisiae* to 121 in *Cryptococcus neoformans*, with the *M. oryzae* protein being 220 amino acids (Table S1). The protein size variation is mainly due to differences in the length of the C-terminal region. We further identified another member of the DASH complex in *M. oryzae*, Ask1 (MGG\_07143), which is known to directly interact with Dam1 in *S. cerevisiae*. To study the subcellular localisation and dynamics of these proteins in relation to those of the nucleus, we tagged Dam1 and Ask1, separately, with GFP in a strain expressing histone H1–mCherry (hH1–mCherry). As a marker for kinetochore position, we also studied the localisation of the middle kinetochore MIND complex protein Mis12 (MGG\_06304) in *Magnaporthe*.

In vegetative hyphae, Mis12–GFP was observed as a single distinct puncta at the periphery of the interphase nucleus (arrowhead, Fig. 1A). In contrast, the DASH complex proteins GFP–Dam1 and Ask1–GFP did not localise predominantly to the nucleus during interphase (Fig. 1A). Occasionally, non-nuclear GFP–Dam1 or Ask1–GFP punctae were seen along the hyphae (arrows, Fig. 1A). We presumed these were DASH complex proteins associated with cytoplasmic MTs. At the onset of mitosis (marked by chromosome condensation), while the Mis12–GFP de-clustered, the GFP–Dam1 punctae appeared at the nucleus and persisted there throughout the mitotic process and the subsequent nuclear migration (arrowheads, Fig. 1B). At the end of mitosis, the Mis12–GFP and GFP–Dam1 spots re-clustered into a single spot per nucleus (Fig. 1B). To determine whether DASH complex proteins had similar dynamics during the early infection process of *M. oryzae*, we studied GFP–Dam1 and Ask1–GFP localisation during appressorium formation. The Ask1–GFP and GFP–Dam1 punctae were associated with the nucleus during nuclear division and migration in the course of appressorial development (lower panels, Fig. 1C; Fig. S1). Thus, while the middle kinetochore layer protein Mis12 was constitutively associated with the *M. oryzae* kinetochore, the outer layer DASH complex proteins were recruited to the nucleus specifically during mitosis.

### Dam1 plays an important role in proper segregation of chromosomes

We monitored the dynamics of nuclei marked with hH1–mCherry and MTs or spindle marked with GFP ( $\beta$  tubulin–sGFP, Tub–GFP hereafter) during mitosis in vegetative hyphae of *M. oryzae*. Concurrently, to investigate the role of DASH complex proteins in mitosis, we generated *DAM1* deletion (*dam1* $\Delta$ ) strains in the wild-type (WT) and the strain expressing hH1–mCherry and Tub–GFP. Additionally, we deleted *ASK1* (*ask1* $\Delta$ ) in a strain expressing GFP–Dam1. At the onset of mitosis in the WT strain, prophase was marked by MT re-organisation and chromosome condensation. It was characterised by the loss of cytoplasmic MT arrays and establishment of a single tubulin focal point at the nucleus, which is probably a site for spindle MT nucleation. This was followed by the assembly of an intensely fluorescent bipolar spindle, which underwent re-orientation to align along the long axis of the hypha. Once formed, the spindle length remained largely constant until its elongation during anaphase. The chromosomes then segregated into two daughter nuclei that migrated to opposite ends (Fig. 2A). The *dam1* $\Delta$  strain showed longer spindles ( $5.37 \pm 0.16 \mu\text{m}$ ) when compared to the WT ( $3.71 \pm 0.07 \mu\text{m}$ ) (mean  $\pm$  s.e.m.) (Fig. 2B). We further determined the time for which the spindle

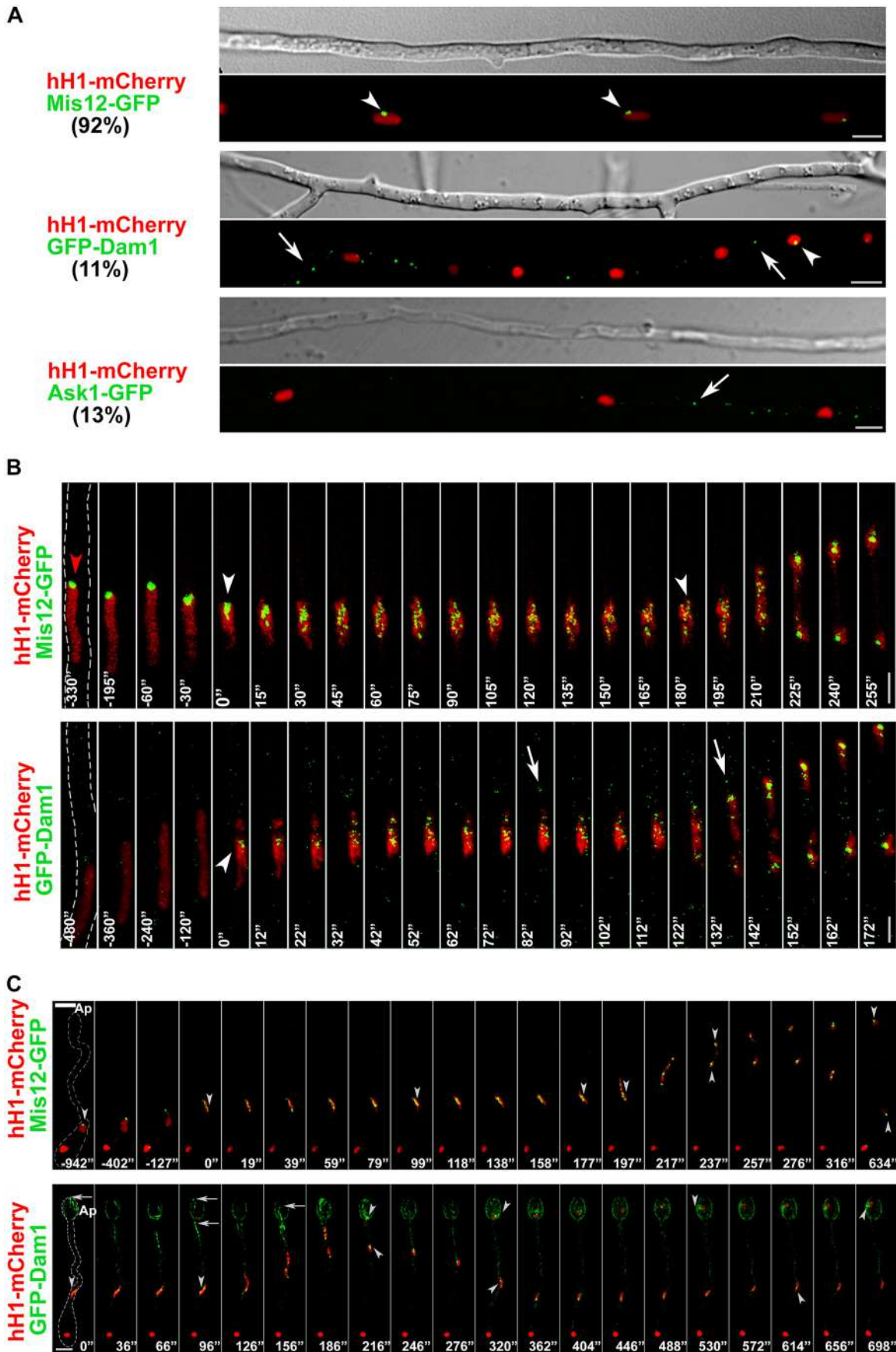


Fig. 1. See next page for legend.

**Fig. 1. Dam1 is recruited to the nucleus at the onset of mitosis.**

(A) Localisation of middle (Mis12–GFP,  $n=207$ ) and outer (GFP–Dam1,  $n=207$ ) and Ask1–GFP,  $n=227$ ) kinetochore proteins during interphase in vegetative hyphae. Numbers indicate percentage of nuclei with associated KT proteins during interphase. Arrowheads indicate nuclear-associated Mis12–GFP or GFP–Dam1. Arrows denote GFP–Dam1 or Ask1–GFP spots probably associated with cytoplasmic MTs. Scale bars: 5  $\mu\text{m}$ . (B) Time-lapse images showing dynamics of Mis12–GFP and GFP–Dam1 during mitosis in vegetative hyphae,  $n=10$ . Numbers indicate time in seconds. Fungal structures are marked with dashed outlines. Arrowheads indicate nuclear-associated Mis12–GFP or GFP–Dam1. Red arrowhead indicates Mis12–GFP associated with the nucleus prior to mitosis. Arrows denote GFP–Dam1 spots probably associated with cytoplasmic MTs along the vegetative hyphae. Scale bars: 3  $\mu\text{m}$ . (C) Localisation of middle (Mis12–GFP) and outer (GFP–Dam1) kinetochore proteins during appressorium (Ap) development,  $n=5$ . Numbers indicate time in seconds. Fungal structures are indicated as dashed outlines. Arrowheads indicate nuclear-associated Mis12–GFP or GFP–Dam1. Arrows indicate non-nuclear spots of GFP–Dam1 in appressorium. Scale bar: 5  $\mu\text{m}$ .

persisted until the onset of anaphase in the WT and *dam1* $\Delta$  strains. The *dam1* $\Delta$  mutant showed a significant delay in spindle elongation compared to the WT (Fig. 2C). While chromosome segregation was mostly initiated within 3 min in the WT ( $2.31 \pm 0.15$  min), anaphase onset in several *dam1* $\Delta$  mutant cells took more than 10 min ( $8.70 \pm 1.29$  min) (Fig. 2C,D). The time spent in metaphase or prior to anaphase varied considerably between individual cells in the *dam1* $\Delta$  strain (3–39 min) (Fig. 2D). The duration of mitosis in the germ tube during appressorium development showed a similar delay in the *dam1* $\Delta$  mutant (Fig. 2E). Importantly, in a few *dam1* $\Delta$  cells, we occasionally observed unequal segregation of nuclear material or lagging chromosomes that moved behind the rest (arrows, Fig. 2C). Thus, Dam1 function probably ensures correct spindle structure and separation of chromosomes at anaphase, allowing proper mitotic progression during both vegetative (hyphal) growth and pathogenic (appressorial) development in *M. oryzae*.

**The DASH complex is involved in polarised hyphal growth**

Next, we looked at the effects of delayed mitosis resulting from the loss of Dam1 or Ask1 function. We found that the *dam1* $\Delta$  (Fig. 3A) and *ask1* $\Delta$  (Fig. S2A) strains had a significantly reduced colony diameter, mainly due to aberrant vegetative hyphal extension and morphology. Radial hyphal growth (in terms of colony diameter) was restored in the complementation strain *dam1* $\Delta$ /*DAM1* (Fig. 3A). In *M. oryzae*, hyphae grow by apical extension and lateral branching. The branches arose close to the septa at acute angles to the growing primary hypha and at fairly regular intervals in the WT. The hyphae of the *dam1* $\Delta$  strain showed a zigzag or curved morphology, unlike the mostly straight hyphae of the WT, and showed more frequent branching (Fig. 3B,C; Fig. S3A). The *dam1* $\Delta$  mutants also showed a higher number of branches emerging at angles  $>60^\circ$  compared to WT (Fig. S3B,C). Since branching is often associated with septation, we asked whether there was a change in cell size upon loss of Dam1 function in *M. oryzae*. Indeed, Calcofluor White (CFW) staining of the *dam1* $\Delta$  hyphae showed smaller sub-apical cell compartments compared to the WT (Fig. 3D,E). A similar septation defect was seen in the vegetative hyphae of the *ask1* $\Delta$  mutant (Fig. S2D). Septation probably leads to branching by acting as a barrier to movement of growth proteins and exocytic vesicles towards the tip, leading to their accumulation.

Interestingly, we observed that GFP–Dam1 localises to the hyphal tip in the form of distinct spots during interphase (Fig. 4A). These intense spots were highly dynamic, and moved forward with the growing tips (Fig. 4B). To check whether this non-conventional localisation during interphase was specific to Dam1 or involved the

DASH complex, we also studied Ask1–GFP localisation. Indeed, Ask1–GFP also localised to the growing hyphal tips in a similar manner. Further, intriguingly, Ask1–GFP (Fig. 4C) and GFP–Dam1 (Fig. 4D) spots showed an oscillatory movement to the tip and back towards the nucleus, suggesting their movement along long tracks. Another stage of the *M. oryzae* life cycle that involves polarised growth is the extension of the germ tube during the early stage of pathogenic development. Dynamic Ask1–GFP and GFP–Dam1 spots, similar to the ones seen in the hyphal tip, were observed at the tips of the germ tubes, suggesting a role for the DASH complex in polarised growth during pathogenic development in *M. oryzae* (Fig. 4E).

We next asked whether the observed localisation and dynamics of Dam1 required the MT network. Upon treatment with the MT-destabilising compound nocodazole, the dynamic GFP–Dam1 punctae became static aggregates, randomly distributed along the germ tube cytoplasm (Fig. 4F). Thus, the MT-based oscillatory behaviour of Dam1 suggests a non-canonical function for this DASH complex protein prior to the onset of mitosis, and that the growth defects seen in the *dam1* $\Delta$  strain are a combined outcome of delayed mitosis and impaired polarised growth upon loss of Dam1 function in *Magnaporthe*.

**Conidiogenesis is marked by three distinct rounds of mitosis**

Production of three-celled conidia is a critical developmental step in the life cycle of *M. oryzae*. However, the mitotic events and cell cycle regulation involved in conidial development have not been studied in any detail to date. We first monitored mitosis during conidium development in the strain expressing hH1–mCherry and Tub–GFP. Development of the three-celled conidium takes 5–7 h, with extremely short mitosis events separated by 1.5–2.5 h interphases characterised by cell growth. It has already been shown that conidial development starts with the shift from polarised to isotropic growth, where the tip of the aerial hypha starts swelling to form an incipient conidium (conidiophore) (Deng et al., 2009). We found that the first nuclear division took place in the stalk and was followed by nuclear migration where one of the daughter nuclei travelled into the conidium cell (mitosis I, Fig. 5A) while the other remained in the stalk. This was followed by cytokinesis (septation), which probably occurred at the neck of the incipient conidium, away from the site of mitosis in the stalk. This spatial uncoupling of cytokinesis from mitosis was similar to the events observed during appressorium development, and different from what was observed in vegetative hyphal growth. The single-celled conidium then grew and elongated into an oval-shaped cell with the nucleus positioned close to the centre. This nucleus underwent division, with one of the daughter nuclei remaining positioned at the base (towards the stalk) of the conidium and the other moving to the opposite end. The process was accompanied by active re-organisation of the MT network and septation at the site of mitosis to form an intermediate two-celled conidium (asterisk, mitosis II, Fig. 5A). Subsequently, the nucleus in the second cell of the developing conidium underwent the third round of division, followed by cytokinesis to form the middle and terminal cells of the mature three-celled conidium (mitosis III, Fig. 5B).

We next studied the localisation of GFP–Dam1 during mitoses in the developing conidia. We observed that GFP–Dam1 localised to the nucleus during all three rounds of nuclear division during conidiation (Fig. 5B). It appeared in the form of multiple spots during mitosis, and then clustered into two distinct spots, one per nucleus, and persisted until nuclear migration and positioning was complete. As in the case of vegetative hyphae, GFP–Dam1 or

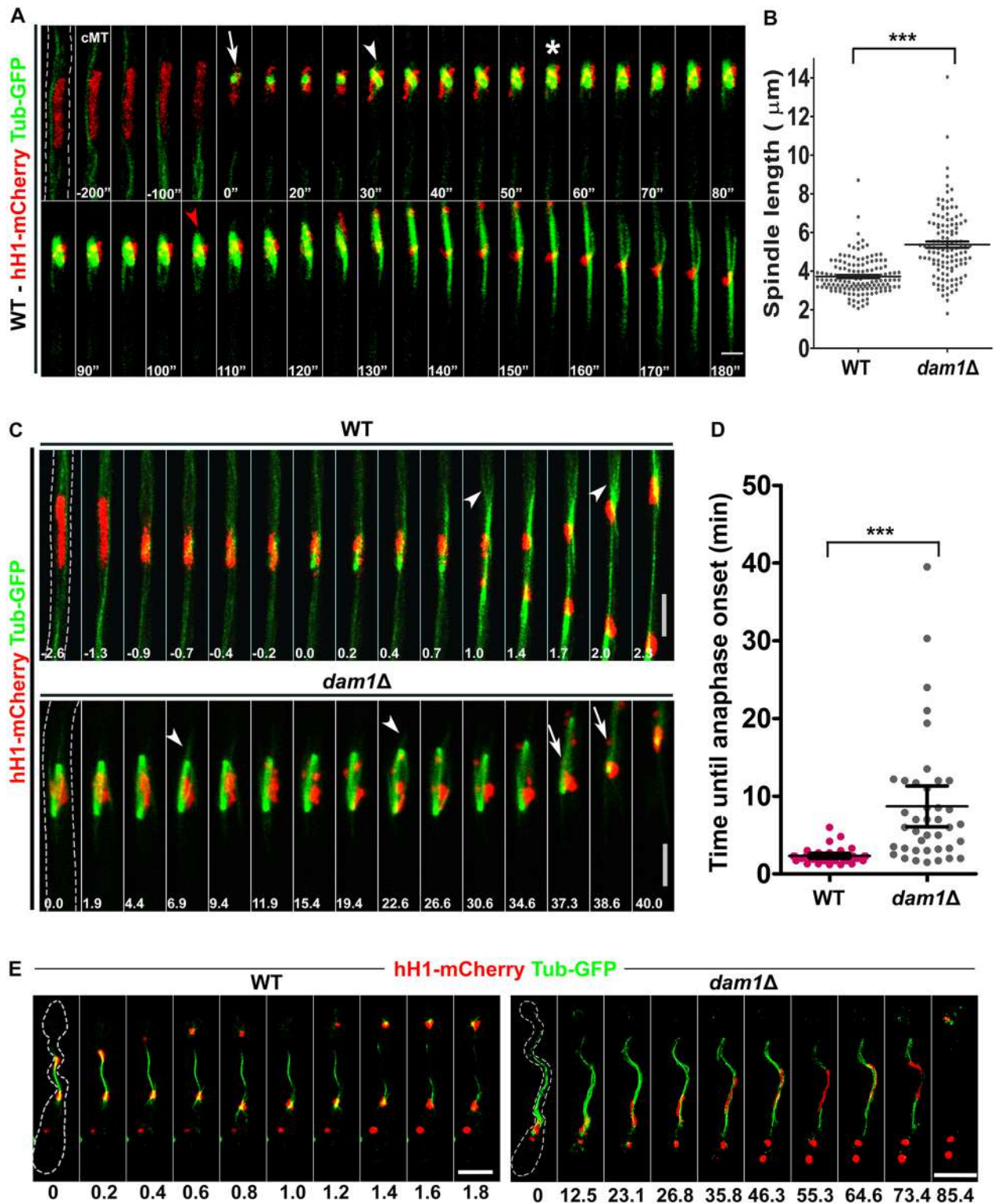


**Fig. 2. Dam1 plays an important role in proper segregation of chromosomes during nuclear division.** (A) Dynamics of the mitotic spindle in WT *M. oryzae* expressing Tub-GFP and hH1-mCherry. Numbers indicate time in minutes. Hyphal borders are indicated with dashed lines. Arrow depicts entry into mitosis, arrowhead indicates assembly of a bipolar spindle, asterisk shows spindle re-orientation, and red arrowhead indicates onset of spindle elongation. Scale bar: 3  $\mu\text{m}$ . cMT, cytoplasmic MTs. (B) Scatter plot showing mean  $\pm$  s.e.m. spindle length in the WT ( $n=143$ ) and *dam1* $\Delta$  ( $n=119$ ) strains during mitosis.  $***P<0.001$ , two-tailed *t*-test. (C) Time-lapse images of mitosis in WT and *dam1* $\Delta$  vegetative hyphae. Numbers indicate time in minutes. Hyphae are marked with dashed outlines. Arrowheads indicate astral MTs and arrows show lagging chromosomes. Scale bars: 5  $\mu\text{m}$ . (D) Scatter plot showing mean  $\pm$  s.e.m. time until spindle elongation in anaphase in WT and *dam1* $\Delta$  strains during mitosis in vegetative hyphae.  $***P<0.001$ , two-tailed *t*-test,  $n=40$ . (E) Time-lapse images of mitosis during appressorium development in the WT and *dam1* $\Delta$  strain. Numbers indicate time in minutes. Fungal structures are marked with dashed outlines. Scale bars: 10  $\mu\text{m}$ .

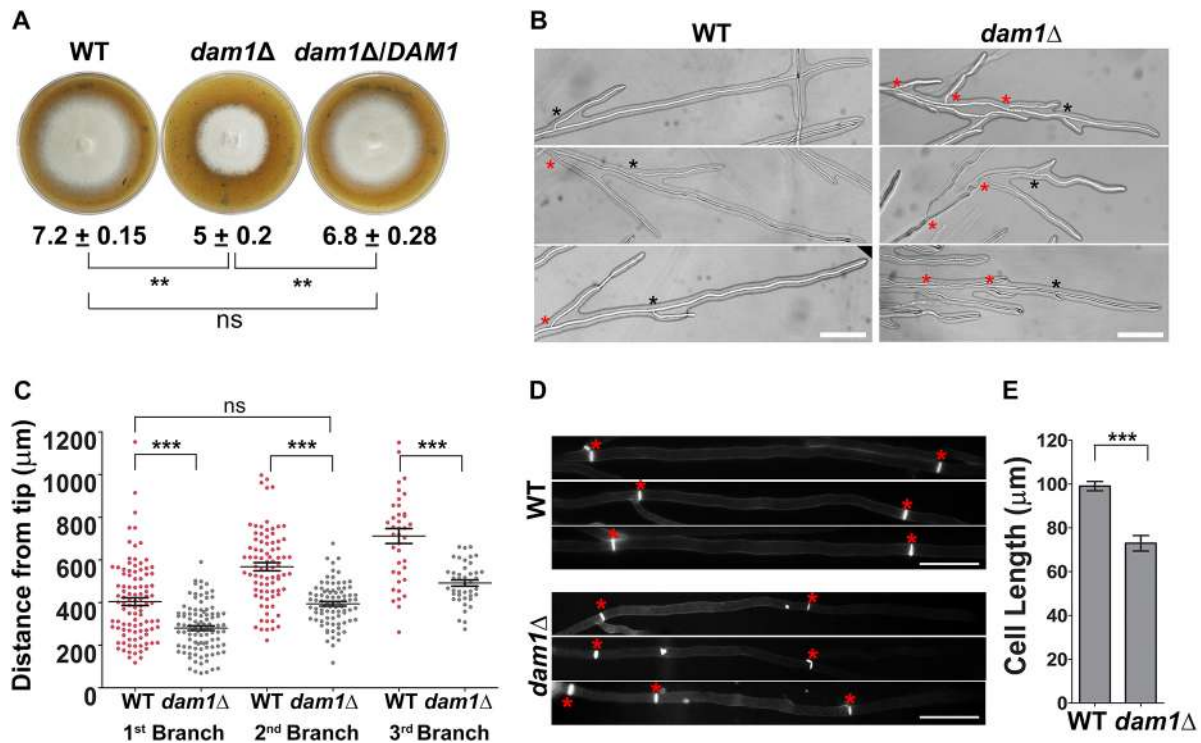


**Fig. 3. The DASH complex is involved in polarised hyphal growth.** (A) Vegetative growth of WT, *dam1Δ* and *dam1Δ/DAM1* strains at 10 dpi on prune agar. Numbers indicate mean±s.e.m. colony diameter in centimetres from three independent experiments with  $n=3$  each.  $**P<0.05$ ; ns, not significantly different; two-tailed *t*-test. (B) Difference in the branching pattern of vegetative hyphae in the WT and *dam1Δ* strain. Black asterisks indicates first branch from the tip. Red asterisks indicate all subsequent branches. Scale bars: 100  $\mu\text{m}$ . (C) Scatter plot showing mean±s.e.m. distance of first ( $n=100$ ), second ( $n=80$ ) and third branch ( $n=40$ ) from the apical tip in the WT and *dam1Δ* vegetative hyphae from three independent experiments.  $***P<0.001$ ; ns, not significantly different, two-tailed *t*-test. (D) Sub-apical cell compartment length in WT and *dam1Δ* vegetative hyphae stained with Calcofluor White (CFW). Red asterisks indicate septa (cell boundaries). Scale bars: 20  $\mu\text{m}$ . (E) Bar chart showing mean±s.e.m. length of sub-apical cell compartments in WT and *dam1Δ* vegetative hyphae from three independent experiments.  $***P<0.0001$ , two-tailed *t*-test,  $n=200$ .

*Ask1*-GFP did not associate with the nucleus during the intermittent interphases. Occasionally, a cytoplasmic spot was seen during the initial conidiophore development prior to the first round of mitosis. Thus, Dam1 function plays a key role in three sequential and essential rounds of mitosis to form a complete three-celled asexual conidium.

#### Dam1 function is crucial for proper conidiation

In addition to reduced radial vegetative growth, the *dam1Δ* strain showed flat and white colonies, in contrast to the fluffy, grey growth of the WT, suggesting defects in the development of aerial hyphae that give rise to conidia. To assess the role of Dam1 protein during asexual conidium development, we studied the growth and morphology of the aerial hyphae and conidiophores in the *dam1Δ* strain. Most of the conidiophores of the *dam1Δ* strain bore only 1–3 conidia as compared to the sympodial cluster of 3–5 conidia observed in the WT (Fig. 6A,B) after 24 h of photo-induction. The total number of conidia in the *dam1Δ* strain was reduced to 10% of the WT, and the mutant conidia were smaller ( $14.61\pm 0.12\ \mu\text{m}$ ) in length than those in the WT ( $23.05\pm 0.47\ \mu\text{m}$ ) (mean±s.e.m. from three independent experiments with  $n=100$  conidia). In addition, the *dam1Δ* mutant showed aberrant morphology compared to the WT when stained with CFW. In contrast to the three-celled pyriform conidia seen in the WT, *dam1Δ* mostly produced one- or two-celled oval conidia (Fig. 6C,D). The WT conidium morphology and cell number were restored in the complementation strain *dam1Δ/DAM1*, expressing the full-length Dam1 protein (Fig. 6D; Fig. S4D).

The *ask1Δ* mutant displayed similar defects in the total conidium number and morphology (Fig. S2B,C). The WT three-celled conidia showed distinct cell boundaries with one nucleus per cell and a prominent MT network, especially along the septa, probably arising from septal microtubule organising centres (MTOCs). We further found that ~50% of the *dam1Δ* conidia had aberrant nuclear and collapsed microtubular structures when compared to the WT (Fig. 6E,F). We infer that Dam1 function is required to ensure precise and orderly mitotic progression for proper conidial development and morphology in *M. oryzae*.

#### Dam1 function is required for proper pathogenic development and virulence

We studied infection-related (appressorial) development in the *dam1Δ* strain, to assess the role of Dam1 in pathogenesis of *M. oryzae*. In *in vitro* assays, the majority of the *dam1Δ* conidia failed to germinate (Fig. 7A). While 81% of the WT conidia formed appressoria, only 15% of the *dam1Δ* mutant conidia formed the infection structure (Fig. 7A,B). A few mutant conidia developed aberrant germ tubes and/or appressoria (Fig. 7A,C), when compared to the WT or the *dam1Δ/DAM1* complementation strain, which showed a single, short, non-septate germ tube giving rise to a mature and functional appressorium (Fig. S4E). While 83% of the WT appressoria could penetrate and colonise the rice leaf sheath tissue 40 h post inoculation, only 28% of the *dam1Δ* cells could do so (Fig. 7D,E). Next, we examined the virulence of the WT and *dam1Δ* mutant strains on susceptible CO-39 seedlings using a standard whole-plant infection assay. While the WT strain developed typical

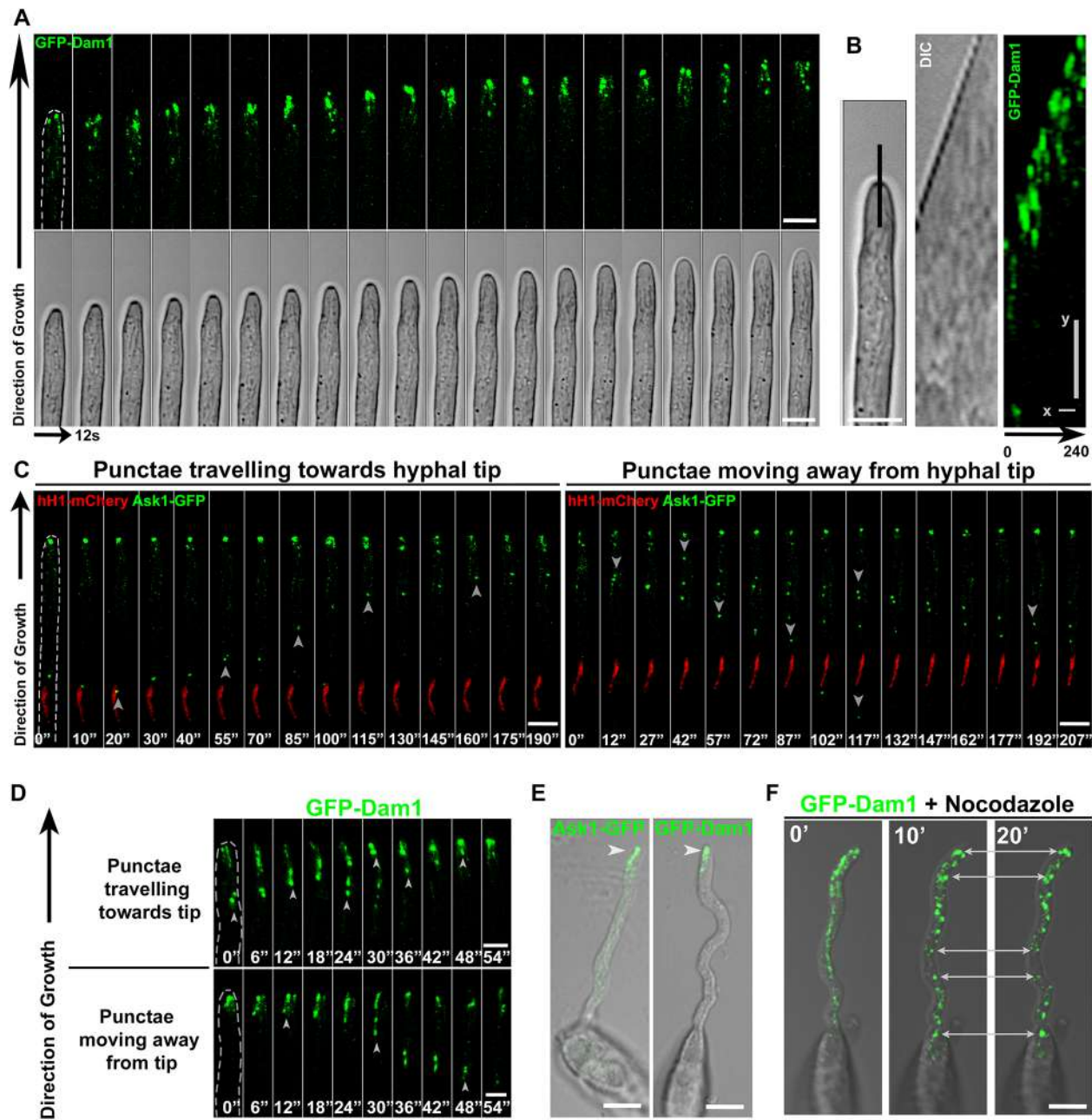


**Fig. 4. DASH complex proteins localise to the hyphal tip during interphase.** (A) Localisation of GFP–Dam1 at the hyphal tip during vegetative growth,  $n=30$ . Hyphal borders are shown with dashed lines. Scale bars: 5  $\mu\text{m}$ . (B) Kymographs of time-lapse images of GFP–Dam1 shown in A. Kymographs are plotted along the black line marked on the hyphal tip in the left-hand panel for 240 s. Scale bars:  $x=48$  s,  $y=1.5$   $\mu\text{m}$ . (C) Oscillation of Ask1–GFP from vegetative hyphal tip during interphase,  $n=20$ . Numbers indicate time in seconds. Hypha is outlined with dashed lines. Arrowheads mark the Ask1–GFP punctae moving towards or away from the tip. Scale bars: 5  $\mu\text{m}$ . (D) Back-and-forth movement of GFP–Dam1 towards vegetative hyphal tip,  $n=10$ . Numbers indicate time in seconds. Hyphae are outlined with dashed lines. Arrowheads mark the GFP–Dam1 punctae moving towards or away from the tip. Scale bars: 3  $\mu\text{m}$ . (E) Ask1–GFP and GFP–Dam1 localise in the form of dynamic punctae to the germ tube tip during polarised growth under pathogenic development on a hydrophobic surface,  $n=25$ . Arrowheads mark Ask1–GFP or GFP–Dam1 at the germ tube tip. Scale bars: 10  $\mu\text{m}$ . (F) Effect of nocodazole treatment on GFP–Dam1 localisation,  $n=20$ . Arrows mark the static large aggregates of Ask–GFP or GFP–Dam1 all along the germ tube post-nocodazole treatment. Arrows mark the static large aggregates of GFP–Dam1 all along the germ tube post-nocodazole treatment. Scale bar: 5  $\mu\text{m}$ .

disease lesions 5 days post-inoculation (dpi), the mutant showed fewer and smaller spots and lesions (Fig. 7F). Thus, our results show that *Magnaporthe* Dam1 is involved in differentiation of the infection structure and plays an important role in host invasion.

Taken together, our results highlight the importance of the dynamics of outer kinetochore proteins in proper chromosome segregation and polarised growth, crucial for asexual and pathogenic development in *M. oryzae*.

## DISCUSSION

A key difference between fungal and metazoan kinetochores is the DASH complex that connects the inner kinetochore to the spindle MTs in fungi. The heterodecameric Dam1 complex is essential for survival in budding yeasts but not in fission yeast. A recent review suggests that in the filamentous fungus *Neurospora crassa*, not all Dam1 complex members may be essential (Freitag, 2017), indicating structural and functional differences in the outer

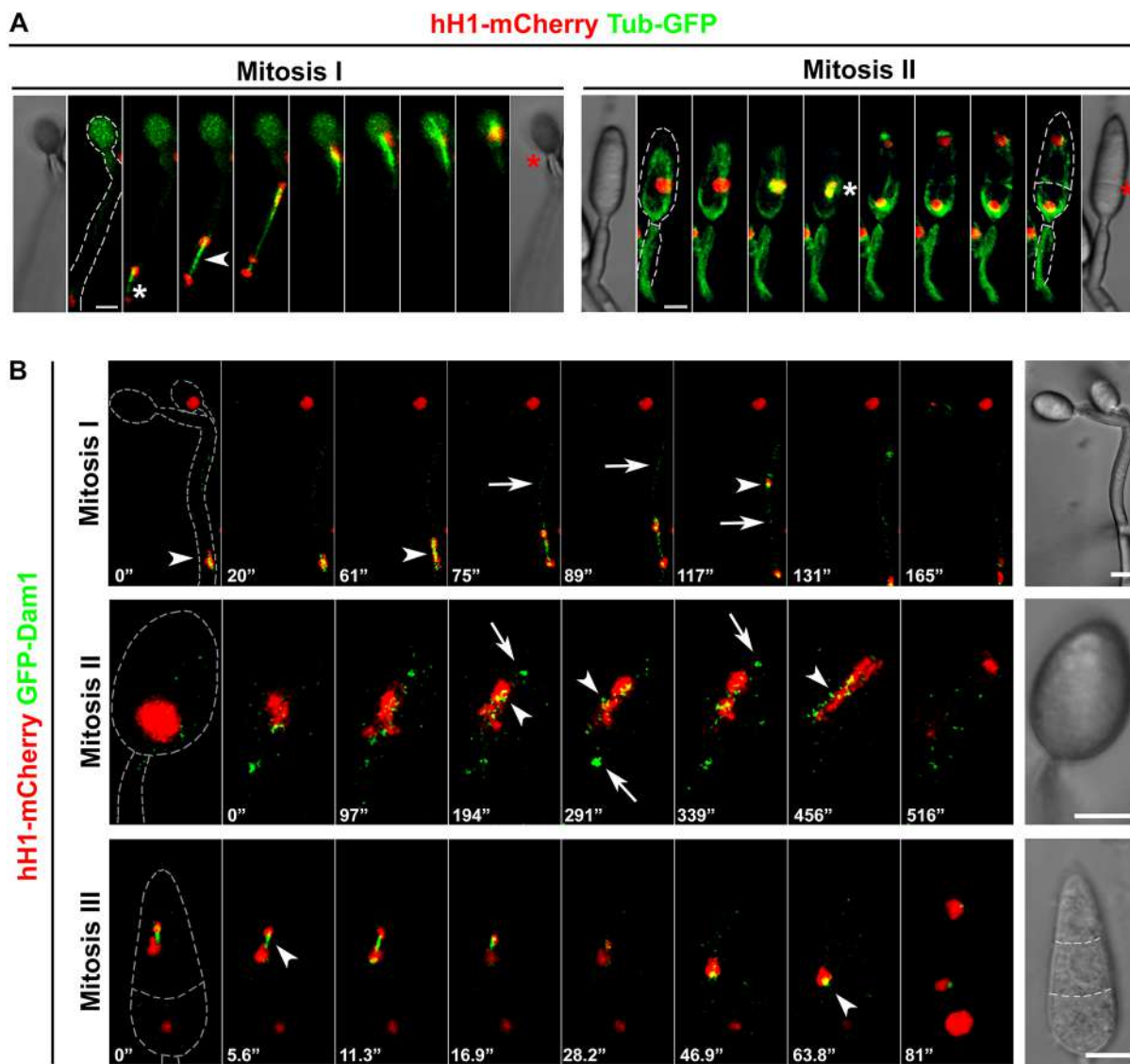


**Fig. 5. Conidium development is marked by three distinct rounds of mitosis.** (A) Dynamics of Tub-GFP-marked MTs or spindle, and hH1-mCherry-marked nuclear division during mitosis in the developing conidium,  $n=3$ . Mitosis I is observed in the stalk of the incipient conidium. Arrowhead marks the spindle, white asterisks indicate the site of mitosis, red asterisks denote the site of cytokinesis. Scale bars: 5  $\mu$ m. (B) Localisation of GFP-Dam1 during three successive rounds of mitosis in the developing conidium,  $n=3$ . Numbers indicate time in seconds. Fungal structures are shown with dashed grey outlines. Arrowheads depict nuclear-associated GFP-Dam1, arrows indicate additional non-nuclear GFP-Dam1 spots. Scale bars: 5  $\mu$ m.

kinetochore of filamentous fungi compared to that of yeasts. In budding yeasts, whether the DASH complex (also known as the Dam1 complex) is required for viability is dependent on the number of MTs attached to the kinetochore (Burrack et al., 2011; Thakur and Sanyal, 2011). However, the relationship between viability, the DASH complex and the number of MTs is not clear in filamentous fungi, where single kinetochore-MT attachment studies are currently lacking. Here, we show that the key members of the DASH complex, Dam1 and Ask1, like the previously studied *M. oryzae* Duo1 homolog, MoDuo1 (MGG\_02484) (Peng et al., 2011), are not individually essential in *M. oryzae*, suggesting that more than one MT probably binds to a kinetochore in the blast fungus, or that other unknown protein interactions stabilise this kinetochore-MT attachment. The fact that we were able to generate deletion mutants of *DAM1* and *ASK1* implies that Dam1 and Ask1 are not essential for viability in *Magnaporthe*. However, although there is no complete cell cycle arrest and loss of viability in all cells within the culture, it is likely that only a fraction of cells progressed

further. This was not obvious during multicellular hyphal growth but became particularly evident during conidiation and appressorium formation. Furthermore, taking into account the greatly reduced capacity of the *dam1* $\Delta$  strain to form conidia and subsequently appressoria that are able to establish infection in hosts, the net capacity for successfully infecting host plants is two orders of magnitude lower than that of the WT. A feature that differs within yeasts and from metazoan kinetochores is the timing of assembly and interdependence of middle and outer kinetochore proteins. The basidiomycete *Cryptococcus neoformans* shows ordered assembly where DASH complex proteins Dad1 and Dad2 are assembled after middle kinetochore protein Mtw1 and released before it (Kozubowski et al., 2013). In *S. cerevisiae* the Dam1 complex is associated with the kinetochore throughout the cell cycle, while all *S. pombe* DASH proteins except for Dad1 are recruited to the kinetochore during mitosis. In *M. oryzae* we found that, while Dam1 and Ask1 localised to the nucleus only at the onset of mitosis and persisted there through chromosome segregation and nuclear

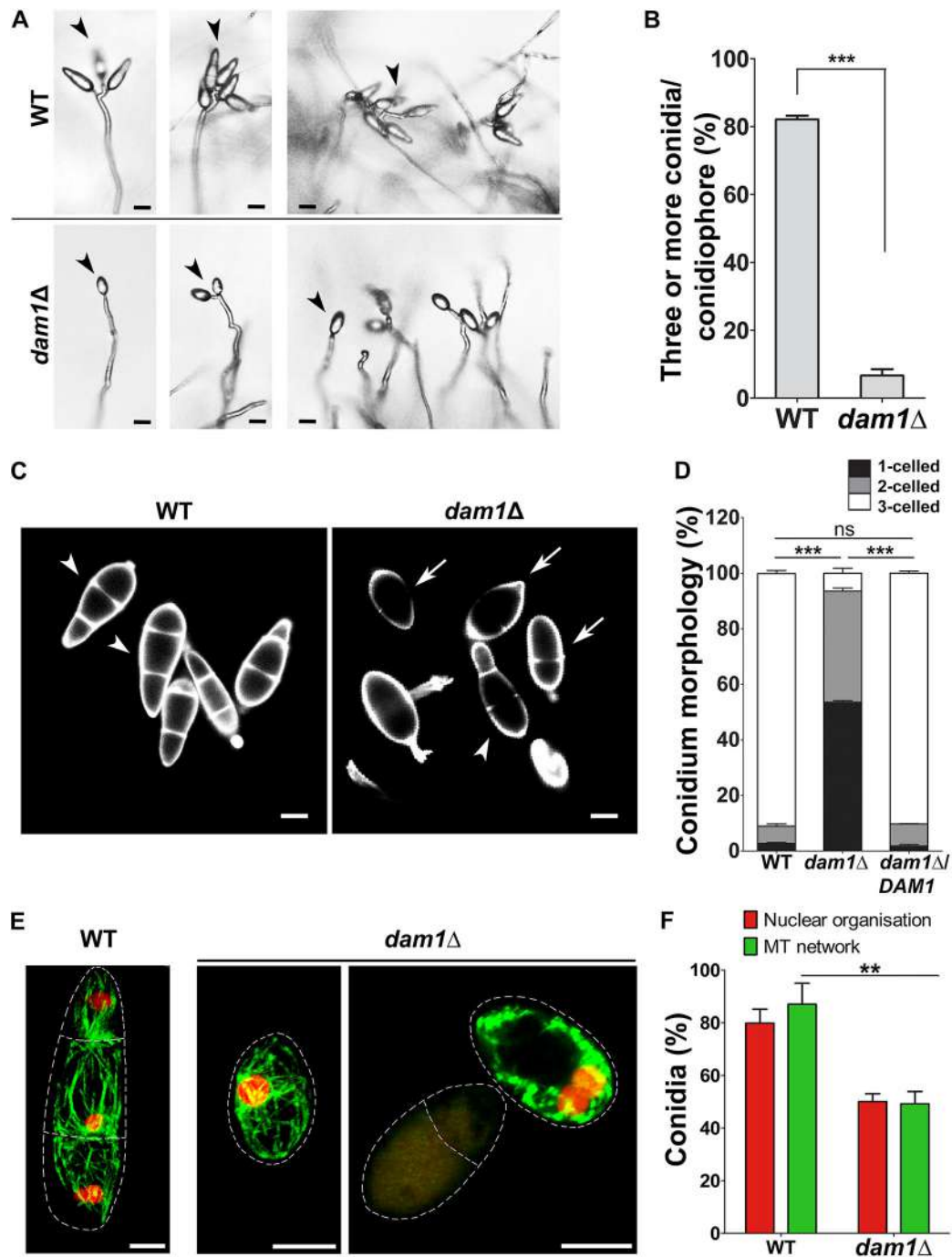


**Fig. 6. Loss of Dam1 function significantly alters conidiation.** (A) Difference in the conidiophore morphology and number of sympodial conidia (arrowheads) between the *dam1Δ* mutant and WT. Scale bars: 10  $\mu$ m. (B) Bar chart showing mean $\pm$ s.e.m. frequency of conidiophores bearing three or more conidia in the *dam1Δ* compared to the WT strain. \*\*\* $P$ <0.0001, two-tailed  $t$ -test,  $n$ =300. (C) Morphology of *dam1Δ* and WT conidia stained with CFW. Arrowheads depict 3-celled conidia and arrows indicate 1- or 2-celled conidia. Scale bars: 5  $\mu$ m. (D) Bar chart showing mean $\pm$ s.e.m. frequency of conidia with different cell numbers (1, 2 or 3) in the WT, *dam1Δ* or *dam1Δ/DAM1* strain. \*\*\* $P$ <0.0001; ns, not significantly different; two-tailed  $t$ -test,  $n$ =300. (E) Nuclear organisation and MT network in the WT or *dam1Δ* conidia expressing hH1-mCherry and Tub-GFP. Conidia borders are shown with dashed lines. Scale bars: 5  $\mu$ m. (F) Bar chart showing mean $\pm$ s.e.m. number of conidia with intact (normal) nuclear and MT organisation in the WT and *dam1Δ* mutant strains from three independent experiments. \*\* $P$ <0.05, two-tailed  $t$ -test,  $n$ =100.

migration, the MIND complex protein Mis12 appeared to be a constitutive member of the kinetochore, associating with the nucleus throughout the cell cycle at all stages of development. *S. pombe* spindle kinesins Klp5/Klp 6, and MT plus-end polymerase Mtc1 (also known as Alp14) also display metaphase-specific kinetochore localisation (Nakaseko et al., 2001; Garcia

et al., 2002). Localisation of *M. oryzae* Mis12 in the form of a single spot per nucleus before mitosis indicates kinetochore clustering during interphase. These single spots of Mis12 resolved into multiple foci during mitosis, highlighting the dynamic behaviour of the kinetochore marker protein. These kinetochore dynamics in *M. oryzae* are similar to those reported in *S. pombe*, where

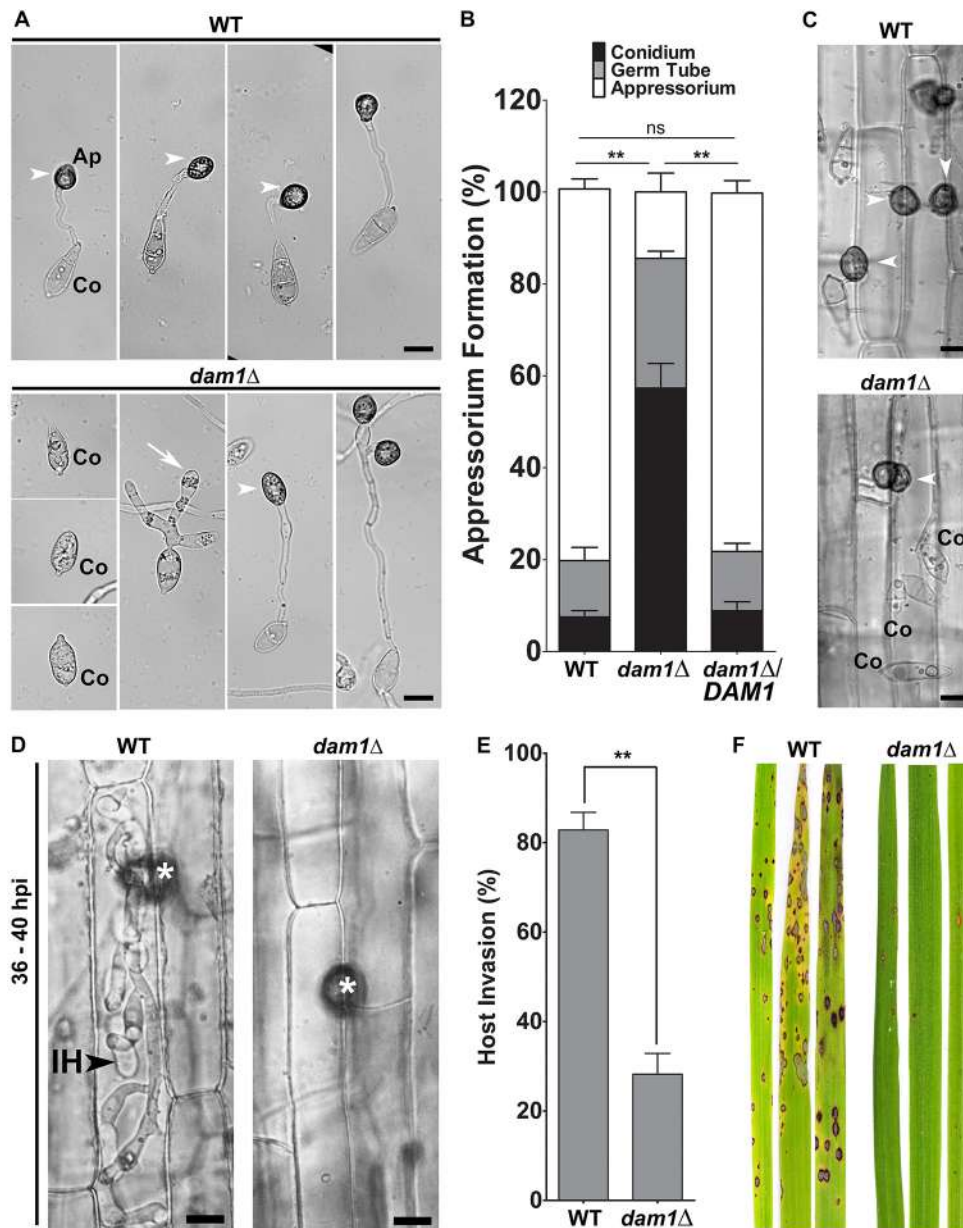


**Fig. 7. Dam1 function is required for proper pathogenic development and virulence.** Micrographs of pathogenic (appressorium) development on a hydrophobic surface (glass coverslips) at 24 hpi. Arrowheads depict appressoria, arrow marks an aberrant germ tube. Scale bars: 5  $\mu$ m. Co, conidia. (B) Bar chart showing mean $\pm$ s.e.m. frequency of appressorium formation at 24 hpi on a hydrophobic surface in the *dam1Δ* and *dam1Δ/DAM1* strain compared to the WT from three independent experiments. \*\* $P$ <0.05; ns, not significantly different; two-tailed  $t$ -test;  $n$ =150 conidia. (C) Micrographs showing appressorium formation on rice leaf sheaths at 24 hpi. Arrowheads depict appressoria. Scale bars: 10  $\mu$ m. Co, conidia. (D) Micrographs showing invasion of rice leaf sheaths inoculated with the WT or *dam1Δ* conidia and observed at 36–40 hpi. Arrowhead shows invasive hyphae (IH), asterisks indicate appressoria. Scale bars: 5  $\mu$ m. (E) Bar chart showing mean $\pm$ s.e.m. frequency of invasive hyphae at 36–40 hpi on rice leaf sheaths in the *dam1Δ* compared to the WT strain from three independent experiments. \*\* $P$ <0.05, two-tailed  $t$ -test,  $n$ =100 appressoria. (F) Whole-plant infection assay using susceptible rice variety CO-39 and  $10^5$  ml $^{-1}$  conidia of WT or *dam1Δ* strains. Leaves from inoculated plants were photographed 5 dpi. Data represent results from two independent experiments.

kinetochore de-clustering is seen in metaphase (Goshima et al., 1999). In contrast, de-clustering of kinetochore during mitosis is not visibly evident in the budding yeasts (Roy et al., 2011). Budding yeast MIND (Mis12) and NDC80 complexes show great plasticity, with many copies of proteins being added to the ‘G1 configuration’ of the kinetochore to form the ‘anaphase configuration’ kinetochore (Dhatchinamoorthy et al., 2017). Such a plastic kinetochore structure probably maintains more stable attachment during chromosome separation, while allowing correction of mis-attached chromosomes during metaphase. Whether this is the case in *M. oryzae* and can be extended to other outer kinetochore complexes in filamentous fungi will require further study. We observed that the size of the *M. oryzae* Mis12 cluster associated with the nucleus before mitosis was larger than the one observed after division (Fig. 1B), probably due to a duplicate set of kinetochores associated with each nucleus, or assembly of additional Mis12 complexes prior to mitosis. Overall, the cell cycle dynamics of DASH complex proteins and Mis12 in *M. oryzae* are more similar to those in *S. pombe* than in budding yeast or humans.

The Dam1 protein in fission yeast is involved in timely anaphase onset and lack of Dam1 leads to lagging chromosomes and sister chromatids occasionally segregating to the same pole (Sanchez-Perez et al., 2005). Along with the spindle kinesin Klp5, Dam1 is involved in chromosome biorientation. In budding yeast, the Dam1 complex proteins play an important role in maintaining spindle structure and integrity, with *DAM1* mutants showing diverse spindle defects ranging from elongated, hyperelongated, extremely short to even broken spindles (Hofmann et al., 1998; Janke et al., 2002; Cheeseman et al., 2001a,b). Similarly, mutations in budding yeast motor proteins, such as Kar3 (kinesin-14 family protein, Klp2 in *S. pombe*), Cin8, Kip1 (kinesin-5 family protein) and Kip3 (kinesin-8 family protein, Klp5/Klp6 in *S. pombe*) involved in MT stability, also display changes in spindle length (Straight et al., 1998; Zeng et al., 1999). Further, Dam1 plays a role in correct kinetochore attachments and bi-orientation in budding as well as fission yeast, lack of which leads to activation of the spindle assembly checkpoint (SAC), delaying the onset of anaphase (Janke et al., 2002; Sanchez-Perez et al., 2005; Buttrick et al., 2012). Dam1 phosphorylation by

Aurora B kinase (also known as Ipl1) in budding yeast and Polo kinase Plo1 in *S. pombe* allows dissociation of incorrect kinetochore–MT attachments. This kinetochore is then free to be captured by a new MT until bi-orientation of sister chromatids is sensed by tension between the two spindle poles. The *M. oryzae* Dam1 sequence also contains the Polo consensus site DTSFVD (amino acids 150–155). In *Magnaporthe*, loss of Dam1 function led to delayed anaphase onset, occasionally ending in unequal nuclear division. Such a delay was probably due to SAC activation resulting from the lack of chromosome bi-orientation in the *dam1Δ* strain of *M. oryzae*. These events of improper nuclear division and cell cycle arrest account for the reduced hyphal growth and loss of viability of conidia. Further, the *dam1Δ* mutant showed altered spindle length with some instances of collapsed spindles. Thus, *Magnaporthe* Dam1 probably plays a key role in both maintenance of spindle structure as well as bi-orientation of chromosomes.

In *M. oryzae*, differentiation of the germ tube into appressorium and the conidiophore into conidium are morphologically similar processes, requiring a switch-over from polarised to isotropic growth associated with asymmetric cell division. While the role of cell cycle checkpoints in appressorium development has been revealed, similar studies into the development of the aerial conidiophore structure have so far proved technically more challenging in *Magnaporthe*. Two different types of cytokinesis, depending on the site of septation, have been described in *M. oryzae*: 1) septation at the site of mitosis in growing vegetative hyphae, and 2) septation spatially uncoupled from mitosis during appressorium formation, where the mitosis occurs in the germ tube while the septum is placed at the neck of the newly formed appressorium (Saunders et al., 2010a,b). We observed both these types of cytokinesis during conidiation. The first septation occurred at the neck of the incipient conidium, away from the site of nuclear division occurring in the conidiophore stalk, similar to the one seen during appressorium development. The deposition of the two subsequent septa in the developing conidium occurred at the site of mitosis as seen in the case of vegetative hyphae. We further showed that nuclear association of Dam1 plays a crucial role in these three rounds of mitosis during conidial development. Conidial development was significantly impaired in the *dam1Δ* mutant with altered septation, most likely resulting from aberrant microtubular dynamics and/or unequal nuclear division. Another DASH complex protein in *M. oryzae*, MoDuo1, has previously been implicated in proper conidiation; however, its precise role in the process remains elusive (Peng et al., 2011). Defective septation, similar to that observed in this study during conidial development in the *dam1Δ* mutant, has also been found in the absence of function of the *M. oryzae* Tea4 homolog, MoTea4 (MGG\_06439), which is mainly involved in cell polarity (Patkar et al., 2010), suggesting a non-canonical role for *M. oryzae* Dam1 and Ask1 during polarised growth. Indeed, loss of Dam1 function led to defects in hyphal morphology and patterning, with the *dam1Δ* mutant exhibiting excessive branching, irregular hyphal diameter and altered cell size. In *M. oryzae*, loss of Spa2, a component of the spindle pole body, also results in excessive branching (Li et al., 2014). Interestingly, independent of the role of Dam1 as a kinetochore protein, dynamic punctae of varying sizes were seen at the hyphal tip under polarised growth during interphase. In *Aspergillus nidulans* hyphal tips, most MTs are arranged with their plus-ends directed towards the tip (Konzack et al., 2005), and kinesin KipA moves along MTs towards the hyphal tip and accumulates at the MT plus-ends. Loss of KipA affects polarity maintenance through changes in the MT–cortex interaction during hyphal growth (Konzack et al., 2005). Taking

into account that DASH complex proteins are plus-end MT-binding proteins in yeasts, the tip signal in *M. oryzae* is probably from Dam1 associated with the MTs at the plus ends, driving hyphal extension. The localisation pattern of Dam1 and Ask1 in *M. oryzae* is also similar to the kinesin KipA and MT polymerase AlpA in *Aspergillus nidulans*. The Dam1 or Ask1 punctae at the tips were highly dynamic, oscillating between the hyphal end and nucleus, suggesting a possible role in scanning until the nucleus is ready to undergo division. In *S. pombe*, Dam1 punctae move along the cytoplasmic MTs, occasionally merging into larger oligomers, or crossing over to neighbouring MT tracks (Gao et al., 2010). *S. pombe* Dam1 also alters the rate of depolymerisation of spindle as well as cytoplasmic MTs. It is likely that in *M. oryzae*, Dam1 is associated with the cytoplasmic MTs during interphase. Indeed, the dynamic Dam1 punctae largely disappeared during interphase upon treatment with the MT-destabilising agent nocodazole. It will also be interesting to see whether Dam1 and Ask1 proteins migrate as a complex to the tip or travel individually to assemble into a complex at the hyphal tip. We have seen that the dynamic localisation pattern of GFP–Dam1 at the hyphal tip is altered in the *ask1Δ* mutant, with relatively fewer and sluggish punctae, suggesting that the movement of Dam1 may depend on Ask1. A dual-tagged strain will provide a better understanding of the association of Dam1 and Ask1 during back-and-forth movement and tip localisation. It would be worth studying interactions, if any, between *M. oryzae* Dam1 and other MT-associated proteins and motor proteins, and their role in regulating the MT network, especially during interphase.

Penetration peg formation during host invasion involves polarised growth and one round of mitosis in the appressorium, to contribute a nucleus to the emerging invasive hyphae (Jenkinson et al., 2017). Although defects were observed in host penetration and colonisation in the *dam1Δ* mutant, it is not clear whether the defects resulted only from aberrant mitotic progression, or a combined effect of impaired penetration peg polarity and development. Determining Dam1 localisation patterns during this early host penetration stage will allow a better understanding of its role in pathogenicity. Here, we propose that in addition to its role in chromosome segregation, Dam1 plays a significant role in polarised growth. To study whether such a non-canonical function is conserved in other filamentous fungi, further characterisation of respective kinetochores would be required. Since model fungi such as *N. crassa* and *Aspergillus*, unlike *Magnaporthe*, are multi-nucleate, detailed studies on DASH complex proteins in these fungi might shed light on some interesting and novel mechanisms underlying KT dynamics.

In conclusion, the DASH complex proteins Dam1 and Ask1, though not essential for viability, have important roles to play in cell cycle progression during fungal development. Given its importance in pathogenesis and specificity to fungi, Dam1 makes a potential target for the development of novel antifungal strategies.

## MATERIALS AND METHODS

### Fungal strains, culture and transformation

*Magnaporthe oryzae* B157 strain (MTCC accession number 12236), belonging to the international race IC9 was previously isolated in our laboratory from infected rice leaves (Kachroo et al., 1994). The fungus was grown and maintained on prune agar (PA). Liquid complete medium (CM) was used to grow biomass for DNA isolation etc. Vegetative growth of the deletion mutants was measured in terms of colony diameter on PA. For conidiation, cultures were grown on PA for 3 days in the dark and then kept under constant light until harvesting. For harvesting conidia, the protocol followed was as described (Patkar et al., 2012). Quantification of conidia was done using a haemocytometer. For gene tagging and deletion, plasmids

were transformed into *M. oryzae* by protoplast transformation or *Agrobacterium tumefaciens* mediated transformation (ATMT) (Mullins et al., 2001). The transformants were selected on yeast-extract glucose agar (YEGA) with 300  $\mu\text{g ml}^{-1}$  Zeocin or 300  $\mu\text{g ml}^{-1}$  hygromycin or basal medium with 100  $\mu\text{g ml}^{-1}$  chlorimuron ethyl or 50  $\mu\text{g ml}^{-1}$  glufosinate ammonium. The selected transformants were screened by locus-specific PCR and microscopy. Single site-specific integration was confirmed by Southern hybridisation.

### Plasmid construction for tagging of genes

Ask1 and Dam1 were tagged with GFP using marker fusion tagging by targeted replacement of the native locus with the GFP-tagged Dam1 construct (Lai et al., 2010). For N-terminal tagging of Dam1 (Fig. S5A,B), the *DAMI* promoter was amplified using primers Dam1-Pro-F/Dam1-Pro-R from B157 genomic DNA and cloned into p718 at EcoRI/SpeI restriction sites to obtain p718-Dam1Pro. The 1052bp *DAMI* ORF and 3'-UTR fragment was amplified using primers Dam1-ORF-F/Dam1-3UTR-R and cloned in p718-Dam1Pro in frame with *BAR-GFP* to give p718-GFPDam1. For C-terminal tagging of Ask1 (Fig. S5C,D), the 3'-end of ASK1 ORF was amplified using primers Ask1tagcdsF-ER1/Ask1tagcdsR-SpeI from B157 genomic DNA and cloned into p718 at EcoRI/SpeI restriction sites to obtain p718-Ask1Up. The ASK1 3'-UTR was amplified using primers Ask1stop3UTRF-HpaI/Ask13UTRR-KpnI and cloned into p718-Ask1Up to give p718-Ask1GFP. For C-terminal tagging of Mis12 (Fig. S5E,F), the Mis123'-UTR was amplified using primers Mis123UTRR-PstI/Mis123UTRR-H3 from B157 gDNA and cloned into pFGL347 at the PstI/HindIII restriction sites to obtain pFGL347-Mis123'UTR. The last 1 kb of the MIS12 ORF was amplified using primers Mis12orf1kbF-E1/Mis12orfR. This fragment was fused with the GFP ORF (amplified using VenusF-Mis12OH/VenusR-KpnI) by PCR. The fusion product was cloned into pFGL347-Mis123'UTR at EcoRI/KpnI restriction sites to give pFGL347-Mis12GFP. All primers used in the study are listed in Table S2. All clones were confirmed by restriction enzyme digestion. PCR was carried out using XT-5 polymerase (Genei Laboratories Pvt. Ltd.) and restriction digestion was done using Fast Digest enzymes (Thermo Fisher Scientific). To mark the *M. oryzae* nucleus, hH1-mCherry-tagged B157 strain was generated using the sulfonyleurea resistance reconstitution (SRR) vector pFGL959-hH1mCherry, a modified version of the pFGL959 plasmid (Yang and Naqvi, 2014) (Fig. S6A). The plasmid carrying a hH1-mCherry expression cassette (*cgl1* promoter: hH1-mCherry) was moved into wild-type *M. oryzae* strain B157 by *Agrobacterium tumefaciens*-mediated transformation (ATMT). The tagged strain was confirmed by PCR, fluorescence microscopy and Southern hybridisation (Fig. S6C). The  $\beta$ -tubulin:sGFP tagging construct was derived from pMF309 (obtained from Michael Freitag, Ohio State University, Columbus, USA) (Fig. S6B). The  $\beta$ -tubulin:sGFP cassette with the *cgl1* promoter was digested from pMF309 with HpaI/SalI and ligated to KS-HPT at HpaI/XhoI restriction sites to generate KS-HPT- $\beta$ -tubulin:sGFP. This KS-HPT- $\beta$ -tubulin:sGFP vector was moved into the hH1:mCherry-tagged B157 strain by protoplast transformation and transformants were selected on hygromycin and confirmed by PCR and Southern hybridisation (Fig. S6D,E). The Ask1-GFP, GFP-Dam1 and Mis12-GFP constructs were transformed into the H1-mCherry tagged strain by ATMT. Targeted replacement of native locus and single copy integration was confirmed by Southern hybridisation (Fig. S5B,D,F). All tagged strains were assessed for their virulence using drop inoculation of conidial suspension on detached barley leaves and were found to be pathogenic (Fig. S5G, Fig. S6F). Details of all strains generated in the study are provided in Table S3. All molecular biology procedures were followed as described previously (Sambrook et al., 1989).

### Construction of plasmids for deletion of genes

The *DAMI* deletion cassette (Fig. S7A) was generated by double-joint PCR. The 972 bp upstream and 530 bp downstream flanking regions were amplified from B157 genomic DNA and fused with the 1.24 kb Zeocin resistance cassette by double-joint PCR. This construct was cloned into an ATMT-based plasmid. For ASK1 deletion (Fig. S7D), the 1080 bp 5'- and 889 bp 3'-flanking regions of the *ASK1* ORF were cloned upstream and downstream of the hygromycin resistance cassette. The deletion

transformants were screened by locus-specific PCR (Fig. S7B,E). Correct deletion of the *DAMI* and *ASK1* ORF was confirmed by Southern hybridisation (Fig. S7C,F).

### Complementation of *dam1* $\Delta$ strain

The N-terminal GFP-Dam1 construct developed earlier for localisation studies was used for complementation of the *dam1* $\Delta$  mutant (Fig. S4A). The construct was transferred into the *dam1* $\Delta$  strain by ATMT. Bialaphos-resistant transformants were screened by PCR (Fig. S4B). Southern hybridisation was used to confirm integration of a single copy of the *DAMI* construct (Fig. S4C). Transformants with a single *DAMI* copy were selected for phenotypic characterisation. The complementation transformants were analysed for hyphal growth (colony diameter), conidiation and appressorial development.

### Microscopy

Bright-field and epifluorescence microscopy were performed on an Olympus BX51 (Olympus) or Nikon Eclipse80i (Nikon) microscope with 40 $\times$  extra-long working distance (ELWD) or 100 $\times$ /1.40 oil immersion objectives using the appropriate filter set. Sub-cellular localisation was studied by laser scanning microscopy on a LSM 700 inverted confocal microscope (Carl Zeiss Inc.). The objectives used were either an EC Plan-Neofluar 40 $\times$ /1.30 or a Plan-Apochromat 63 $\times$ /1.40 oil immersion lens. GFP and mCherry were imaged with the 488 nm and 555 nm laser, respectively. For live-cell imaging, fungal cultures were inoculated on glass-bottom Petri dishes. To study protein dynamics, fungal structures were captured as a time series of z-stack images. The images were acquired through ZEN 2010 software with the Zeiss AxioCam MR camera and processed and analysed using ImageJ (<https://imagej.nih.gov/ij/download.html>) and Adobe Photoshop CS6 software. 3  $\mu\text{g ml}^{-1}$  Calcofluor White (Whitener 28, Sigma-Aldrich) was used to stain the cell wall and septa of conidia and vegetative hyphae. To study hyphal morphology, methods described for studying *Neurospora* hyphal growth and branching (Riquelme et al., 1998; Riquelme and Bartnicki-Garcia, 2004) were adapted for *M. oryzae*. The cultures were grown in 35 mm plates with a 3–5 mm-thick basal medium until the colony grew to a size of 2 cm. The growing edge of the colony was then observed using a 40 $\times$  or 100 $\times$  objective. The hyphal lengths and angles were measured using ImageJ. For fluorescence microscopy, the cultures were inoculated in plates with 2 mm thick medium. To examine the effects of the MT inhibitor nocodazole on GFP-Dam1 dynamics in germ tubes, germinating conidia were treated with 0.5  $\mu\text{M}$  nocodazole for 15 min and images were taken every 5 min.

### Pathogenicity assays

For appressorial assays, *M. oryzae* conidia were harvested from 10-day-old prune agar cultures. Aliquots (20  $\mu\text{l}$ ) of conidial suspensions ( $5 \times 10^4$  conidia  $\text{ml}^{-1}$  in sterile water with streptomycin) were applied on hydrophobic glass coverslips and incubated under humid conditions at room temperature. Conidial germination and appressorium formation were examined 24 h post-inoculation (hpi). The percentage of appressoria formed was calculated. For penetration assays, rice leaf sheath inoculation assays were performed with conidial suspensions as described (Kankanala et al., 2007) and assessed 36–40 hpi. Penetration pegs and infection hyphae were detected by microscopy. For detached leaf assay, 8–12-day-old barley leaves were inoculated with three drops of 10  $\mu\text{l}$  each of conidial suspension in 0.2% gelatine. The disease outcome was recorded 5 days post-inoculation. For *in-planta* infection assays, susceptible rice CO-39 seedlings were sprayed with  $10^5 \text{ ml}^{-1}$  of wild-type *M. oryzae* and mutant conidia in 0.2% gelatine and disease symptoms were recorded 5 dpi.

### Acknowledgements

We thank the Bharat Chattoo Genome Research Centre Group for useful discussions and suggestions on the manuscript. We thank Kaustuv Sanyal (Jawaharlal Nehru Centre for Advanced Scientific Research, India) for valuable and constructive discussions. We thank Naweel Naqvi (Temasek Lifesciences Laboratory, Singapore) for sharing backbone vectors used to develop gene deletion and tagging constructs in the study. We are grateful to Michael Freitag

(Ohio State University, USA) for sharing the pMF309 plasmid used to develop the tubulin-GFP tagging construct. We acknowledge late Prof. Bharat B. Chattoo who encouraged us to take up this work and made it possible with the infrastructure and facilities he established at the Bharat Chattoo Genome Research Centre.

#### Competing interests

The authors declare no competing or financial interests.

#### Author contributions

Conceptualization: H.S., R.P., J.M.; Methodology: H.S., R.P., J.M.; Validation: H.S., K.R., H.A.; Formal analysis: H.S.; Investigation: H.S., K.R., H.A.; Resources: R.P., J.M.; Writing - original draft: H.S.; Writing - review & editing: H.S., R.P., J.M.; Visualization: H.S., R.P., J.M.; Supervision: R.P., J.M.; Project administration: R.P., J.M.; Funding acquisition: H.S., R.P., J.M.

#### Funding

The work was supported by a Shyama Prasad Mukherjee Fellowship from the Council of Scientific and Industrial Research, India to H.S. [SPM-09/114(0129)/2012-EMR-I] and Ramalingaswami Re-Entry Fellowship from the Department of Biotechnology, Ministry of Science and Technology to R.P. (BT/RLF/Re-entry/32/2014).

#### Supplementary information

Supplementary information available online at <http://jcs.biologists.org/lookup/doi/10.1242/jcs.224147.supplemental>

#### References

- Burrack, L. S., Applen, S. E. and Berman, J. (2011). The requirement for the Dam1 complex is dependent upon the number of kinetochore proteins and microtubules. *Curr. Biol.* **21**, 889-896. doi:10.1016/j.cub.2011.04.002
- Buttrick, G. J., Lancaster, T. C., Meadows, J. C. and Millar, J. B. A. (2012). Plo1 phosphorylates Dam1 to promote chromosome bi-orientation in fission yeast. *J. Cell Sci.* **125**, 1645-1651. doi:10.1242/jcs.096826
- Cheeseman, I. M., Brew, C., Wolyniak, M., Desai, A., Anderson, S., Muster, N., Yates, J. R., Huffaker, T. C., Drubin, D. G. and Barnes, G. (2001a). Implication of a novel multiprotein Dam1p complex in outer kinetochore function. *J. Cell Biol.* **155**, 1137-1146. doi:10.1083/jcb.200109063
- Cheeseman, I. M., Enquist-Newman, M., Muller-Reichert, T., Drubin, D. G. and Barnes, G. (2001b). Mitotic spindle integrity and kinetochore function are linked by the Duo1p/Dam1p complex. *J. Cell Biol.* **152**, 197-212. doi:10.1083/jcb.152.1.197
- Dhatchinamoorthy, K., Shivaraju, M., Lange, J. J., Rubinstein, B., Unruh, J. R., Slaughter, B. D. and Gerton, J. L. (2017). Structural plasticity of the living kinetochore. *J. Cell Biol.* **126**, 3551-3570. doi:10.1083/jcb.201703152
- Dean, R., Van Kan, J. A., Pretorius, Z. A., Hammond-Kosack, K. E., Di Pietro, A., Spanu, P. D., Rudd, J. J., Dickman, M., Kahmann, R., Ellis, J. et al. (2012). The top 10 fungal pathogens in molecular plant pathology. *Mol. Plant Pathol.* **13**, 414-430. doi:10.1111/j.1364-3703.2011.00783.x
- Deng, Y. Z., Ramos-Pamplona, M. and Naqvi, N. I. (2009). Autophagy-assisted glycogen catabolism regulates asexual differentiation in *Magnaporthe oryzae*. *Autophagy* **5**, 33-43. doi:10.4161/aut.5.1.7175
- Franco, A., Meadows, J. C. and Millar, J. B. A. (2007). The Dam1/DASH complex is required for the retrieval of unclustered kinetochores in fission yeast. *J. Cell Sci.* **120**, 3345-3351. doi:10.1242/jcs.013698
- Freitag, M. (2017). The kinetochore interaction network (KIN) of ascomycetes. *Mycologia* **108**, 485-505. doi:10.3852/15-182
- Gao, Q., Courtheoux, T., Gachet, Y., Tournier, S. and He, X. (2010). A non-ring-like form of the Dam1 complex modulates microtubule dynamics in fission yeast. *Proc. Natl. Acad. Sci. USA* **107**, 13330-13335. doi:10.1073/pnas.1004887107
- Garcia, M. A., Koonruga, N. and Toda, T. (2002). Two kinesin-like Kin I family proteins in fission yeast regulate the establishment of metaphase and the onset of anaphase A. *Curr. Biol.* **12**, 610-621. doi:10.1016/S0960-9822(02)00761-3
- Goshima, G., Saitoh, S. and Yanagida, M. (1999). Proper metaphase spindle length is determined by centromere proteins Mis12 and Mis6 required for faithful chromosome segregation. *Genes Dev.* **13**, 1664-1677. doi:10.1101/gad.13.13.1664
- Hofmann, C., Cheeseman, I. M., Goode, B. L., McDonald, K. L., Barnes, G. and Drubin, D. G. (1998). *Saccharomyces cerevisiae* Duo1p and Dam1p, novel proteins involved in mitotic spindle function. *J. Cell Biol.* **143**, 1029-1040. doi:10.1083/jcb.143.4.1029
- Janke, C., Ortiz, J., Tanaka, T. U., Lechner, J. and Schiebel, E. (2002). Four new subunits of the Dam1-Duo1 complex reveal novel functions in sister kinetochore biorientation. *EMBO J.* **21**, 181-193. doi:10.1093/emboj/21.1.181
- Jenkinson, C. B., Jones, K., Zhu, J., Dorhmi, S. and Khang, C. H. (2017). The appressorium of the rice blast fungus *Magnaporthe oryzae* remains mitotically active during post-penetration hyphal growth. *Fungal Genet. Biol.* **98**, 35-38. doi:10.1016/j.fgb.2016.11.006
- Jones, K., Jenkinson, C. B., Araújo, M. B., Zhu, J., Kim, R. Y., Kim, D. W. and Khang, C. H. (2016). Mitotic stopwatch for the blast fungus *Magnaporthe oryzae* during invasion of rice cells. *Fungal Genet. Biol.* **93**, 46-49. doi:10.1016/j.fgb.2016.06.002
- Kachroo, P., Leong, S. A. and Chattoo, B. B. (1994). Pot2, an inverted repeat transposon from the rice blast fungus *Magnaporthe grisea*. *Mol. Gen. Genet.* **245**, 339-348. doi:10.1007/BF00290114
- Kankanala, P., Czymmek, K. and Valent, B. (2007). Roles for rice membrane dynamics and plasmodesmata during biotrophic invasion by the blast fungus. *Plant Cell* **19**, 706-724. doi:10.1105/tpc.106.046300
- Konzack, S., Rischitor, P. E., Enke, C. and Reinhard, F. (2005). The role of the kinesin motor KipA in microtubule organization and polarized growth of *Aspergillus nidulans*. *Mol. Biol. Cell* **16**, 497-506. doi:10.1091/mbc.e04-02-0083
- Kozubowski, L., Yadav, V., Chatterjee, G., Sridhar, S., Yamaguchi, M., Kawamoto, S., Bose, I., Heitman, J. and Sanyal, K. (2013). Ordered kinetochore assembly in the human-pathogenic basidiomycetous yeast *Cryptococcus neoformans*. *MBio* **4**, e00614-e00613. doi:10.1128/mBio.00614-13
- Lai, J., Ng, S. K., Liu, F. F., Patkar, R. N., Lu, Y., Chan, J. R., Suresh, A., Naqvi, N. and Jedd, G. (2010). Marker fusion tagging, a new method for production of chromosomally encoded fusion proteins. *Eukaryot. Cell* **9**, 827-830. doi:10.1128/EC.00386-09
- Legal, T., Zou, J., Sochaj, A., Rappsilber, J. and Welburn, J. P. I. (2016). Molecular architecture of the Dam1 complex-microtubule interaction. *Open Biol.* **6**, 1-9. doi:10.1098/rsob.150237
- Li, C., Yang, J., Zhou, W., Chen, X.-L., Huang, J.-G., Cheng, Z.-H., Zhao, W.-S., Zhang, Y. and Peng, Y.-L. (2014). A spindle pole antigen gene MoSPA2 is important for polar cell growth of vegetative hyphae and conidia, but is dispensable for pathogenicity in *Magnaporthe oryzae*. *Curr. Genet.* **60**, 255-263. doi:10.1007/s00294-014-0431-4
- Liu, X., McLeod, I., Anderson, S., Yates, J. R. and He, X. (2005). Molecular analysis of kinetochore architecture in fission yeast. *EMBO J.* **24**, 2919-2930. doi:10.1038/sj.emboj.7600762
- Mullins, E. D., Chen, X., Romaine, P., Raina, R., Geiser, D. M. and Kang, S. (2001). *Agrobacterium*-mediated transformation of *Fusarium oxysporum*: an efficient tool for insertional mutagenesis and gene transfer. *Phytopathology* **91**, 173-180. doi:10.1094/PHYTO.2001.91.2.173
- Nakaseko, Y., Goshima, G., Morishita, J. and Yanagida, M. (2001). M phase specific kinetochore proteins in fission yeast: microtubule-associating Dis1 and Mtc1 display rapid separation and segregation during anaphase. *Curr. Biol.* **11**, 537-549. doi:10.1016/S0960-9822(01)00155-5
- Ng, C. T., Deng, L., Chen, C., Lim, H. H., Shi, J., Surana, U. and Gan, L. (2019). Electron cryotomography analysis of Dam1C/DASH at the kinetochore-spindle interface *in situ*. *J. Cell Biol.* **218**, 455-473. doi:10.1083/jcb.201809088
- Patkar, R. N., Suresh, A. and Naqvi, N. I. (2010). MoTea4-mediated polarized growth is essential for proper asexual development and pathogenesis in *Magnaporthe oryzae*. *Eukaryot. Cell* **9**, 1029-1038. doi:10.1128/EC.00292-09
- Patkar, R. N., Ramos-Pamplona, M., Gupta, A. P., Fan, Y. and Naqvi, N. I. (2012). Mitochondrial beta-oxidation regulates organellar integrity and is necessary for conidial germination and invasive growth in *Magnaporthe oryzae*. *Mol. Microbiol.* **86**, 1345-1363. doi:10.1111/mmi.12060
- Peng, H., Feng, Y., Zhu, X., Lan, X., Tang, M., Wang, J., Dong, H. and Chen, B. (2011). MoDUO1, a Duo1-like gene, is required for full virulence of the rice blast fungus *Magnaporthe oryzae*. *Curr. Genet.* **57**, 409-420. doi:10.1007/s00294-011-0355-1
- Riquelme, M. and Bartnicki-Garcia, S. (2004). Key differences between lateral and apical branching in hyphae of *Neurospora crassa*. *Fung. Genet. Biol.* **41**, 842-851. doi:10.1016/j.fgb.2004.04.006
- Riquelme, M., Reynaga-Peña, C. G., Gierz, G. and Bartnicki-Garcia, S. (1998). What determines growth direction in fungal hyphae? *Fung. Genet. Biol.* **24**, 101-109. doi:10.1006/fgbi.1998.1074
- Roy, B., Burrack, L. S., Lone, M. A., Berman, J. and Sanyal, K. (2011). CaMtw1, a member of the evolutionarily conserved Mis12 kinetochore protein family, is required for efficient inner kinetochore assembly in the pathogenic yeast *Candida albicans*. *Mol. Microbiol.* **80**, 14-32. doi:10.1111/j.1365-2958.2011.07558.x
- Sambrook, J., Fritsch, E. F. and Maniatis, T. (1989). *Molecular Cloning: A Laboratory Manual*, 2nd edn. New York: Cold Spring Harbour Laboratory Press.
- Sanchez-Perez, I., Renwick, S. J., Crawley, K., Karig, I., Buck, V., Meadows, J. C., Franco-Sanchez, A., Fleig, U., Toda, T. and Millar, J. B. (2005). The DASH complex and Klp5/Klp6 kinesin coordinate bipolar chromosome attachment in fission yeast. *EMBO J.* **24**, 2931-2943. doi:10.1038/sj.emboj.7600761
- Saunders, D. G. O., Aves, S. J. and Talbot, N. J. (2010a). Cell cycle-mediated regulation of plant infection by the rice blast fungus. *Plant Cell* **22**, 497-507. doi:10.1105/tpc.109.072447
- Saunders, D. G. O., Dagdas, Y. F. and Talbot, N. J. (2010b). Spatial uncoupling of mitosis and cytokinesis during appressorium-mediated plant infection by the rice blast fungus *Magnaporthe oryzae*. *Plant Cell* **22**, 2417-2428. doi:10.1105/tpc.110.074492
- Straight, A. F., Sedat, J. W. and Murray, A. W. (1998). Time-lapse microscopy reveals unique roles for kinesins during anaphase in budding yeast. *J. Cell Biol.* **143**, 687-694. doi:10.1083/jcb.143.3.687

- Thakur, J. and Sanyal, K.** (2011). The essentiality of the fungus-specific Dam1 complex is correlated with a one-kinetochore-one-microtubule interaction present throughout the cell cycle, independent of the nature of a centromere. *Eukaryot. Cell* **10**, 1295-1305. doi:10.1128/EC.05093-11
- Van Hooff, J. J. E., Tromer, E., van Wijk, L. M., Snel, B. and Kops, G. J. P. L.** (2017). Evolutionary dynamics of the kinetochore network as revealed by comparative genomics. *EMBO Rep.* **18**, 1559-1571. doi:10.15252/embr.201744102
- Yang, F. and Naqvi, N. I.** (2014). Sulfonyleurea resistance reconstitution as a novel strategy for ILV2-specific integration in *Magnaporthe oryzae*. *Fungal Genet. Biol.* **68**, 71-76. doi:10.1016/j.fgb.2014.04.005
- Zeng, X., Kahana, J. A., Silver, P. A., Morpew, M. K., McIntosh, J. R., Fitch, I. T., Carbon, J. and Saunders, W. S.** (1999). Slk19p is a centromere protein that functions to stabilize mitotic spindles. *J. Cell Biol.* **146**, 415-425. doi:10.1083/jcb.146.2.415

## FIRST PERSON

# First person – Hiral Shah

First Person is a series of interviews with the first authors of a selection of papers published in Journal of Cell Science, helping early-career researchers promote themselves alongside their papers. Hiral Shah is first author on 'Dual role for fungal-specific outer kinetochore proteins during cell cycle and development in *Magnaporthe oryzae*', published in JCS. Hiral is a PhD student in the lab of Johannes Manjrekar and the late Prof. Bharat Chattoo at Bharat Chattoo Genome Research Centre, Gujarat, India, investigating the role of microtubule-associated proteins in fungal development.

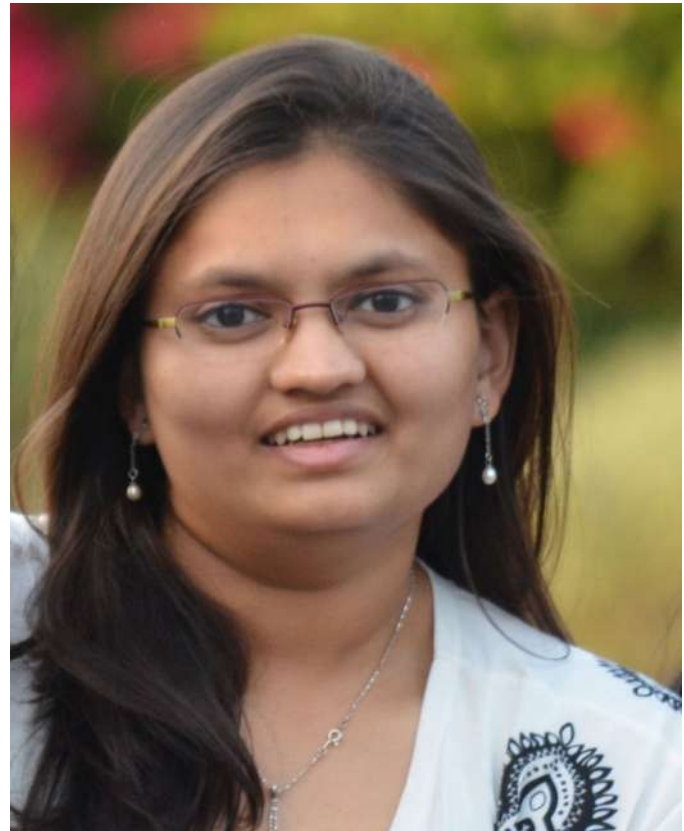
### How would you explain the main findings of your paper in lay terms?

The rice blast fungus *Magnaporthe oryzae* infects rice and many other cereal crops, destroying a vast number of plants that would be sufficient to feed millions of people around the world. In order to enter plant tissue and multiply within it, the fungus goes through many different stages during its life cycle. An important step that controls fungal development is mitosis, which involves the equal segregation of chromosomes (DNA) between the two newly formed daughter cells. During segregation, chromosomes are pulled to the two opposite poles by microtubules through the multi-protein motor called the kinetochore. A component unique to the fungal kinetochore is the Dam1 protein complex. We studied Dam1 and its associated protein Ask1 during fungal development. We found that apart from mitosis, Dam1 plays an additional role in the extension of fungal hyphae, and without Dam1 the fungus forms a more branched network with irregular cell size. In addition, without Dam1, the DNA is not segregated properly and the fungus does not grow, produce spores or infect leaves as it normally would. Spores are generally spindle-shaped with three cells. In the absence of Dam1, the number of spores is reduced and most spores have only one or two cells. Since Dam1 is so important for the fungus and is not found in rice plants, if we find a way to block it, we could potentially control rice blast disease without adversely affecting the crop.

### Were there any specific challenges associated with this project? If so, how did you overcome them?

The biggest challenge was to carry out live-cell imaging of all the different fungal structures with meaningful spatio-temporal resolution to capture mitosis that lasts just about 3 min, while avoiding any phototoxicity. The rice blast fungus in its life cycle forms three-celled conidia, a polarised germ tube, a dome-shaped appressorium (infection structure), bulging invasive hyphae and a branching vegetative hyphal network, each one having different growth trajectories. For instance, while the germ tube and appressoria are substratum, attached conidia are borne on aerial hyphae. The challenges were overcome through the optimization of growth conditions, incubation times, laser intensity and imaging

Hiral Shah's contact details: Bharat Chattoo Genome Research Centre, Department of Microbiology and Biotechnology Centre, The Maharaja Sayajirao University of Baroda, Vadodara 390002, Gujarat, India.  
E-mail: hiralshah1586@gmail.com



Hiral Shah

speed and frequency. Great support came from my co-authors, Kanika Rawat and Harsh Asher, who were always up for the challenge and enthusiastic to try new things.

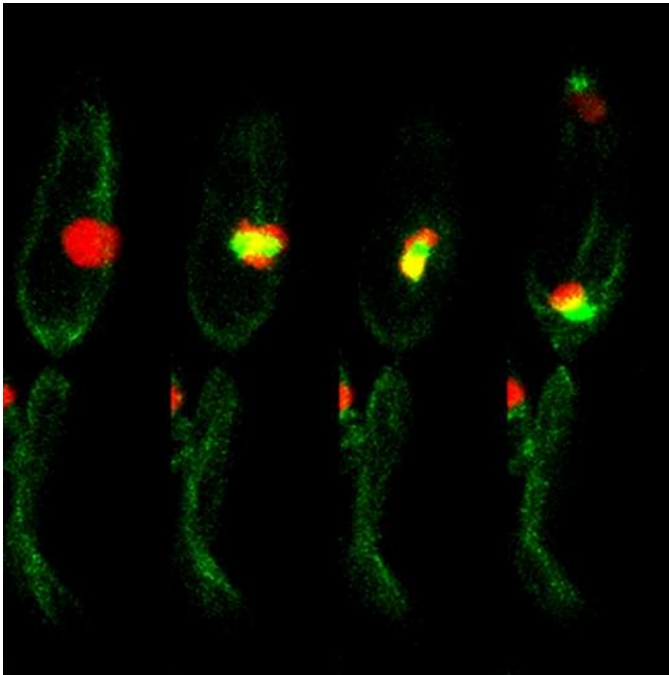
**...every time I look into a microscope is special. No matter how many mitosis events I see, each spindle is even more magical than the first.**

### When doing the research, did you have a particular result or 'eureka' moment that has stuck with you?

I think it was when we realized that Dam1 function at the kinetochore during mitosis was only one of the many roles of the DASH complex in microtubule-associated proteins, and its contribution during other stages of the cell cycle was just as important to fungal development. Apart from this, every time I look into a microscope is special. No matter how many mitosis events I see, each spindle is even more magical than the first and there is always something more to learn.

### Why did you choose Journal of Cell Science for your paper?

We wanted to share our work with a broad cell biology audience. For a fungal pathology lab venturing into cell biology, we were looking for a journal that would be the best fit. Having seen previous



**Mitosis in the rice blast fungus during conidium development as it goes from the one-cell to two-cell stage.**

papers in the journal on *Aspergillus*, *Ustilago* and *Colletotrichum* cell biology, we felt that JCS was open to moving away from typical cell biology model systems and decided to give it try. Thank you for a smooth peer review process.

**Have you had any significant mentors who have helped you beyond supervision in the lab? How was their guidance special?**

I was lucky to have two amazing PhD supervisors, Johannes Manjrekar and the late Prof. Bharat Chattoo. I am grateful to Johannes Manjrekar who was always open to scientific discussion and debate. He gave me the freedom to pursue my own interests and nudged me along when I was stuck. Most importantly, he raised the right questions, forcing me to think and think again and sometimes even reconsider my conclusions. He set a great example of work–life balance, often encouraging us to pursue a hobby. Prof. Bharat Chattoo was instrumental in me joining the lab and taking up this project. He encouraged me to set my goals high and do my best to achieve them.

During my PhD, mentorship has come in different ways from multiple sources and I am grateful for all of them. I thank Rajesh Patkar for sharing his experience on working with fungal pathogens, writing manuscripts and in general advising on the challenges and enthusiasm of a scientific career. My colleagues Hashim Reza, Divya Purohit, Akhil Thaker, Khyati Mehta and Anand Parnandi,

from whom I've learnt many techniques, presentation skills, lab management, a consistent work culture, and the importance of persistence and clarity, have been great mentors. My parents Anju and Bharat and my sister Kushal have been extremely generous with their time, resources and motivation, constantly standing by my side through my education journey.

**What motivated you to pursue a career in science, and what have been the most interesting moments on the path that led you to where you are now?**

My career in science and particularly biology started as a love for nature and its infinite diversity. As a child, I would spend hours staring at every emerging leaf, the monsoon snails and every splash of colour from the spring flowers. To a student interested in numbers and geometry, the forms, shapes and patterns of living forms were simply fascinating. In high school, I was introduced to Mendel's peas, the cardiovascular system and the different stages of mitosis, which the teacher had so carefully shown us on an onion peel. It encouraged me to take up biology for my undergraduate studies at Ruia College. It was while performing experiments during my bachelor's and master's courses at the Maharaja Sayajirao University of Baroda that I first found my motivation to pursue science. Reading 'how something works' in textbooks was fun, but performing the experiment and seeing for oneself was way more enlightening and I found an altogether new meaning in my life. It was during these years that I also found my love for microscopy; it allowed me to see nature at a whole new level. My PhD, for which I studied kinetochore proteins, introduced me to the beauty of cell biology and the amazing world of fungi. Along the way, meeting and listening to scientists talk about their work and paths to discovery inspired me to keep going. More importantly, I realized that while I was performing an experiment or looking through the lens of a microscope, nothing else in the world mattered and irrespective of the outcome, I could come back to this again and again every morning.

**What's next for you?**

I'm looking for a postdoctoral position to answer interesting questions in cell biology. With all the technological advancements in quantitative microscopy, reconstitution studies, chemical biology tools and support from the physical and mathematical sciences, I think we are in a great position to address processes governing the emergence of cell form and function at previously unimaginable space and time scales.

**Tell us something interesting about yourself that wouldn't be on your CV**

I like gardening, painting and cooking!

**Reference**

Shah, H., Rawat, K., Ashar, H., Patkar, R. and Manjrekar, J. (2019). Dual role for fungal-specific outer kinetochore proteins during cell cycle and development in *Magnaporthe oryzae*. *J. Cell Sci.* **132**, 224147. doi:10.1242/jcs.224147

RESEARCH ARTICLE

# Magnesium Uptake by CorA Transporters Is Essential for Growth, Development and Infection in the Rice Blast Fungus *Magnaporthe oryzae*

Md. Hashim Reza, Hiral Shah, Johannes Manjrekar, Bharat B. Chattoo\*

Genome Research Centre, Department of Microbiology & Biotechnology Centre, Faculty of Science, The Maharaja Sayajirao University of Baroda, Vadodara 390 002, Gujarat, India

\* [bharat.chattoo@bcsu.ac.in](mailto:bharat.chattoo@bcsu.ac.in)



**OPEN ACCESS**

**Citation:** Reza M.H, Shah H, Manjrekar J, Chattoo BB (2016) Magnesium Uptake by CorA Transporters Is Essential for Growth, Development and Infection in the Rice Blast Fungus *Magnaporthe oryzae*. PLoS ONE 11(7): e0159244. doi:10.1371/journal.pone.0159244

**Editor:** Richard A Wilson, University of Nebraska-Lincoln, UNITED STATES

**Received:** May 16, 2016

**Accepted:** June 29, 2016

**Published:** July 14, 2016

**Copyright:** © 2016 Reza et al. This is an open access article distributed under the terms of the [Creative Commons Attribution License](https://creativecommons.org/licenses/by/4.0/), which permits unrestricted use, distribution, and reproduction in any medium, provided the original author and source are credited.

**Data Availability Statement:** All relevant data are within the paper and its Supporting Information files.

**Funding:** The work was funded by Department of Biotechnology (DBT) and Department of Science & Technology through J.C. Bose National Fellowship awarded to Bharat B. Chattoo by the Government of India. The authors thank University Grants Commission (UGC-NET) and Council of Scientific & Industrial Research-Shyama Prasad Mukherjee Fellowship (CSIR-SPMF) for providing the fellowship to Md. Hashim Reza and Hiral Shah respectively. The funders had no role in study design, data collection

## Abstract

*Magnaporthe oryzae*, the causative organism of rice blast, infects cereal crops and grasses at various stages of plant development. A comprehensive understanding of its metabolism and the implications on pathogenesis is necessary for countering this devastating crop disease. We present the role of the CorA magnesium transporters, MoAlr2 and MoMnr2, in development and pathogenicity of *M. oryzae*. The *MoALR2* and *MoMNR2* genes individually complement the Mg<sup>2+</sup> uptake defects of a *S. cerevisiae* CorA transporter double mutant. *MoALR2* and *MoMNR2* respond to extracellular Mg<sup>2+</sup> and Ca<sup>2+</sup> levels and their expression is elevated under Mg<sup>2+</sup> scarce conditions. RNA silencing mediated knockdown of *MoALR2* (WT+siALR2,  $\Delta mnr2$ +siALR2 and ALR2+MNR2 simultaneous silencing) drastically alters intracellular cation concentrations and sensitivity to metal ions. *MoALR2* silencing is detrimental to vegetative growth and surface hydrophobicity of mycelia, and the transformants display loss of cell wall integrity. *MoALR2* is required for conidiogenesis and appressorium development, and is essential for infection. Investigation of knockdown transformants reveal low cAMP levels and altered expression of genes encoding proteins involved in MoMps1 cell wall integrity and cAMP MoPmk1 driven MAP Kinase signaling pathways. In contrast to *MoALR2* knockdowns, the *MoMNR2* deletion ( $\Delta mnr2$ ) shows increased sensitivity to CorA inhibitors as well as altered cation sensitivity, but has limited effect on surface hydrophobicity and severity of plant infection. Interestingly, *MoALR2* expression is elevated in  $\Delta mnr2$ . Impairment of development and infectivity of knockdown transformants and altered intracellular cation composition suggest that CorA transporters are essential for Mg<sup>2+</sup> homeostasis within the cell, and are crucial to maintaining normal gene expression associated with cell structure, signal transduction and surface hydrophobicity in *M. oryzae*. We suggest that CorA transporters, and especially *MoALR2*, constitute an attractive target for the development of antifungal agents against this pathogen.

and analysis, decision to publish, or preparation of the manuscript.

**Competing Interests:** The authors have declared that no competing interests exist.

## Introduction

Rice blast disease caused by *Magnaporthe oryzae* continues to be a serious and recurring problem in all rice growing regions across the world. The rice blast fungus attacks rice plants at all stages of development and can infect leaves, stems, nodes, panicles and roots. Foliar infection occurs by formation of a dome-shaped infection structure called the appressorium, which upon maturation generates turgor pressure by accumulating high concentrations of compatible solutes such as glycerol [1] and is important for breaching the rice cuticle; thereby the fungal hyphae invade and ramify through the plant tissue and grow within the host cells. The fungus sporulates profusely from disease lesions under conditions of high humidity, allowing the disease to spread rapidly to adjacent rice plants by wind and dewdrop splash [2]. Considering the poor durability of many blast-resistant cultivars of rice, which have a typical field life of only 2–3 growing seasons before disease resistance is overcome, and increasing energy costs which affect fungicide and fertilizer prices, there is a need for better understanding of rice blast disease to combat this deadly crop destroyer [3]. Rice blast control strategies that can be deployed as part of an environmentally sustainable plan for increasing the efficiency of cereal cultivation are therefore urgently required [4].

The development of spores leading to appressorium formation is initiated through recognition of environmental cues and is mediated by cross-talk between signal transduction pathways within the cell. In the past two decades, studies on signaling pathways, which include Mitogen Activated Protein Kinase (MAPK) signaling cascade and signaling pathways dependent on secondary messengers like  $\text{Ca}^{2+}$  [5] and cAMP [6, 7], which regulate various stages of the *M. oryzae* infection cycle, have been initiated. Although the cell cycle and signal transduction pathways tightly regulate *M. oryzae* development and infection, studies of how metal ions affect these developmental pathways have been largely limited to calcium signaling. The ability to grow, divide, respond to cell wall stress, sporulate and infect are complex but critical processes in *M. oryzae* for its colonization and establishment in the host as a successful pathogen. Magnesium being a co-factor for a wide range of enzymes is important in a variety of biochemical processes.  $\text{Mg}^{2+}$  is utilized by twice as many metalloenzymes as Zinc [8]. Free  $\text{Mg}^{2+}$  is essential for stabilizing cell membrane, cell wall [9–12] and ribosomes. It is essential for neutralizing the negatively charged phosphate groups of nucleic acids [13], DNA repair, and is indispensable for DNA replication fidelity.  $\text{Mg}^{2+}$  regulates electrolyte transport across the cell membrane [13], as well as activity of the sodium potassium pump (Na/K-ATPase) and the calcium pump (Ca-ATPase) [14]. In the fission yeast *Schizosaccharomyces pombe* and the budding yeast *Kluyveromyces fragilis*, intracellular levels of  $\text{Mg}^{2+}$  regulate the timing of cell cycle progression [15]. Among pathogens,  $\text{Mg}^{2+}$  is also required for germ tube formation in *Candida albicans* vegetative cells and consequently affects its morphogenesis and pathogenicity [16]. Regulation of intracellular concentration of  $\text{Mg}^{2+}$  is achieved by three mechanisms: uptake systems, efflux from the cell and sequestration within organelles [17]. However, the relation between  $\text{Mg}^{2+}$  concentrations and morphogenesis has not been investigated in fungal plant pathogens, including *M. oryzae*.

The molecular identity, function and regulation of  $\text{Mg}^{2+}$  transporters have been studied extensively to understand the basis of  $\text{Mg}^{2+}$  homeostasis in eukaryotic cells. The CorA (or Metal Ion Transporter) superfamily is an important group of  $\text{Mg}^{2+}$  transporters in both prokaryotes and eukaryotes [17]. Despite divergent primary protein sequence, the CorA  $\text{Mg}^{2+}$  transporters are characterized by two or three conserved transmembrane domains near the carboxy terminus, one of which is followed by the conserved motif (F/W) GMN [18] that is essential for  $\text{Mg}^{2+}$  transport. In *Salmonella typhimurium* and *Escherichia coli*, three proteins (CorA, MgtA, and MgtB) have been shown to be involved in  $\text{Mg}^{2+}$  transport across the plasma

membrane [18]. Magnesium uptake by CorA is essential for viability of *Helicobacter pylori* [19]. Eukaryotic CorA proteins have diversified in function, facilitating both  $Mg^{2+}$  uptake and distribution between sub-cellular compartments. *Saccharomyces cerevisiae* Alr1 is the first characterized  $Mg^{2+}$  transport system in eukaryotes and is distantly related to the bacterial CorA  $Mg^{2+}$  transporter family [18]. Subsequently a second CorA protein, Alr2, was identified in *S. cerevisiae*. Alr1 and Alr2 are present on the plasma membrane; loss-of-function mutations in Alr1 result in reduced  $Mg^{2+}$  uptake and growth defects restorable by external  $Mg^{2+}$  supplementation [18, 20]. Alr2 makes only a minor contribution to  $Mg^{2+}$  homeostasis, due to low expression and activity [14]. The Alr1 clade of CorA proteins includes a subgroup represented by Mnr2, a vacuolar membrane protein required for access to intracellular magnesium stores [21]. Another subfamily includes the yeast Mrs2 protein, which supplies  $Mg^{2+}$  to the mitochondrial matrix [22]. In *Arabidopsis thaliana*, a family of 10  $Mg^{2+}$  transporters which is homologous to the yeast *MRS2* gene and to the CorA family in bacteria has been identified, most of which have been shown to be expressed in a range of plant tissues [23].

Given its diverse metabolic roles, magnesium is indispensable for cellular functioning. However, the regulation and role of CorA  $Mg^{2+}$  transporters in development and pathogenicity of *M. oryzae* are still unexplored. Considering the diverse roles of  $Mg^{2+}$  ions, understanding the regulation of  $Mg^{2+}$  in *M. oryzae* is of considerable interest.

In the present study we identified the *M. oryzae* orthologs of *S. Cerevisiae* *ALR1*, Mgg\_08843 (*MoALR2*) and Mgg\_09884 (*MoMNR2*). Both *MoALR2* and *MoMNR2* can complement the  $Mg^{2+}$  uptake defects in a *S. cerevisiae* *alr1 alr2* double mutant. As a first step towards understanding  $Mg^{2+}$  regulation, we show that CorA transporters in *M. oryzae* affect intracellular  $Mg^{2+}$  concentration and are in turn themselves regulated by levels of extracellular  $Mg^{2+}$  and other divalent cations. Using knockout and knockdown transformants we show that  $Mg^{2+}$  uptake by CorA transporters is required for fungal development, progression of the infection cycle and cell wall integrity. We find that in the knockdown transformants cAMP levels are reduced and expression of genes involved in key signaling pathways is altered. We show that depletion of CorA transporters mimics the phenotypes produced by extracellular  $Mg^{2+}$  scarcity and brings about changes in gene expression previously not known to be affected by  $Mg^{2+}$  in fungal pathogens. Analysis of both the transporters indicates that the role of *MoALR2* is more critical than that of *MoMNR2*, and that *MoALR2* may be indispensable for the growth and pathogenesis in *M. oryzae*. Our results indicate that both *MoALR2* and *MoMNR2* play important roles in  $Mg^{2+}$  homeostasis in *M. oryzae*, in which Alr2 appears to be more central than Mnr2.

## Results

### Identification of *MoALR2* and *MoMNR2*

We identified CorA Magnesium transporters from the *M. oryzae* genome ([http://www.broadinstitute.org/annotation/genome/magnaporthe\\_grisea/MultiHome.html](http://www.broadinstitute.org/annotation/genome/magnaporthe_grisea/MultiHome.html)) by a BLAST\_P search using the full length *S. cerevisiae* Alr1 protein sequence (859 amino acids). We obtained two putative orthologs in the *M. oryzae* genome: Mgg\_08843 (47% identity) and Mgg\_09884 (49% identity), which are named MoAlr2 and MoMnr2 respectively. Both these proteins have two transmembrane domains towards the carboxy terminus, which are followed by conserved residues of (W/F) GMN, and hence belong to the CorA superfamily of  $Mg^{2+}$  transporters. MoAlr2 is a 622 amino acid protein with a CorA domain spanning amino acids 310–617 (Pfam). Strongly preferred model (ExPASy) for MoAlr2 predicts that the protein has two transmembrane helices (565–582; in-out) and (596–615; out-in), with the N-terminus facing the cytosol; the protein has been predicted to be localized to the plasma membrane

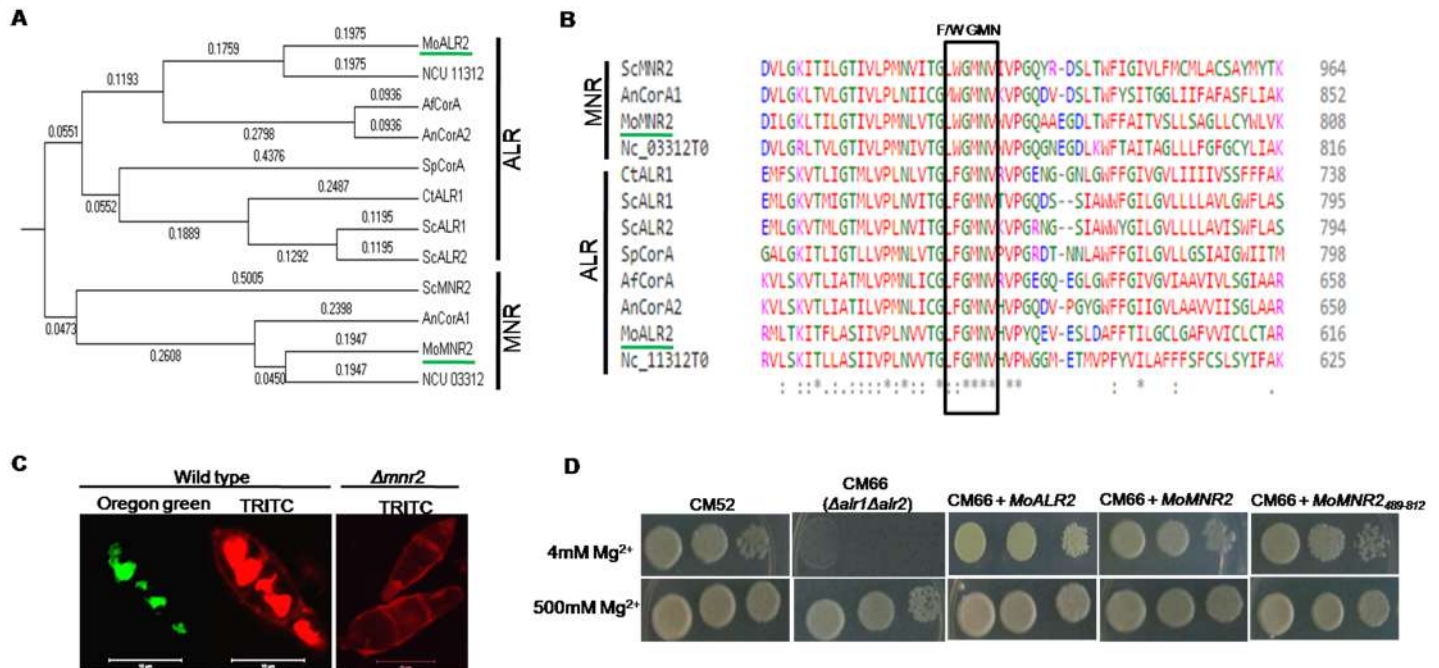


**Fig 1. Identification of *MoAlr2* and *MoMnr2*.** (A) The tree was constructed using the Neighbor-Joining method based on alignment of full length sequences of CorA proteins of *Magnaporthe oryzae* (XP\_003713862, XP\_003709977), *Saccharomyces cerevisiae* (EDV10489, EDV09793, YKL064W), *Aspergillus fumigatus* (XP\_754049), *Aspergillus nidulans* (CBF70700, CBF77902), *Candida tropicalis* (XP\_002548119), *Schizosaccharomyces pombe* (NP\_595545) and *Neurospora crassa* (NCU11312, NCU03312). The evolutionary distances were computed using the Poisson correction method and are in the units of the number of amino acid substitutions per site. All positions containing gaps and missing data were eliminated. Evolutionary analyses were done using MEGA5. (B) Amino acid sequence alignment of CorA proteins *Magnaporthe oryzae* (XP\_003713862, XP\_003709977), *Saccharomyces cerevisiae* (EDV10489, EDV09793, and YKL064W), *Aspergillus fumigatus* (XP\_754049), *Aspergillus nidulans* (CBF70700, CBF77902), *Candida tropicalis* (XP\_002548119), *Schizosaccharomyces pombe* (NP\_595545) and *Neurospora crassa* (NCU11312, NCU03312) was performed using Clustal Omega. CorA consensus sequence motifs (Y/FGMN) for the above proteins are highlighted. (C) Conidia were harvested and treated with polyclonal antibodies raised against the CorA domain of MoMnr2. TRITC labeled secondary antibodies were used for staining. Oregon green 488 staining was used to visualize the vacuole. (D) *S. cerevisiae*  $\Delta alr1\Delta alr2$  mutant (CM66) was transformed with pYES2-*MoAlr2*, pYES2-*MoMnr2* and pYES2-*MoMnr2*<sub>489-812</sub>. The transformants were grown overnight on SD+Gal+leu+lys-ura+500mM Mg<sup>2+</sup> and different dilutions were spotted on SD+Gal-ura+leu+lys containing 4mM Mg<sup>2+</sup> and 500mM Mg<sup>2+</sup> and grown at 28°C for 4 days. The experiments were repeated in triplicate, N = 3.

doi:10.1371/journal.pone.0159244.g001

(WoLFPSORT). MoMnr2 is a 814 amino acid protein with a CorA domain spanning amino acids 491–809 (Pfam). MoMnr2 is predicted to have two transmembrane helices (756–773; in-out) and (788–806; out-in), with the N-terminus facing the cytosol. In *S. cerevisiae*, the ScMnr2 protein has been shown to be localized to vacuolar membrane. The MoAlr2 and MoMnr2 CorA domains have ~ 48% identity with that of the *S. cerevisiae* CorA domain. Multiple sequence alignment of CorA superfamily transporters across different species including yeast and several filamentous pathogenic and non-pathogenic fungi was done using full length protein sequence and the phylogenetic relationship of these CorA proteins is presented (Fig 1A). The CorA transporters included in the analysis form two clades. The MNR clade has W (tryptophan) just before the conserved sequence motif of GMN, while the ALR clade has F (phenylalanine) prior to the GMN sequence (Fig 1B).

CorA transporters are known to be present on the plasma membrane as well as on organelles to form a system of Mg<sup>2+</sup> uptake and compartmentalization that maintains cytoplasmic Mg<sup>2+</sup> homeostasis. In yeast, ScAlr2 has been shown to be a plasma membrane protein while ScMnr2 is a vacuolar membrane protein. The subcellular localization of CorA transporters in *M. oryzae* was done by indirect immunolocalization using polyclonal antibodies against the MoMnr2 CorA domain. In wild type, the CorA transporters localized to plasma membrane

and vacuole (Fig 1C). Vacuolar localization was seen by co-localization with Oregon Green 488 staining (which stains vacuolar lumen). In the *MoMNR2* knockout ( $\Delta mnr2$ ), the MoAlr2 protein was found to be restricted to the plasma membrane (Fig 1C).

To confirm the nature of these  $Mg^{2+}$  transporters functionally, complementation with the *M. oryzae* genes was carried out in yeast. The *S. cerevisiae*  $\Delta alr1\Delta alr2$  mutant CM66 [23] is a haploid disruptant for both *ALR1* and *ALR2* genes. Unlike the wild type, the double mutant is unable to grow at 4mM  $Mg^{2+}$ , indicating a defect in  $Mg^{2+}$  uptake. To test the ability of *MoALR2* and *MoMNR2* to complement the  $Mg^{2+}$  uptake defect in the double mutant CM66, transformants over-expressing either *MoALR2* or *MoMNR2*, were first grown in SD media containing 500mM  $Mg^{2+}$  and then different dilutions were spotted on SD media containing 4mM  $Mg^{2+}$ . The transformants were able to grow even at 4mM  $Mg^{2+}$  like the wild type, while the mutant could not (Fig 1D), suggesting that both *MoALR2* and *MoMNR2* could rescue the  $Mg^{2+}$  uptake defect and hence have a role in  $Mg^{2+}$  transport. Further, a truncated *MoMNR2* was also able to complement the function in the yeast mutant, suggesting that amino acids of the CorA domain at the Carboxyl terminus (489–812 amino acids) are sufficient for  $Mg^{2+}$  transport.

### CorA $Mg^{2+}$ transporters alter metal ion composition in *M. oryzae*

Targeted disruption of *MoALR2* and *MoMNR2* through homologous recombination was attempted to investigate the functions of CorA  $Mg^{2+}$  transporters in *M. oryzae*. *MoMNR2* knockouts ( $\Delta mnr2$ ) were generated using a Zeocin resistance cassette in the wild type strain B157 (WT). Three independent transformants were confirmed by Southern blotting for targeted gene deletion (S1B Fig). Immunostaining of  $\Delta mnr2$  with CorA antibodies showed staining only of plasma membrane due to MoAlr2, while vacuolar staining was absent (Fig 1C). In contrast, only non-homologous (ectopic) transformants were obtained for *MoALR2* despite multiple attempts using different conditions of selection (S1 Table). Knockout of *MoALR2* was also attempted in the  $\Delta ku80$  background known to aid homologous integration. But screening of all the transformants resulted only in ectopic integrants (S1 Table). Thus, we speculate that *MoALR2* is essential for viability of *M. oryzae*.

To establish the role of *MoALR2* by an alternative approach, the gene was silenced in both WT and  $\Delta mnr2$  backgrounds using a stretch of 110bp complementary to the 5' UTR of *MoALR2* [24], cloned in the vector pSD2. The knockdown was validated by analysis of relative expression of *MoALR2* and *MoMNR2* by quantitative Real Time PCR (qRT-PCR) in the transformants. Transformants in the WT background showed transcript levels of *MoALR2* ranging from 48% to 85%, while those in the background of  $\Delta mnr2$  showed transcript levels ranging from 66% to 88% compared to WT (S2 Table). No transcripts of *MoMNR2* were detected in  $\Delta mnr2$  background transformants, while the levels of *MoMNR2* did not change in the *MoALR2* knockdown transformants in wild type background, thereby confirming the specificity of the cassette used for *MoALR2* silencing. Since *MoALR2* could not be silenced more strongly in the  $\Delta mnr2$  background, to obtain transformants with further reduced transcript levels of *MoALR2*, an alternative knockdown approach for simultaneous silencing of both *MoALR2* and *MoMNR2* was also used. As these two genes show high similarity in the CorA domain, we carried out simultaneous silencing using an antisense construct targeted to this region. The knockdown was validated by qRT-PCR of *MoALR2* and *MoMNR2* in the transformants. The transformants showed transcript levels ranging from 30% to 80% and 37% to 90% for *MoALR2* and *MoMNR2* respectively, compared to WT (S2 Table).

To be sure that reduced transcript levels translated into decline in transporter levels, we used a Co(III) Hexaammine sensitivity test. Unlike WT, growth of CorA knockout/knockdown strains is not sensitive to cation hexaammines, demonstrating that the inhibition is mediated

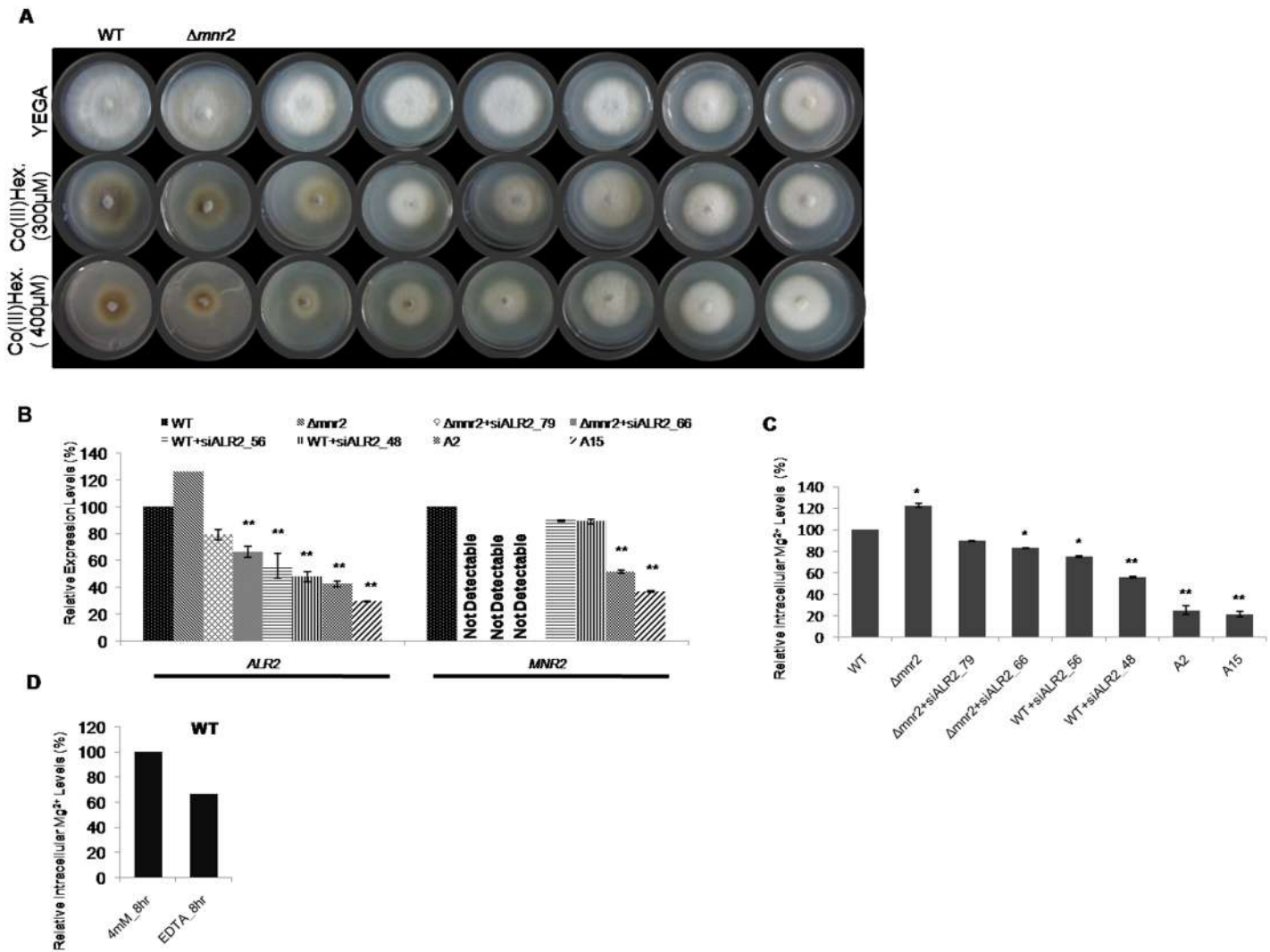


**Fig 2. CorA  $Mg^{2+}$  transporters affect metal ion composition in *M. oryzae*.** (A) CorA specific inhibitor (Cobalt (III) hexaammine (Co (III) Hex.) was added to YEGA medium at concentrations of 300 $\mu$ M and 400 $\mu$ M. Sensitivity was assessed relative to Wild type (WT) five days post inoculation and growth was measured for WT,  $\Delta mnr2$  and knockdown transformants. (B) mRNA levels of *MoALR2* and *MoMNR2* were estimated by qRT-PCR. Transcript levels were normalized to that of WT. (C) Intracellular levels of  $Mg^{2+}$  in the knockout and knockdown transformants were estimated by XRF. The values are expressed as percentage values, with 100 corresponding to WT at 4mM  $Mg^{2+}$ . (D) Intracellular levels of  $Mg^{2+}$  in WT were estimated in presence of 4mM extracellular  $Mg^{2+}$  and EDTA at 8hrs. The values are expressed as percentage values, with 100 corresponding to 4mM  $Mg^{2+}$ . \*\* means P value at <0.0001 and \* means significant at P value <0.05. Values are the mean of two independent experiments with each performed in triplicates.

doi:10.1371/journal.pone.0159244.g002

by an interaction between CorA and the hexaammines [25]. We tested the sensitivity of knock-down transformants as compared to WT. Two independent knockdown transformants from each category, namely Alr2 silencing (WT+siALR2),  $\Delta mnr2$ +siALR2 and simultaneously silenced for *MoALR2* and *MoMNR2*, which were least sensitive to Co(III)Hex., were selected for further study. Southern blot analysis confirmed single site integration in these knockdown transformants (S2A Fig). The degree of resistance to Co(III)Hex. of the selected transformants,  $\Delta mnr2$ +siALR2\_79,  $\Delta mnr2$ +siALR2\_66, WT+siALR2\_56, WT+siALR2\_48, A2 and A15 (Fig 2A) correlated with the degree of silencing of *MoALR2*. The expression levels (%) of *MoALR2* and *MoMNR2* in the transformants relative to WT were  $\Delta mnr2$  (126, 0),  $\Delta mnr2$ +siALR2\_79 (79, 0),  $\Delta mnr2$ +siALR2\_66 (66, 0), WT+siALR2\_56 (56, 90), WT+siALR2\_48 (48, 89), A2 (43,

52) and A15 (30, 37) (Fig 2B). Interestingly, the  $\Delta mnr2$  knockout was more sensitive to Co(III) Hex. than wild type, possibly due to up-regulation of *MoALR2* transcripts observed in the three independent  $\Delta mnr2$  knockouts. Failure of  $\Delta mnr2$  to show Co(III)Hex. resistance, once again suggests its intracellular localization, since cation hexaammines are known to affect only surface transporters, as seen with *MoALR2* knockdowns.

Western blot analysis of selected transformants was done to determine whether protein levels were also reduced in them. The sequence of the CorA domain from MoMnr2 has 50% identity with that of MoAlr2, so the antibodies raised against the CorA domain detected both MoAlr2 (70 kDa) and MoMnr2 (90 kDa). The transformants studied showed lower protein levels of these CorA Mg<sup>2+</sup> transporters than wild type B157 (S2B Fig).

We next investigated whether a decrease in Mg<sup>2+</sup> transporter levels affects the intracellular levels of metal ions (mainly Mg<sup>2+</sup> and Ca<sup>2+</sup>), using X-ray Fluorescence Analysis (XRF) of hyphae obtained under standard growth conditions (medium containing 4mM Mg<sup>2+</sup>). We found a decrease in the intracellular levels of Mg<sup>2+</sup> in the knockdown transformants (Fig 2C) while intracellular levels of Ca<sup>2+</sup> did not change significantly (data not shown). Significant decreases in Mg<sup>2+</sup> levels were seen when the silencing of *MoALR2* was >50%. For instance, XRF analysis of A2 and A15 showed that Mg<sup>2+</sup> levels were reduced to 25% and 21% of WT levels respectively. Thus we show that CorA Mg<sup>2+</sup> transporters play a significant role in maintenance of intracellular metal ion composition. Next, to look at the effect of extracellular Mg<sup>2+</sup> availability, we determined the intracellular Mg<sup>2+</sup> levels in presence of extracellular EDTA (a Mg<sup>2+</sup> chelator). The intracellular levels of Mg<sup>2+</sup> in WT decreased in presence of EDTA (Fig 2D) indicating a need for extracellular Mg<sup>2+</sup> and its uptake for maintenance of the intracellular ionic milieu.

To investigate whether extracellular Mg<sup>2+</sup> supplementation restores intracellular Mg<sup>2+</sup>, the two knockdown transformants which showed maximum silencing of *MoALR2*, A2 and A15, were grown in presence of higher concentrations of extracellular Mg<sup>2+</sup> (50mM and 250mM). When supplemented with 50mM Mg<sup>2+</sup>, the intracellular Mg<sup>2+</sup> levels in A2 and A15 increased to 62% and 42% (from 25% and 21%) respectively (Fig 3A) and rose further at 250mM Mg<sup>2+</sup> (Fig 3B). This could be either due to enhanced uptake by the CorA transporters in the knockdown transformants, or due to non-specific transport at higher levels of Mg<sup>2+</sup> by other metal ion transporters. In WT, while intracellular Mg<sup>2+</sup> levels remained unchanged at 50mM extracellular Mg<sup>2+</sup>, there was a drastic increase at 250mM Mg<sup>2+</sup> (Fig 3A and 3B). The increased Ca<sup>2+</sup>/Mg<sup>2+</sup> ratio observed in A2 and A15 at 4mM Mg<sup>2+</sup>, also returned to lower levels in presence of 50mM Mg<sup>2+</sup> (Fig 3C).

## Mg<sup>2+</sup> dependent expression of *MoALR2* and *MoMNR2*

The expression profile of *MoALR2* and *MoMNR2* was studied in WT grown in presence of EDTA, 50mM and 250mM extracellular Mg<sup>2+</sup> for different lengths of time (2 hours and 6 hours). The addition of EDTA resulted in up-regulation of both *MoALR2* and *MoMNR2*. *MoALR2* showed a biphasic mode of regulation with respect to different concentrations of Mg<sup>2+</sup>; transcript levels decreased at 50mM Mg<sup>2+</sup> both at 2 hours and 6 hours, while at 250mM Mg<sup>2+</sup>, the transcript level increased both at 2 hours and 6 hours (Fig 4A). The transcript levels of *MoMNR2* decreased with increasing concentrations of Mg<sup>2+</sup> (Fig 4B). To examine how the levels of MoAlr2 and MoMnr2 proteins change with extracellular Mg<sup>2+</sup> levels, Western blot analysis was also done. The levels of both proteins increased in presence of EDTA. In the presence of 50mM Mg<sup>2+</sup> the level of MoAlr2 was comparable to that seen with 4mM Mg<sup>2+</sup> alone (i.e. no EDTA), both at 2 hours and 6 hours, but increased at 250mM Mg<sup>2+</sup> both at 2 hours and 6 hours compared to that at 4mM Mg<sup>2+</sup> (Fig 4C). The level of MoMnr2 protein showed the same trend as seen at transcript level, decreasing with increasing concentration of Mg<sup>2+</sup> and with increasing time interval (Fig 4D).

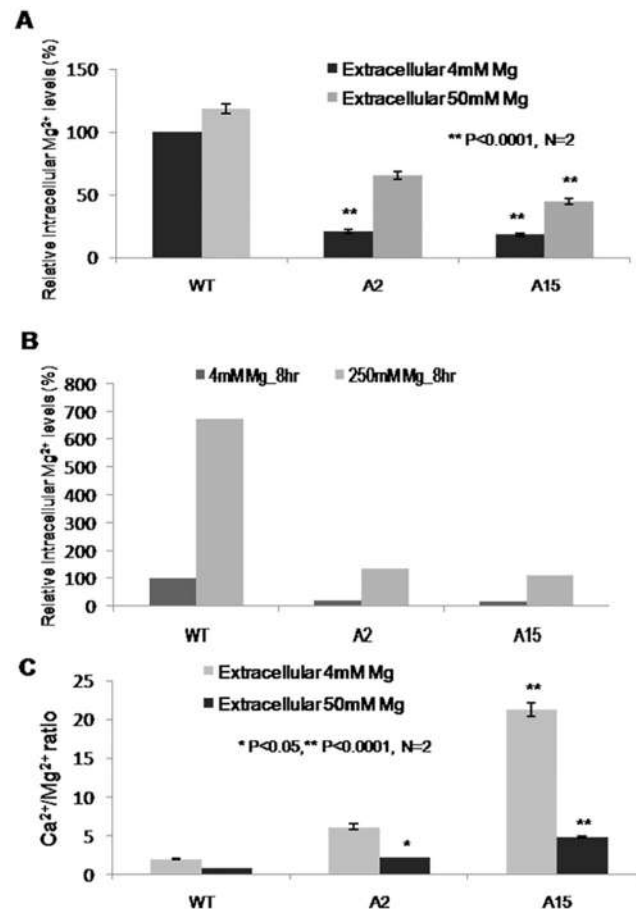


**Fig 3. XRF analysis of knockdown transformants.** (A), (B) Intracellular levels of Mg<sup>2+</sup> at 4mM, 50mM and 250mM extracellular Mg<sup>2+</sup> in WT and the double knockdown transformants, A2 and A15. The values are expressed as percentages, with 100 corresponding to the WT at 4mM Mg<sup>2+</sup>. (C) Ratios of Ca<sup>2+</sup> to Mg<sup>2+</sup> at two different concentrations of Mg<sup>2+</sup> in WT, A2 and A15. Values are the mean of two independent experiments with each performed in triplicates. Error bar denote SD. \*\* means P value at <0.0001 and \* means significant at P value <0.05.

doi:10.1371/journal.pone.0159244.g003

### Ca<sup>2+</sup> dependent expression of *MoALR2* and *MoMNR2*

Calcium (Ca<sup>2+</sup>) is a natural antagonist of Mg<sup>2+</sup> [23, 9, 14]. To evaluate how expression of the plasma membrane Mg<sup>2+</sup> transporter *MoALR2* changes with increasing concentration of Ca<sup>2+</sup>, transcript and protein levels were studied in WT. The transcript level of *MoALR2* increased at 50mM and 250mM extracellular Ca<sup>2+</sup> compared to control (where extracellular Ca<sup>2+</sup> was chelated with EGTA) (Fig 5A). Protein level of MoAlr2 was higher than in the EGTA-treated control, but MoMnr2 protein level remained constant even at high concentrations of Ca<sup>2+</sup> (Fig 5B). It is likely that high intracellular concentration of Ca<sup>2+</sup> induced increased expression of *MoALR2* as part of a feedback mechanism to maintain a favorable Ca<sup>2+</sup>/Mg<sup>2+</sup> ratio.

### Altered Cation sensitivity in knockdown transformants

Mg<sup>2+</sup> is the most abundant divalent cation in the cell. A change in Mg<sup>2+</sup> levels affects metal ion homeostasis and may alter sensitivity to heavy metal ions. We assayed the sensitivity of  $\Delta mnr2$  and the knockdown transformants to various cations in comparison to WT. A2 and A15 showed enhanced sensitivity to Aluminium (Al<sup>3+</sup>) (Table 1).

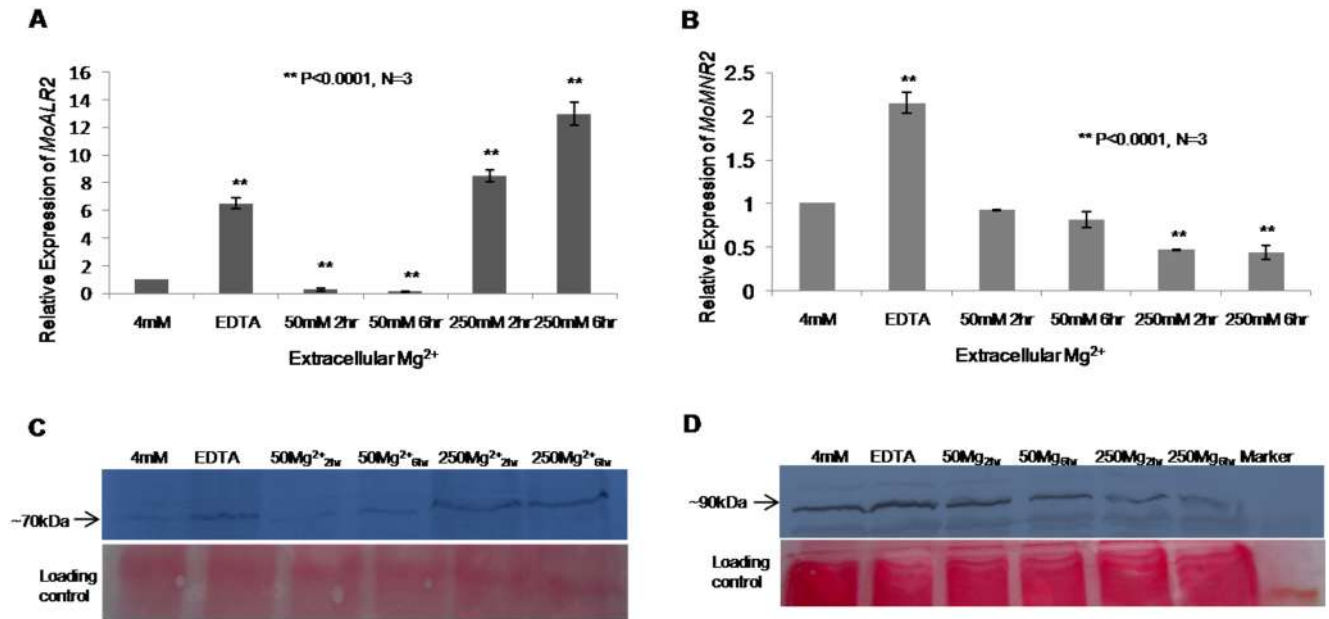


**Fig 4. Regulation of *MoALR2* and *MoMNR2* at mRNA and protein level with respect to extracellular  $Mg^{2+}$ .** (A) mRNA levels of *MoALR2* were estimated in WT by qRT-PCR at different concentrations of extracellular  $Mg^{2+}$ . (B) mRNA levels of *MoMNR2* were estimated by qRT-PCR at different concentrations of extracellular  $Mg^{2+}$ . Transcript levels were expressed as relative values, with 1 corresponding to levels at 4mM. (C) Western blot analysis of WT for MoAlr2 at different concentrations of extracellular  $Mg^{2+}$ . (D) Western blot analysis for MoMnr2 at different concentrations of extracellular  $Mg^{2+}$ . \*\* means P value at <0.0001 and \* means significant at P value <0.05. The experiments were repeated in triplicate, N = 3.

doi:10.1371/journal.pone.0159244.g004

This is consistent with the observation in *S. cerevisiae* that over-expression of the  $Mg^{2+}$  transporter provides resistance to  $Al^{3+}$ , justifying the ALR (Aluminium Resistance) nomenclature. The knockdown transformants were also more sensitive to Copper ( $Cu^{2+}$ ) and Iron ( $Fe^{3+}$ ) (Table 1). Their increased sensitivity towards these cations suggests that the level of  $Mg^{2+}$

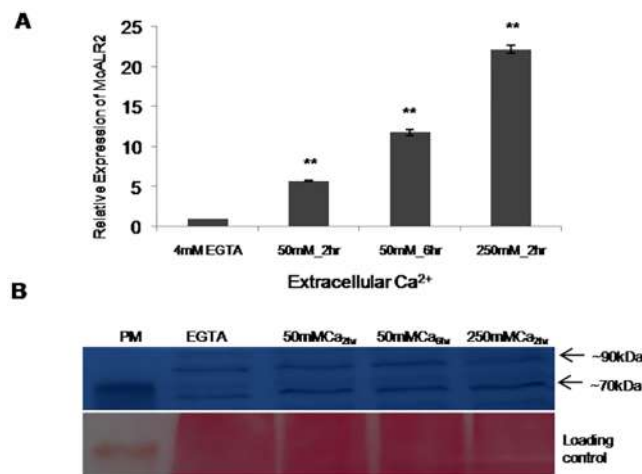


**Fig 5. Regulation of *MoALR2* in WT at mRNA and protein level with respect to extracellular  $Ca^{2+}$ .** (A) mRNA levels of *MoALR2* were estimated in WT by qRT-PCR at different concentrations of extracellular  $Ca^{2+}$ . The transcript levels were expressed as relative values, with 1 corresponding to levels at 4mM. Error bar denote SD. (B) Western blot analysis for MoAlr2 at different concentrations of extracellular  $Ca^{2+}$ . \*\* means P value at <0.0001 and \* means significant at P value <0.05. The experiments were repeated in triplicate, N = 3.

doi:10.1371/journal.pone.0159244.g005

**Table 1. Altered Cation Sensitivity in the knockdown transformants.**

Transformants	Growth diameter (centimeters)							
	YEGA	800µM Al <sup>3+</sup>	750µM Cu <sup>2+</sup>	2mM Fe <sup>3+</sup>	200µM Ni <sup>2+</sup>	150µM Co <sup>2+</sup>	500µM Zn <sup>2+</sup>	3mM Mn <sup>2+</sup>
WT	2.5 ±0.06	2.03 ±0.09	1.97 ±0.04	0.74 ±0.03	0.83 ±0.03	0.37 ±0.04	0.34 ±0.04	1.57 ±0.04
<i>Δmnr2</i>	2.47 ±0.03	2.25 ±0.03 <sup>a</sup>	1.94 ±0.04	0.57 ±0.04 <sup>b</sup>	0.54 ±0.04 <sup>a</sup>	0.36 ±0.03	0.33 ±0.04	0.37 ±0.04 <sup>a</sup>
<i>Δmnr2</i> +siALR2_79	2.3 ±0.07 <sup>b</sup>	1.47 ±0.03 <sup>a</sup>	1.3 ±0.06 <sup>a</sup>	0.38 ±0.04 <sup>a</sup>	0.87 ±0.04	0.37 ±0.03	0.33 ±0.04	0.37 ±0.04 <sup>a</sup>
<i>Δmnr2</i> +siALR2_66	2.28 ±0.02 <sup>a</sup>	1.43 ±0.03 <sup>a</sup>	1.23 ±0.03 <sup>a</sup>	0.34 ±0.04 <sup>a</sup>	1.02 ±0.05 <sup>b</sup>	0.34 ±0.04	0.67 ±0.03 <sup>a</sup>	0.84 ±0.03 <sup>a</sup>
WT +siALR2_56	2.27 ±0.01 <sup>a</sup>	1.36 ±0.03 <sup>a</sup>	1.07 ±0.04 <sup>a</sup>	0.34 ±0.03 <sup>a</sup>	1.03 ±0.04 <sup>b</sup>	0.33 ±0.04	0.66 ±0.02 <sup>a</sup>	1.27 ±0.04 <sup>a</sup>
WT +siALR2_48	2.25 ±0.03 <sup>a</sup>	1.23 ±0.04 <sup>a</sup>	0.87 ±0.03 <sup>a</sup>	0.33 ±0.03 <sup>a</sup>	1.07 ±0.03 <sup>a</sup>	0.40 ±0.01	0.87 ±0.03 <sup>a</sup>	1.20 ±0.06 <sup>a</sup>
A2	2.08 ±0.05 <sup>a</sup>	1.02 ±0.04 <sup>a</sup>	0.9 ±0.01 <sup>a</sup>	0.30 ±0.01 <sup>a</sup>	1.04 ±0.04 <sup>a</sup>	0.87 ±0.04 <sup>a</sup>	1.63 ±0.04 <sup>a</sup>	1.80 ±0.02 <sup>a</sup>
A15	1.95 ±0.03 <sup>a</sup>	0.74 ±0.03 <sup>a</sup>	0.73 ±0.04 <sup>a</sup>	0.29 ±0.01 <sup>a</sup>	1.27 ±0.04 <sup>a</sup>	1.03 ±0.04 <sup>a</sup>	2.03 ±0.03 <sup>a</sup>	1.97 ±0.03 <sup>a</sup>

WT, *Δmnr2* and knockdown transformants were inoculated on YEG and YEG supplemented with different cations. The sensitivity to cation was assessed relative to growth of WT. Data are presented as mean±SD from three independent experiments. Two-way ANOVA followed by Fisher's LSD test was performed at 95% confidence interval.

<sup>a</sup> means significantly different from WT at P value <0.0001

<sup>b</sup> means significantly different from WT at P value <0.05.

doi:10.1371/journal.pone.0159244.t001

required to provide resistance against these cations is dependent on *MoALR2* function. Conversely, A2 and A15 were more resistant to Nickel (Ni<sup>2+</sup>), Cobalt (Co<sup>2+</sup>), Zinc (Zn<sup>2+</sup>) and Manganese (Mn<sup>2+</sup>) (Table 1). The *Δmnr2* knockout, on the other hand, showed greater sensitivity to Ni<sup>2+</sup>, Co<sup>2+</sup>, Zn<sup>2+</sup> and Mn<sup>2+</sup>. These cations have been reported to be transported by CorA transporters [26, 27], so the higher resistance of the knockdown transformants to them is likely to be due to reduced uptake by the lower number of Mg<sup>2+</sup> transporters. This is also supported by the intracellular levels of Zn<sup>2+</sup> in A2 and A15, in which Zn<sup>2+</sup> levels were reduced to 78% and 61% of WT levels (S3A Fig).

### CorA transporters are required for mycelial growth and surface hydrophobicity in *M. oryzae*

We next set out to evaluate the effect of reduced Mg<sup>2+</sup> transport on development in *M. oryzae*. *Δmnr2* showed ~5% reduction in colony diameter as compared to WT and failed to produce melanin in the aerial hyphae (S3B Fig). The *MoALR2* knockdown transformants showed ~6% to 25% reduction in growth on Oat Meal Agar (OMA) medium (S3B Fig) (S3 Table) and this reduction was correlated with the degree of silencing of *MoALR2*. In comparison to WT, *Δmnr2* formed fewer aerial hyphae, while the knockdown transformants showed very sparse aerial hyphae, as seen in A2 and A15 (Fig 6A).

To investigate whether similar growth defects are also observed in situations of low Mg<sup>2+</sup> availability in *M. oryzae*, growth of WT was assayed in Mg<sup>2+</sup> limiting conditions, using EDTA to lower Mg<sup>2+</sup> availability. Growth on OMA was severely reduced with increasing concentrations of EDTA, being retarded significantly at 0.5mM EDTA (S4A Fig). On supplementing this medium with 50mM and 250mM extracellular Mg<sup>2+</sup>, growth was restored to normal (S4B Fig). At a concentration of 0.6mM EDTA, there was complete growth inhibition. Under 0.5mM EDTA stress, WT frequently formed sectorial colonies with certain sectors showing phenotypic differences (less melanized whitish sectors and melanized grayish sectors). Given the frequency with which such sectors appeared, it is likely that their altered phenotypes were due to epigenetic changes. When the phenotypically different sectors (grown on OMA without EDTA) were grown again in the absence of 0.5mM EDTA stress, these differences (less melanized and whitish) persisted, as observed up to 6 sub-culturings (S4B Fig).

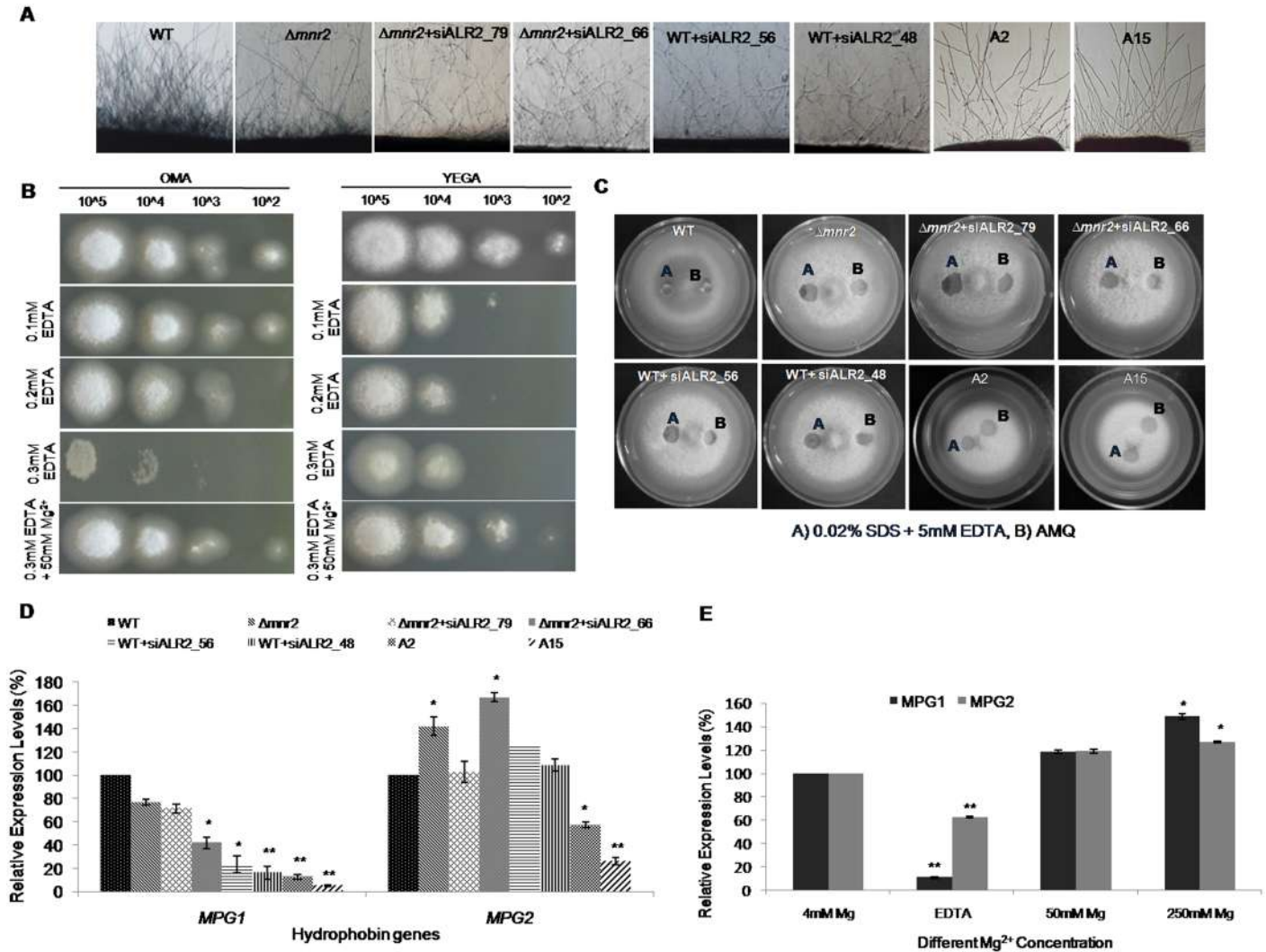


**Fig 6. CorA transporters are required for mycelial growth and surface hydrophobicity in *M. oryzae*.** (A) Microscopic examination of the hyphal growth of WT,  $\Delta mnr2$  and knockdown transformants was assessed. Pictures were taken after 2dpi grown on 0.8% agarose. (B) Ability of WT spores to form vegetative hyphal growth following germination was assessed on OMA (left) and YEGA (right) with different concentrations of EDTA. 10 $\mu$ l of spores with increasing dilution was spotted onto the plates. The ability of Mg<sup>2+</sup> to restore the germination capability of spores was also checked on Mg<sup>2+</sup> supplemented medium in presence of EDTA. (C) 10  $\mu$ l of water or detergent solution containing 0.02% SDS+5mM EDTA were placed on the surfaces of the WT,  $\Delta mnr2$  and knockdown transformants and photographed after 1 min. (D) mRNA levels of *MoMPG1* and *MoMPG2* were estimated by qRT-PCR in  $\Delta mnr2$  and knockdown transformants. All transcript levels were normalized to that of WT. (E) mRNA levels of *MoMPG1* and *MoMPG2* were estimated by qRT-PCR at two different concentrations of extracellular Mg<sup>2+</sup> in WT. All transcript levels were expressed as relative values, with 1 corresponding to levels at 4mM. Error bar denote SD. \*\* means P value at <0.0001 and \* means significant at P value <0.05. The experiments were repeated in triplicate, N = 3.

doi:10.1371/journal.pone.0159244.g006

Vegetative hyphal growth from WT spores following germination was checked on OMA and YEGA with increasing concentrations of EDTA. At 0.3mM EDTA growth from spores was severely restricted, while 50mM Mg<sup>2+</sup> could rescue the growth defect (Fig 6B).

Hydrophobins are surface proteins produced by filamentous fungi that are important for growth of aerial hyphae, hyphal surface hydrophobicity and attachment to solid supports [28–31]. Reduced surface hydrophobicity leads to a “wettable” phenotype where water droplets are not retained as beads on aerial hyphae. Such a wettable phenotype has been observed previously in *M. oryzae* in hydrophobin (*MoMHP1*, *MoMPG1*) and phosphodiesterase (*MoPDEH*)

mutants [6, 32–34].  $\Delta mnr2$  and *MoALR2* knockdown transformants were tested for their ability to retain drops of water and detergent solution to assess effects of *MoALR2* and *MoMNR2* on surface hydrophobicity. Compared to WT,  $\Delta mnr2$  showed a wettable phenotype both with water and detergent solution, but could hold water longer than the *MoALR2* knockdown transformants, which showed an easily wettable phenotype (did not retain solution at all) (Fig 6C). Thus, while *MoMNR2* has some effect on surface hydrophobicity, *MoALR2* appears to be the critical determinant. To investigate whether this wettable phenotype was mediated through hydrophobins, we measured the expression levels of hydrophobins, *MoMPG1* (Mgg\_10315) and *MoMPG2* (Mgg\_01173), in the  $\Delta mnr2$  and knockdown transformants. There was substantial decrease in the expression of *MoMPG1* in the knockdown transformants and in A15 the levels decreased by ~95%. The levels of *MoMPG2* did not change significantly (at  $P < 0.0001$ ) (Fig 6D).

To check whether extracellular  $Mg^{2+}$  availability affects expression of *MoMPG1* and *MoMPG2*, their transcript levels in WT were studied at different concentrations of  $Mg^{2+}$  and in presence of EDTA. In presence of EDTA, the expression of *MoMPG1* decreased to as little as 10% while *MoMPG2* still showed 60% expression (significant at  $P < 0.0001$ ) (Fig 6E). At 50mM and 250mM  $Mg^{2+}$  the expression of *MoMPG1* and *MoMPG2* was similar to that of control at 4mM. Thus, we show for the first time that in *M. oryzae*, decrease in  $Mg^{2+}$  levels, either by silencing of transporter function (in the knockdown transformants), or by using EDTA (in WT), has a direct effect on the expression of both hydrophobins, especially *MoMPG1*.

Hyphal growth on OMA was observed at regular time intervals post inoculation. As early as 12 days post inoculation (dpi),  $\Delta mnr2$  and *MoALR2* knockdown transformants displayed autolysis at the centre of the colony (Fig 7A). WT did not show any such phenotype even up to three weeks. The autolysis was more severe in transformants with *MoALR2* expression below 50%, namely, WT+siALR2\_48, A2 and A15 (Fig 7A). We followed  $\Delta mnr2$  for a longer time period under different extracellular  $Mg^{2+}$  concentrations. Though at 12dpi  $\Delta mnr2$  showed autolysis only at the centre, by 16 dpi, autolysis had spread to include a large proportion of the  $\Delta mnr2$  colony. 50mM and 250mM extracellular  $Mg^{2+}$  supplement delayed the onset of autolysis and as a result the autolysis area observed at 16 dpi was reduced (Fig 7B). On the contrary, EDTA hastened the process with  $\Delta mnr2$  displaying the phenotype even at 11 dpi with increasing severity on subsequent days (Fig 7B). In spite of wild type levels of *MoALR2*,  $\Delta mnr2$  showed early autolysis compared to WT, suggesting that *MoMNR2* is essential for long term survival of *M. oryzae*.

## Magnesium uptake by CorA transporters is essential for progression of the infection cycle in *M. oryzae*

The ability of pathogenic fungi to sporulate is critical to the spread of infection.  $\Delta mnr2$  knock-out showed a 23% reduction in spore count. In the *MoALR2* knockdowns, sporulation efficiency decreased with a reduction in the expression of *MoALR2*, to as low as 20% in WT +siALR2\_48 (Fig 8A). A2 and A15 completely failed to sporulate, suggesting that maintenance of *MoALR2* levels is critical for conidiogenesis.

We studied the ability of WT to sporulate in presence of EDTA. Sporulation increased up to 0.3mM EDTA as compared to control (OMA with no EDTA), and then decreased at higher concentrations (S5A Fig). At 0.5mM EDTA, sporulation was severely decreased.  $Mg^{2+}$  supplementation of 250mM was able to rescue this decrease in the sporulation at 0.5mM EDTA, suggesting that adequate  $Mg^{2+}$  levels are required for sporulation.

During infection, the spores germinate and differentiate into appressoria. To evaluate the role of *MoALR2* and *MoMNR2* in germination and appressorium formation in WT and

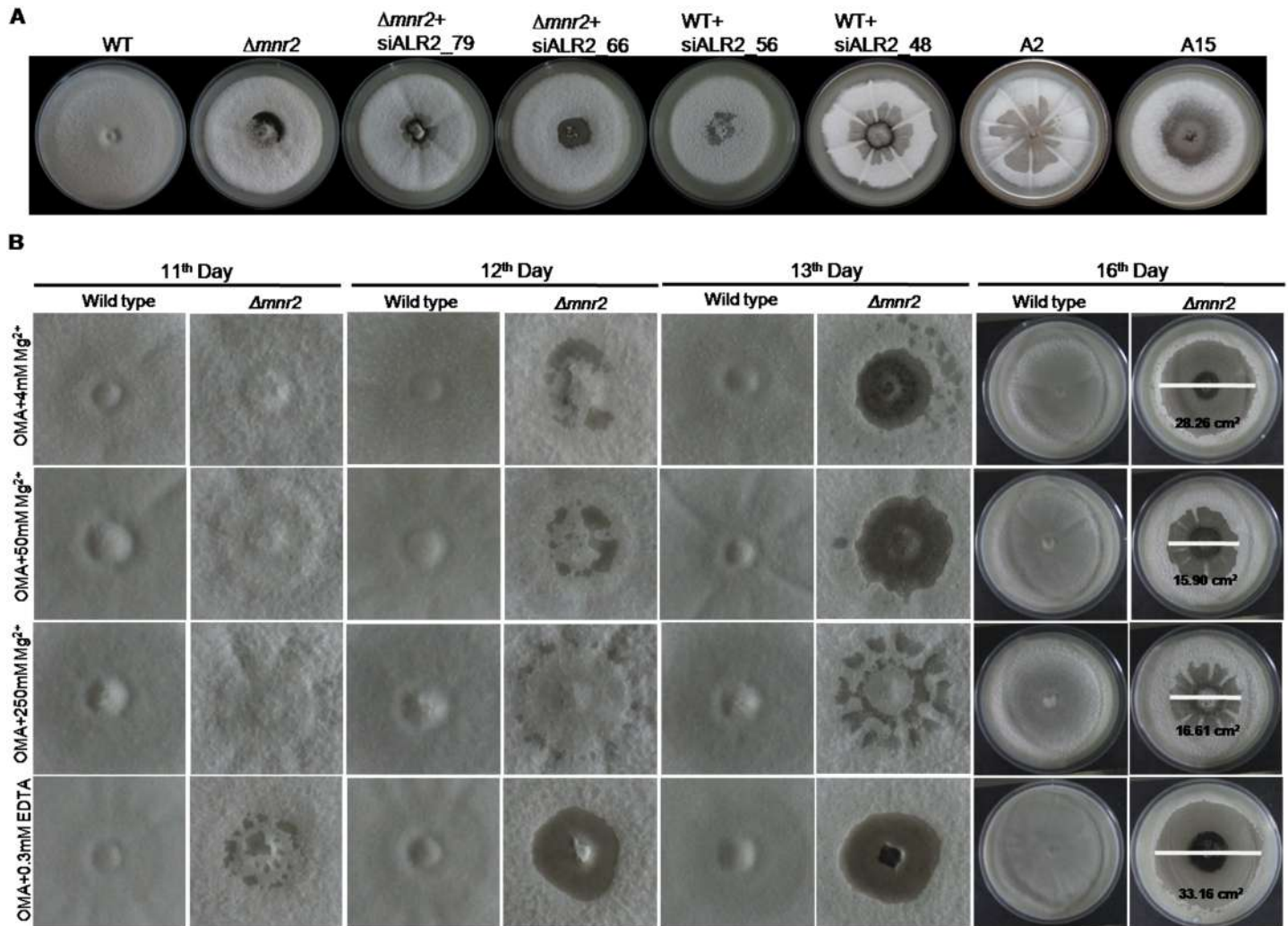


**Fig 7. CorA transporters are required for preventing autolysis.** (A) WT,  $\Delta mnr2$  and knockdown transformants were grown on OMA for 12 days. Early autolysis was monitored compared to WT. (B) WT and  $\Delta mnr2$  were grown on OMA supplemented with 4mM, 50mM, 250mM extracellular Mg<sup>2+</sup> and 0.3mM EDTA. Autolysis was monitored from 10 dpi to 16 dpi and area under autolysis was measured at 16dpi.

doi:10.1371/journal.pone.0159244.g007

knockdown transformants, percentage of spores that germinated and formed appressoria at 6 and 12 hours was determined (Fig 8B and 8C). While in WT 90% of spores had germinated by 12 hours, in knockdown transformants the percentage of ungerminated spores ranged from 33% in  $\Delta mnr2+$ siALR2\_79 to 41% in WT+siALR2\_48. In WT, the percentage of appressoria formed increased from 41% at 6 hours to 85% at 12 hours. In  $\Delta mnr2$  the percentage of appressoria formed at 12 hours was 83%, which is comparable to WT. In the *MoALR2* knockdown transformant WT+siALR2\_48, the percentage of appressoria formed at 12 hours was only 33%. The percentage of spores that failed to germinate and form appressoria increased with higher level of silencing in the knockdown transformants (Fig 8C). Since A2 and A15 failed to sporulate, mycelial plugs from these transformants were inoculated on hydrophobic surface and incubated under moist conditions for 48 hours (as mycelial tips are also capable of forming appressoria-like structures). The mycelial tips of A2 and A15 failed to develop any appressorium-like structure of the kind seen in the WT (Fig 8B). Thus it is evident that a minimum

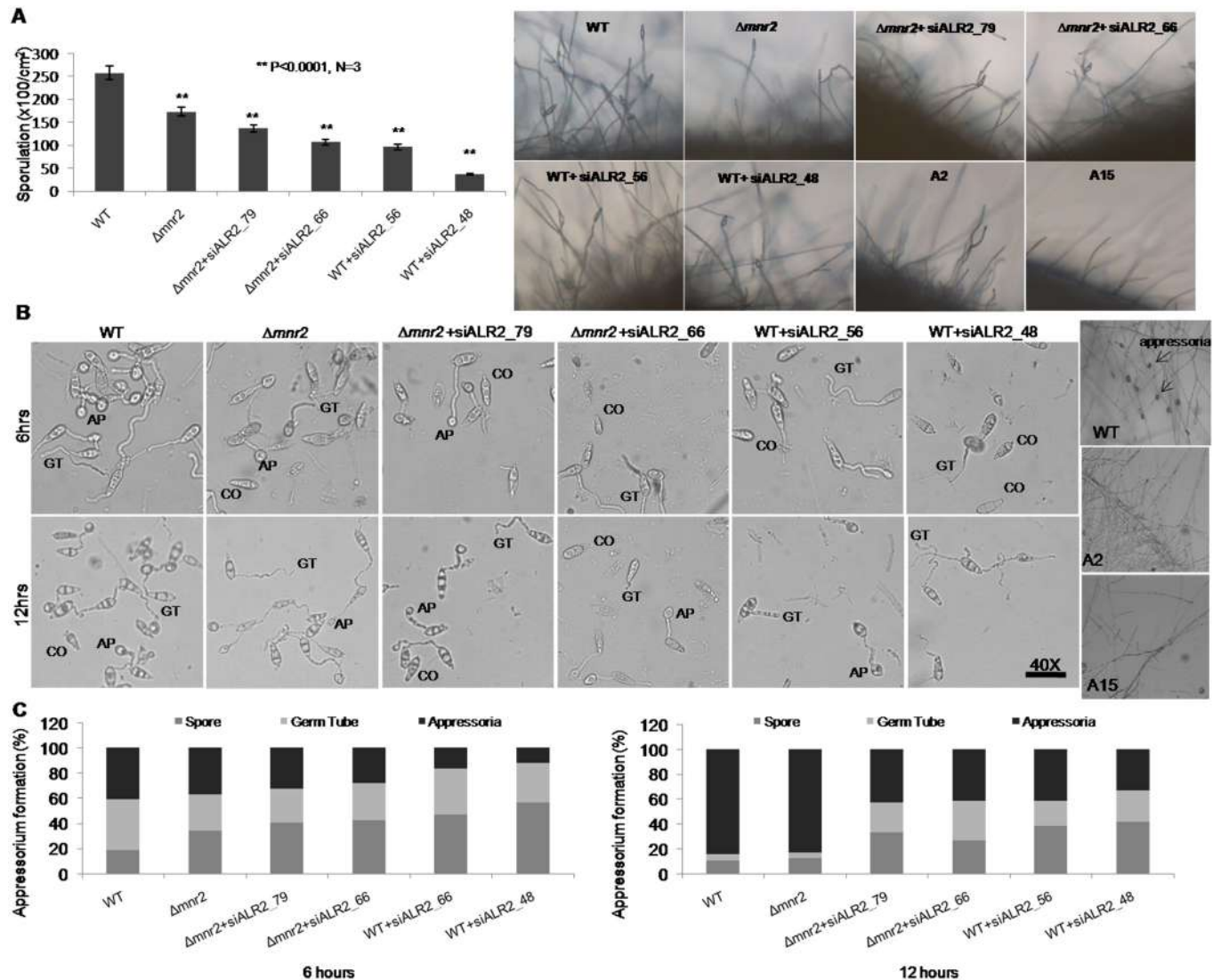


**Fig 8. CorA transporters are required for Sporulation and Appressorium formation.** (A) Ability of  $\Delta mnr2$  and knockdown transformants to sporulate was checked on OMA 8 days post inoculation and quantified. Aerial hyphal and conidial development were also assessed for  $\Delta mnr2$  and knockdown transformants at 48 hpi. (B), (C) Appressorial assay for  $\Delta mnr2$  and knockdown transformants was performed on hydrophobic gel bond film and the ability to form infection structure was assessed and quantified at 6 hours and 12 hours (CO-Conidium, GT-Germ tube, AP-Appressorium). The values are represented as percentage of spore (ungerminated), germ tube and appressoria formed at the given time interval. Mycelial blocks were placed on hydrophobic surface and incubated upto 72 hours at 28°C for non-sporulating transformants. The experiments were repeated in triplicate, N = 3.

doi:10.1371/journal.pone.0159244.g008

level of *MoALR2* expression is critical for appressorium formation from germinated spores as well as from hyphae.

To test the ability of the conidia to germinate and form appressoria in presence of EDTA and EDTA with 50mM Mg<sup>2+</sup> supplementation, appressorium formation was studied at different time points in WT (Fig 9A). In the presence of 0.25mM EDTA, even at 24 hours the spores failed to form appressoria (for every time point n>100). Most of the spores (63%) were stalled in the germ tube stage (S5B Fig). Extracellular Mg<sup>2+</sup> (50mM) was able to rescue the defect in appressorium formation in presence of EDTA in WT. At 24 hours, approximately 53% of the spores had formed appressoria in presence of 50mM Mg<sup>2+</sup> and 0.25mM EDTA (S5B Fig).

Rice detached leaf infection test showed that the severity of infection decreased in the knockdown transformants (Fig 9B), where small brown lesions were observed as compared to the typical brown bordered gray centered lesions of the WT. The decrease was consistent with the decrease in the levels of *MoALR2*, indicating the importance of *MoALR2* for pathogenicity

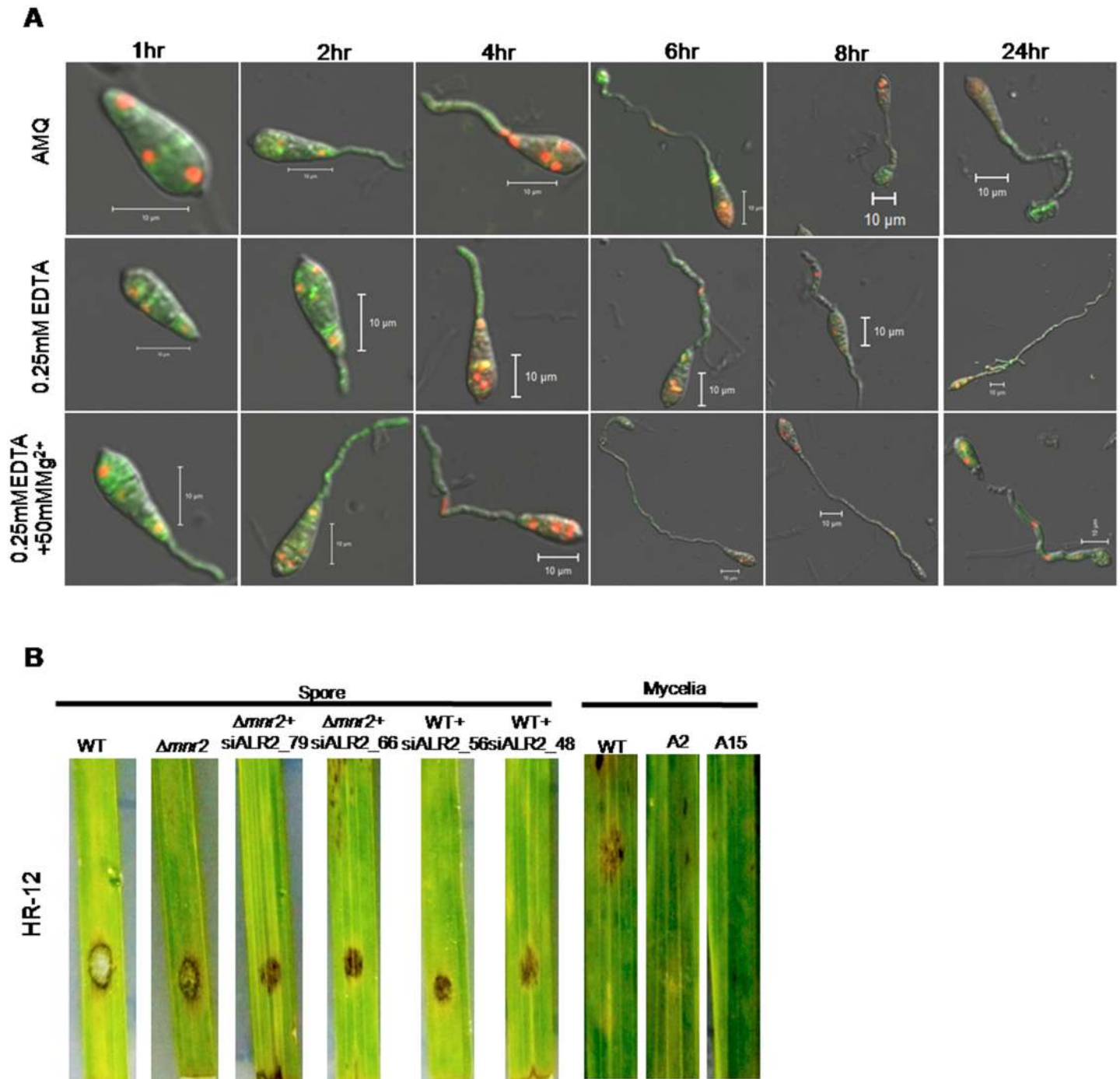


**Fig 9. Mg<sup>2+</sup> uptake by CorA transporters is essential for progression of the infection cycle.** (A) Ability to form appressoria in water, 0.25mMEDTA and 0.25mMEDTA+50mM Mg<sup>2+</sup> was observed at different time intervals in WT tagged with H1:RFP and Tub:GFP. (B) Detached rice leaves of cultivar HR12 were inoculated with spores (1x10<sup>4</sup>/ml) and mycelial plugs. Disease symptoms (lesions) were assessed 4 days post inoculation. The experiments were repeated in triplicate, N = 3.

doi:10.1371/journal.pone.0159244.g009

in *M. oryzae*. Thus, extracellular Mg<sup>2+</sup> availability and transport are critical at all stages of the infection cycle including hyphal growth, conidiation, spore germination, appressorium formation and disease progression in *M. oryzae*.

### MoALR2 affects intracellular cAMP levels in *M. oryzae*

In *M. oryzae*, cAMP mediated signaling through *MoPMK1* (Mgg\_09565) is crucial for conidiation and appressorium initiation [7, 35]. cAMP is synthesized by Mg<sup>2+</sup> dependent adenylate cyclase [14, 36]. In view of the low Mg<sup>2+</sup> levels in the knockdown transformants, we looked for changes in intracellular cAMP levels. The levels of cAMP in  $\Delta mnr2$  and the knockdown transformants ranged from 97 to 20 fmol mg<sup>-1</sup> as compared to 105 fmol mg<sup>-1</sup> in WT (Fig 10A). The

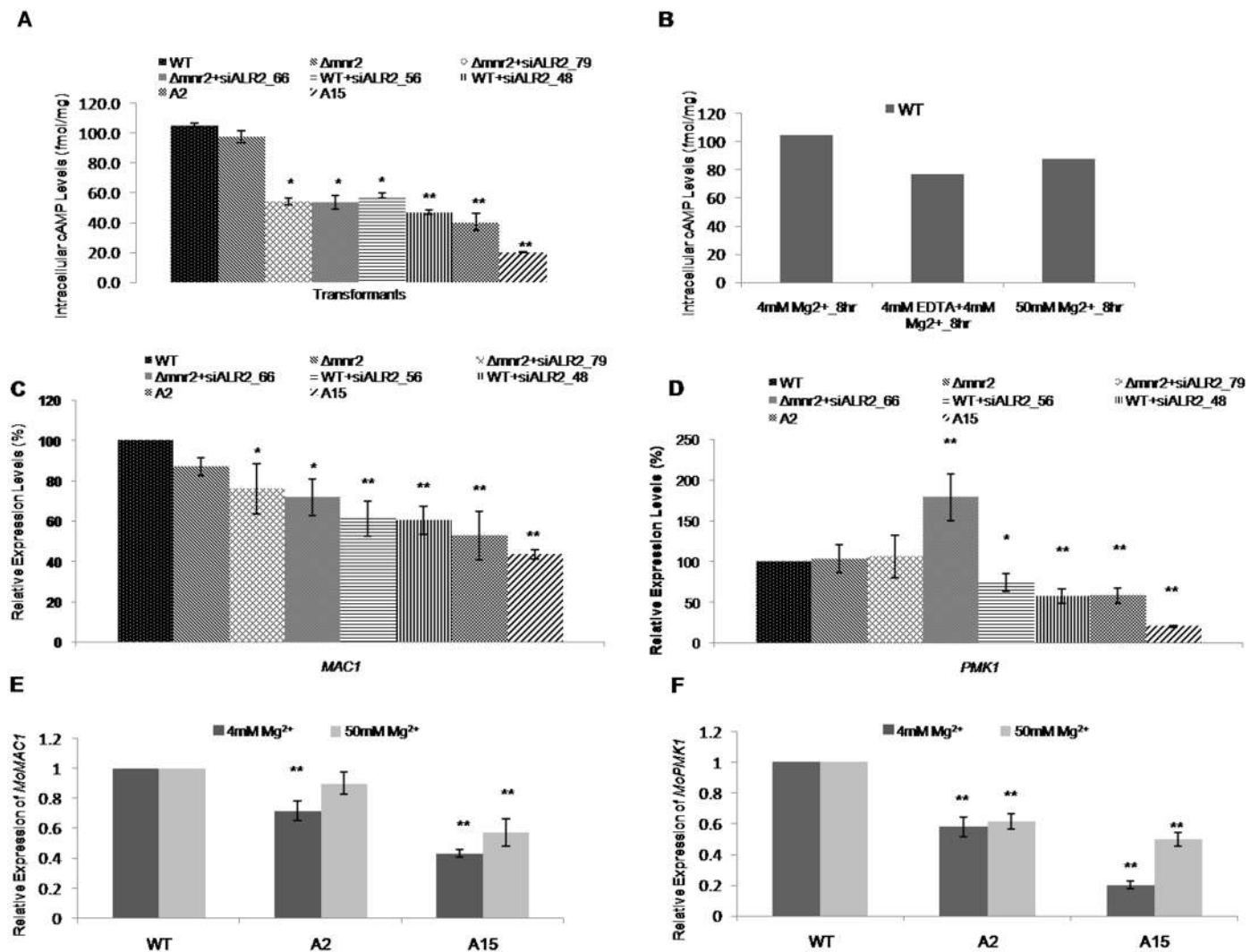


**Fig 10. *MoALR2* affects intracellular cAMP levels and cAMP mediated signaling in *M. oryzae*.** (A) Intracellular cAMP levels were estimated in WT,  $\Delta mnr2$  and knockdown transformants. The bar graph represents cAMP levels in fmol mg<sup>-1</sup>. (B) Estimation of intracellular levels of cAMP at 50mM extracellular Mg<sup>2+</sup> in the double knockdown transformants, A2 and A15 in presence of 4mM Mg<sup>2+</sup>, 4mM Mg<sup>2+</sup> + 4mM EDTA and at 50mM Mg<sup>2+</sup>. The values are expressed in fmol mg<sup>-1</sup>. (C), (D) mRNA levels of *MoMAC1* and *MoPMK1* were estimated by qRT-PCR in WT,  $\Delta mnr2$  and knockdown transformants. (E), (F) mRNA levels of *MoMAC1* and *MoPMK1* were estimated by qRT-PCR at two different concentrations of extracellular Mg<sup>2+</sup> in WT, A2 and A15. The transcript levels were normalized to that of WT. Error bar denote SD. \*\* means P value at <0.0001 and \* means significant at P value <0.05. The experiments were repeated in triplicate, N = 3.

doi:10.1371/journal.pone.0159244.g010

cAMP levels correlated with the transcript levels of *MoALR2* and intracellular  $Mg^{2+}$  levels in the transformants. In WT, cAMP levels decreased in presence of EDTA (Fig 10B) and were consistent with the intracellular levels of  $Mg^{2+}$  in presence of EDTA described earlier (Fig 2D). cAMP levels were restored at 50mM  $Mg^{2+}$  at 8 hours in WT (Fig 10B). In presence of EDTA, cAMP levels in A2 and A15 did not correlate to intracellular  $Mg^{2+}$  levels (data not shown).

We studied the expression of the adenylate cyclase gene, *MoMAC1* (Mgg\_09898) and of *MoPMK1* (encoding MAPK) in the knockdown transformants and found significant decrease in expression, with the transcript levels decreasing to 43% and 20% respectively in A15 (Fig 10C and 10D). To study whether extracellular  $Mg^{2+}$  affects expression of *MoMAC1* and *MoPMK1*, we looked at their transcript levels in A2 and A15 with 50mM  $Mg^{2+}$  supplementation, and found that expression was restored to WT levels (Fig 10E and 10F). Since the knockdown transformants of *MoALR2* showed decreased ability to conidiate and form appressoria, the low level of intracellular cAMP is likely to be one of the factors contributing to the defect seen in appressorium formation in knockdown transformants.

### MoALR2 knockdown transformants show altered cell wall integrity

$Mg^{2+}$  is vital for the integrity of the cell wall and cell membrane [37, 9–12]. We asked whether decreased  $Mg^{2+}$  levels lead to changes in cell wall integrity (CWI). Growth was measured on media containing the cell wall stressors Congo Red (CR) [38] and Caffeine [39–41]. *Δmnr2* transformants were resistant to 1.5 and 2 mg ml<sup>-1</sup> CR, similar to WT. However the knockdown transformants, both in WT and *Δmnr2* backgrounds, were more sensitive to CR, with A15 showing the maximum sensitivity (Table 2).

The degree of sensitivity towards cell wall stressors increased in proportion to silencing of *MoALR2*.  $Mg^{2+}$  supplementation could restore the normal (lower) sensitivity to cell wall stressors (S6 Fig). These results indicate that maintenance of  $Mg^{2+}$  levels dependent on *MoALR2* is critical for the integrity of the cell wall.

To understand the cell wall defects in the knockdown transformants better, we looked at expression of cell wall maintenance related genes. We found decreased expression of two chitin synthase genes, *MoCHS1* (Mgg\_01802) and *MoCHS4* (Mgg\_09962), in the knockdown transformants (Fig 11E).

**Table 2. Cell Wall Integrity assay.**

Transformants	Growth diameter (centimeters)				
	YEGA	1.5 mg/ml Congo Red	2.0 mg/ml Congo Red	2.5mM Caffeine	3mM Caffeine
WT	2.5 ±0.063	2.26 ±0.020	1.25 ±0.029	1.74 ±0.006	1.40 ±0.013
<i>Δmnr2</i>	2.47 ±0.032	1.63 ±0.016 <sup>a</sup>	1.20 ±0.010	1.57 ±0.016 <sup>a</sup>	1.34 ±0.013
<i>Δmnr2</i> +siALR2_79	2.3 ±0.073 <sup>a</sup>	1.69 ±0.020 <sup>a</sup>	1.19 ±0.011	1.21 ±0.010 <sup>a</sup>	1.06 ±0.020 <sup>a</sup>
<i>Δmnr2</i> +siALR2_66	2.28 ±0.018 <sup>a</sup>	1.57 ±0.016 <sup>a</sup>	1.19 ±0.010 <sup>b</sup>	1.03 ±0.013 <sup>a</sup>	0.87 ±0.017 <sup>a</sup>
WT+siALR2_56	2.27 ±0.012 <sup>a</sup>	1.57 ±0.019 <sup>a</sup>	1.17 ±0.013 <sup>b</sup>	1.11 ±0.006 <sup>a</sup>	1.03 ±0.013 <sup>a</sup>
WT+siALR2_48	2.25 ±0.032 <sup>a</sup>	1.22 ±0.017 <sup>a</sup>	1.03 ±0.019 <sup>a</sup>	1.01 ±0.006 <sup>a</sup>	0.97 ±0.016 <sup>a</sup>
A2	2.08 ±0.048 <sup>a</sup>	1.22 ±0.010 <sup>a</sup>	1.02 ±0.018 <sup>a</sup>	0.71 ±0.020 <sup>a</sup>	0.69 ±0.005 <sup>a</sup>
A15	1.95 ±0.032 <sup>a</sup>	1.02 ±0.006 <sup>a</sup>	0.87 ±0.006 <sup>a</sup>	0.51 ±0.023 <sup>a</sup>	0.35 ±0.003 <sup>a</sup>

2X2 mm mycelial plugs of WT, *Δmnr2* and knockdown transformants were inoculated on YEG and YEG supplemented with Congo Red and Caffeine. Growth was assessed 5 days post inoculation. Data are presented as mean±SD from three independent experiments. Two-way ANOVA followed by Fisher's LSD test was performed at 95% confidence interval.

<sup>a</sup> means significantly different from WT at P value <0.0001

<sup>b</sup> means significantly different from WT at P value <0.05.

doi:10.1371/journal.pone.0159244.t002

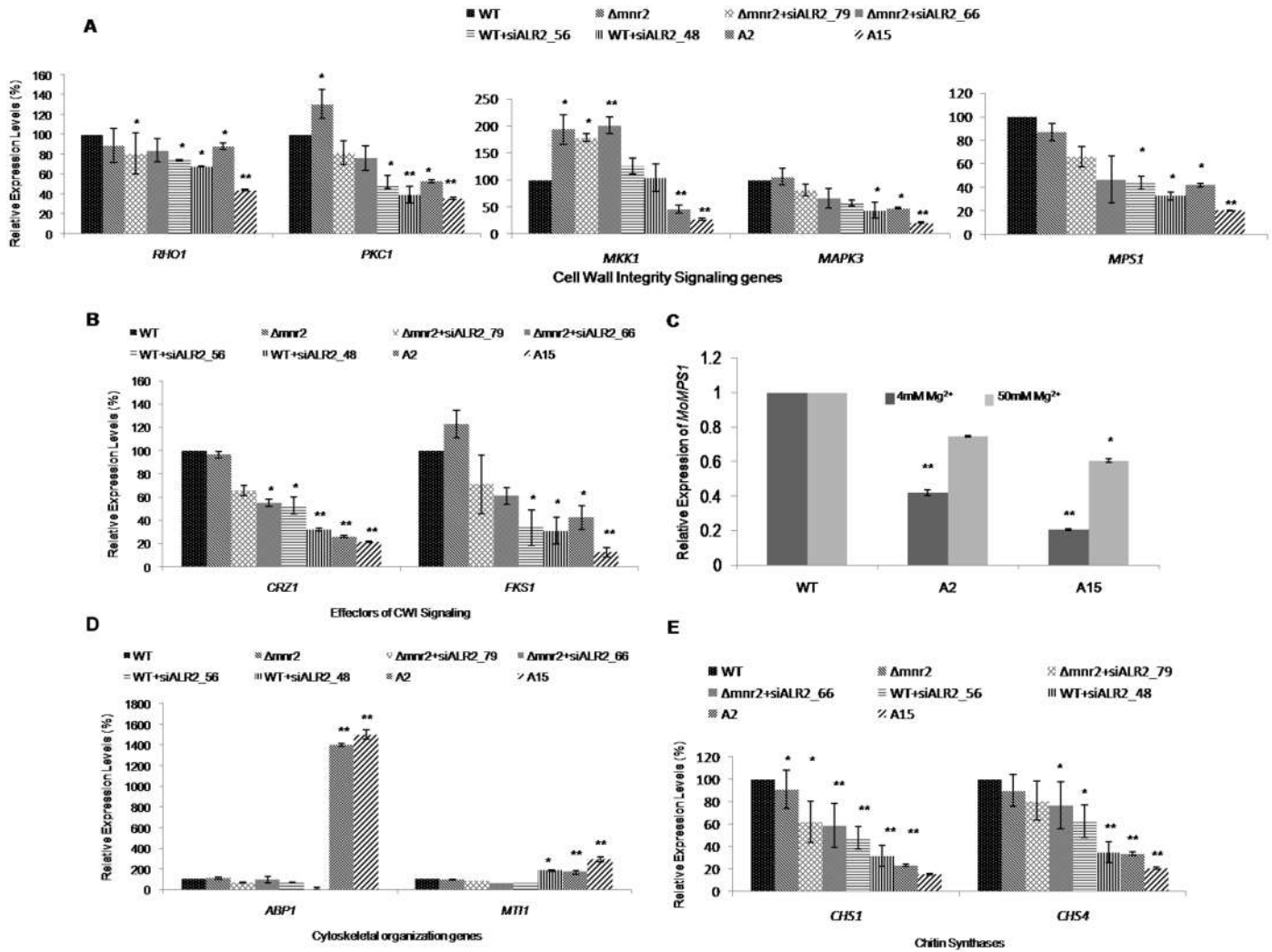


**Fig 11. Expression analysis of genes involved in the CWI Pathway in knockout and knockdown transformants.** (A) mRNA levels of *MoGTBP1*, *MoPKC1*, *MoMAPK3*, *MoMKK1* and *MoMPS1* were estimated by qRT-PCR. (B) mRNA levels of *MoCRZ1* and *MoFKS1* were estimated by qRT-PCR. (C) mRNA levels of *MoMPS1* were estimated by qRT-PCR at two different concentrations of extracellular  $Mg^{2+}$  in WT, A2 and A15. (D) mRNA levels of *MoABP1* and *MoMT1* were estimated by qRT-PCR. (E) mRNA levels of *MoCHS1* and *MoCHS4* were estimated by qRT-PCR. All transcript levels were normalized to that of WT. Error bar denote SD. \*\* means P value at <0.0001 and \* means significant at P value <0.05. The experiments were repeated in triplicate, N = 3.

doi:10.1371/journal.pone.0159244.g011

We studied the expression of genes involved in the CWI pathway in  $\Delta mnr2$  and knockdown transformants. In simultaneously silenced transformants (for *MoALR2* and *MoMNR2*), A2 and A15, there was significant down-regulation of genes involved in the Pkc1 activated mitogen activated protein (MAP) kinase cascade including *MoPKC1*, *MoMKK1*, *MoMAPK3* and *MoMPS1* (at  $P < 0.05$ ) (Fig 11A) only for *MoGTBP1* (Mgg\_07176) (*Rho1*), did expression not change significantly (at  $P < 0.0001$ ). In contrast  $\Delta mnr2$  showed increased expression of *MoPKC1* and *MoMKK1*. Increased expression of *MoMKK1* was also observed in  $\Delta mnr2$ +siALR2\_79 and  $\Delta mnr2$ +siALR2\_66 (*MoALR2* silencing in  $\Delta mnr2$  background), while no significant changes were observed in WT+siALR2\_56 and WT+siALR2\_48 (*MoALR2* silencing in WT background).

The expression of downstream effectors of CWI signaling, *MoFKS1* (Mgg\_00865) and *MoCRZ1* (Mgg\_05133) was also significantly decreased in the knockdown transformants (Fig 11B). The expression of *MoMPS1* in A2 and A15 was restored to WT levels when

supplemented with 50mM  $Mg^{2+}$  (Fig 11C), indicating that  $Mg^{2+}$  levels affect the expression of *MoMPS1*. The decreased expression of CWI signaling genes in the knockdown transformants explains the sensitivity towards cell wall stress and demonstrates the role of *MoALR2* in maintenance of  $Mg^{2+}$  levels critical for cell wall integrity.

Actin cytoskeletal reorganisation is an important aspect of the compensatory response to cell wall defects [37]. We analyzed the expression of the genes *MoABP1* (Mgg\_06358) and *MoMTI1* (Mgg\_04116), in  $\Delta mnr2$  and the knockdown transformants by qRT-PCR. There was significantly increased expression of both *MoABP1* and *MoMTI1* in A2 and A15 (at  $P < 0.05$ ) (Fig 11D). The expression of *MoABP1* was 15 fold higher, implying that MoAbp1 might play a role in stabilizing the cytoskeleton and membranes to compensate for the lack of  $Mg^{2+}$ , which is known to be crucial for maintenance of cell shape and membrane integrity.

## Discussion

Magnesium is an essential mineral nutrient with roles in stability of DNA structure, cell membrane maintenance, activity of ATP, and as a cofactor of several enzymes. In spite of the importance of  $Mg^{2+}$  in cellular physiology, there is little information about the transport, regulation and storage of  $Mg^{2+}$  in fungi. In this study, we show that the CorA  $Mg^{2+}$  transporters MoAlr2 and MoMnr2 play important roles in development and virulence of the model fungal pathogen, *Magnaporthe oryzae*. Our results, supported by the phenotypic defects seen in the knockout and knockdown transformants— $\Delta mnr2$ , WT+siALR2,  $\Delta mnr2$ +siALR2 and transformants in which both genes were simultaneously knocked down (A2 and A15)—show that CorA  $Mg^{2+}$  transporters are intimately involved at all stages of the infection cycle of *M. oryzae*. Chemical inhibition of  $Mg^{2+}$  transport by the CorA specific inhibitor Co(III)Hex. in wild type also produced growth defects. We also used the  $Mg^{2+}$  chelator EDTA to deplete  $Mg^{2+}$  to study the effect of extracellular magnesium availability in the wild type strain B157. Higher levels of EDTA completely abolish growth in WT, while lower levels inhibit spore germination, and an even lower concentration of EDTA is sufficient to inhibit the process of appressorium formation. A corresponding gradation of phenotypes is also observed in the different knockdown transformants, where effects of low silencing are seen on appressorium development. With stronger silencing spore germination too is affected, and at the highest level of silencing we see drastic effects even on hyphal growth, suggesting that during the course of the infection cycle from vegetative hyphal growth to sporulation to appressorium formation, the requirement for  $Mg^{2+}$  transport into the cell goes up. Recently, it has been shown that *MoALR2* is down-regulated during *in planta* growth in barley and rice at 72 hours post inoculation (hpi) [42].

The severity of growth defects of transformants was further intensified in low  $Mg^{2+}$  conditions; for instance,  $\Delta mnr2$  knockout showed less growth than WT in presence of EDTA (S7 Fig). This high  $Mg^{2+}$  requirement could be for processes like cell wall remodeling, cell division and maintenance of surface hydrophobicity that form a critical part of the differentiation process. Spore germination and appressorium formation, where we have shown a requirement for MoAlr2, are part of the early events of infection on the plant host and are completed well before 72 hpi. Due to failure to obtain a true knockout for *MoALR2* in spite of the use of diverse approaches, and from the drastic defects observed in the knockdown transformants, we conclude that *MoALR2* is likely essential for viability of the rice blast fungus. Further, we did not obtain any knockdown transformants with less than 30% expression of *MoALR2*, indicating that a critical minimum level of *MoALR2* expression is essential for viability (although it cannot be ruled out that our silencing procedure is unable to achieve a higher level of silencing). Previous large scale random mutagenesis screens for pathogenicity have also not uncovered any mutants of this gene. In all, our results show that the knockdown transformants have

defects in hyphal growth, conidiation, spore germination, appressorium formation and infection. Given this requirement for  $Mg^{2+}$  transport at all stages of the *M. oryzae* infection cycle, CorA transporters may be good targets for the development of antifungal agents. Ion channel blockers, agents that sequester  $Mg^{2+}$  from the fungal environment and rice lines expressing RNAi targeting  $Mg^{2+}$  transporter could prove fatal to fungal proliferation.

Element analysis in the knockdown transformants showed that decreased levels of MoAlr2 transporter led to lowered intracellular levels of  $Mg^{2+}$  (Fig 2C). The knockdown transformant A15, which showed maximum silencing of *MoALR2* and *MoMNR2*, also had the lowest intracellular levels of  $Mg^{2+}$ . Complementation studies in *S. cerevisiae* also suggest that *MoALR2* and *MoMNR2* have a definite role in  $Mg^{2+}$  transport. We used the 489–812 amino acid region encompassing the CorA transmembrane helices to carry out complementation and have shown that these 324 amino acids at the C terminus of MoMnr2 are sufficient for the function of  $Mg^{2+}$  transport (Fig 1D). Earlier mutagenesis experiments in *ScAlr1* showed similar effects where the 239 amino acids at the N-terminal and 53 amino acids at the C-terminal are not essential for  $Mg^{2+}$  uptake [43].

Regulation of  $Mg^{2+}$  involves localization, compartmentalization, and sequestration [44]. Higher expression of *MoALR2* was observed in  $\Delta mnr2$  transformants. The maximum sensitivity of  $\Delta mnr2$  to Co(III)Hex. and higher intracellular levels of  $Mg^{2+}$  in  $\Delta mnr2$  correlated with the increased levels of *MoALR2*. We suggest that absence of an organellar transporter MoMnr2 in the  $\Delta mnr2$  knockout transformant may lead to up-regulation of expression of *MoALR2* encoding the plasma membrane transporter. The external environment of the fungus is dynamic with respect to the levels of divalent cations like  $Mg^{2+}$  and  $Ca^{2+}$ . In *S. cerevisiae*, under  $Mg^{2+}$  limiting conditions, vacuolar  $Mg^{2+}$  contributes towards the maintenance of cytosolic  $Mg^{2+}$  levels through the activity of *MNR2* [45]. We show that CorA transporters are regulated in response to changes in the extracellular ionic milieu. *MoALR2* and *MoMNR2* are induced by the depletion of extracellular  $Mg^{2+}$ , while their levels decreased at higher concentrations of  $Mg^{2+}$ . *MoMNR2* may be down-regulated to reduce the efflux of  $Mg^{2+}$  from organellar stores, thereby preventing toxicity due to increased cytoplasmic levels of  $Mg^{2+}$ . We found that with increasing concentrations of  $Ca^{2+}$ , both the transcript and protein levels of *MoALR2* increased. The severity of panicle blast has previously been shown to be positively correlated with  $Mg^{2+}$  levels and negatively affected by  $Ca^{2+}$  concentration in the plant tissue [46]. Determination of the ionic composition of the leaf and transporter levels in the fungus during invasion and proliferation will shed further light on the significance of  $Mg^{2+}$  uptake by CorA transporters at the site of infection.

The *MPG1* hydrophobin gene plays a key role in the development of *M. oryzae* and its expression is regulated in response to diverse morphogenetic and environmental signals. The Mpg1 protein at the cell surface perceives stimuli such as surface hydrophobicity and conveys the signal through G protein coupled receptors to activate adenylate cyclase, which in turn activates Pka and Pmk1 dependent MAP kinase, vital for appressorium development and maturation [35]. While MoPmk1 acts downstream of MoMpg1, it is also known in turn to regulate the expression of the *MoMPG1* gene [47]. MoMpg1 is essential for conidiogenesis and appressorium formation and it has been proposed that MoMpg1 may exert positive feedback on its own expression through the cAMP response pathway [47].  $\Delta mnr2$  knockout and *MoALR2* knockdown transformants showed fewer aerial hyphae, surface hydrophobicity defects and a wettable phenotype. Decrease in hydrophobicity in presence of low levels of  $Mg^{2+}$  has been previously observed in *S. cerevisiae* [48]. Our knockdown transformants also showed lower expression of hydrophobin genes (Fig 7D). We demonstrate that a reduction in  $Mg^{2+}$  levels, either by knockdown of transporter function or by using EDTA in the WT, has an effect on the expression of the hydrophobin gene *MoMPG1*.  $\Delta mnr2$  showed an early autolysis phenotype.

The autolysis occurred even earlier in the knockdown transformants both in WT and  $\Delta mnr2$  background and the degree of autolysis correlated with the degree of knockdown of *MoALR2*.

We also found that the intracellular levels of cAMP are lower in the *MoALR2* knockdown transformants. cAMP is an important secondary messenger in the cell and its levels regulate appressorium formation in *M. oryzae* [7, 35]. Decrease in intracellular cAMP reduces the flux through the Pmk1 pathway and in turn reduces the expression of *MoMPG1*, thus possibly contributing to the defects in conidiation, appressorium formation and infection seen in *MoALR2* knockdown transformants.

We found that silencing of the  $Mg^{2+}$  transporters led to a loss of cell wall integrity, indicating that  $Mg^{2+}$  transport is vital for cell wall structure. The cell wall integrity (CWI) signaling cascade has been studied extensively in *S. cerevisiae* and involves a Rho1 'master regulator' which activates Pkc1 activated mitogen activated protein (MAP) kinase cascade involving effectors like Pkc1, Bck1, Mkk 1/2 and Mpk1. These effectors regulate a diverse set of processes including  $\beta$ -glucan synthesis at the site of cell wall remodeling, gene expression related to cell wall biogenesis, organization of the actin cytoskeleton, and secretory vesicle targeting to growth sites [49]. We hypothesized that a decrease in  $Mg^{2+}$  levels in knockdown transformants affects cell wall structure by alteration of the CWI signaling. Consistent with this, we found a decrease in expression of genes involved in CWI signaling in the knockdown transformants. CWI signaling is important for invasive growth, conidiation and plant penetration in *M. oryzae* [50]. The decreased expression of hydrophobins, *PMK1* and genes encoding members of the MoMps1-dependent CWI pathway, and low levels of cAMP in *MoALR2* knockdown transformants are among the major factors contributing to their decreased ability to conidiate, form appressoria and cause infection.

We show that *MoALR2* regulates intracellular  $Mg^{2+}$  concentration and modulates key signaling pathways necessary for development and pathogenicity in *M. oryzae*. Decrease in the expression of the CorA  $Mg^{2+}$  transporter *MoALR2* leads to defects in growth, conidiation and appressorium formation, which are critical features for successful establishment of the pathogen within the host. Overall, we show that the CorA transporter *MoAlr2* is the dominant factor for maintenance of  $Mg^{2+}$  homeostasis during growth and differentiation in *M. oryzae*. Knockdown of CorA  $Mg^{2+}$  transporters below a critical level makes the pathogen lose its virulence and hence these transporters are potential targets for anti-fungals. In future, the role of CorA transporters in sub-cellular  $Mg^{2+}$  distribution and dynamics of cations between the organelles and the cytoplasm needs to be addressed in greater detail.

## Materials and Methods

### Fungal strain and culture conditions

*Magnaporthe oryzae* B157 strain (MTCC accession number 12236), belonging to the international race IC9 was previously isolated in our laboratory from infected rice leaves [51]. The  $\Delta ku80$  mutant used in the present study was generated by replacing *MoKU80* ORF with Zeocin selection marker in wild type B157 strain (WT) in our laboratory. The fungus was grown and maintained on YEG medium (Glucose 1 g, yeast extract 0.2 g, H<sub>2</sub>O to 100 ml) or Oatmeal agar (Hi-Media, Mumbai, India).

### Complementation of a *S. cerevisiae* $\Delta alr1 \Delta alr2$ mutant

*S. cerevisiae*  $\Delta alr1 \Delta alr2$  mutant (CM66) having the genotype *Mata alr1::HIS3, alr2::TRP1, his3-200, ura3-52, leu2-1, lys2-202, trp1-63* and the strain from which it was derived (CM52) having the genotype *Mata his3-200, ura3-52, leu2-1, lys2-202, trp1-63* was used for functional complementation studies. The full length gene of *MoALR2* (1.9kb) was amplified from genomic DNA

and cloned at *PvuII* site in the yeast episomal vector pYES2 (Invitrogen, California, USA) to generate pYES2-*MoALR2*. The full length gene of *MoMNR2* (2.5kb) was amplified from genomic DNA and cloned first at *EcoRV* site in pBluescript KS (+). The full length gene was moved into pYES2 vector at *HindIII* and *BamHI* site under Gal1 promoter to give pYES2-*MoMNR2*. For *MoMNR2*<sub>489-812</sub> cloning, the CorA domain of *MoMNR2* was PCR amplified from genomic DNA and cloned first in pBluescript KS (+) at *EcoRV* site. The CorA domain of *MoMNR2* was moved into pYES2 vector at *XhoI* and *BamHI* site under Gal1 promoter to give pYES2-*MoMNR2*<sub>489-812</sub>. This construct was used to transform the *S. cerevisiae*  $\Delta$ *alr1* $\Delta$ *alr2* double mutant (CM66). Colonies were selected on SD medium lacking uracil and having lysine, leucine, 2% Galactose and 500mM MgSO<sub>4</sub>. Transformed colonies obtained were grown in SD media (lysine + leucine + 2% Galactose + 500mM MgSO<sub>4</sub>) till saturation and cells were spotted on SD media having leucine, lysine, 2% Galactose and 4mM MgSO<sub>4</sub>/500mM MgSO<sub>4</sub>. The growth of colonies was seen 4 days post inoculation at 28°C. All primers used in the study are listed in [S4 Table](#).

### Raising of antibodies against MoAlr2 and MoMnr2

The CorA domains of MoAlr2 and MoMnr2 have 50% identity at the protein level and the size of the proteins is 70kDa and 90kDa respectively. The CorA domain from *MoMNR2* was amplified (1kb) from genomic DNA as it has no intron. The amplified product was cloned in pBluescript KS (+) vector at *EcoRV* site and then was ligated in bacterial expression vector pET30a (+) vector at *NdeI* and *KpnI* site translationally in frame with a (His)<sub>6</sub> tag at the C terminus. *E. coli* BL21 DE3 cells were transformed with the protein expression construct. The transformed colonies were grown in Luria Bertani (LB) medium O/N. 1% inoculum was used the next day and the culture was grown to an O.D. ( $\lambda_{600}$ ) of 0.4 to 0.6 O.D. 1mM IPTG was used for induction of the protein for another 4 hours. The induced protein having Polyhistidine at the carboxyl terminus was purified using Ni-NTA affinity chromatography (Novagen, Darmstadt, Germany) according to manufacturer's protocol. The purified protein was used to raise polyclonal antibodies in New Zealand White Rabbit. Antibody titer was estimated by indirect-enzyme linked immunosorbent analysis (ELISA) using HRP conjugated anti-rabbit IgG (Bangalore Genie, Bangalore, India) as the secondary antibody.

### Indirect immunolocalization of MoAlr2 and MoMnr2 in *M. oryzae*

The wild type B157 spores were fixed with 10% formaldehyde, 5% acetic acid, and 85% ethanol for 30 minutes at room temperature and the fixed sample was incubated in PBS + 0.1% Triton X-100 for 2–5 minutes. The sample was given wash with PBS for 10 to 15 minutes. The fixed samples were further treated as described [52] with few modifications. Primary antibodies used were against CorA domain of MoMnr2. Secondary antibody, TRITC-conjugated anti-rabbit IgGs raised in goat, (Sigma Chemical Co, St Louis, MO, USA) diluted to 1:20 in PBS was used for staining for 2 hours. Three washes each of 15 minutes were given with PBST which was followed by vacuolar staining with Oregon green 488 carboxylic acid diacetate (cDFFDA) (Molecular Probes, Invitrogen, California, USA) for 10 minutes followed by three washes with PBST. The slides were observed under 63X using LSM 700 microscope (Carl Zeiss, Jena, Germany) at 557nm excitation and 576nm emission for TRITC and at 501nm excitation and 526nm emission for Oregon green 488. Image analysis was done using ZEN software.

### Plasmid construction and transformation of *M. oryzae*

The vector pGKO2-*MoALR2* was constructed for carrying out targeted disruption in WT. Full length gene of *MoALR2* (1.9kb) was PCR amplified, end filled and cloned at *EcoRV* site in

pBluescript KS (+) to give KS-*MoALR2*. The HPT cassette used for disrupting the gene *MoALR2* was taken out from pAN7.1 [27] vector using *Bgl*II and *Hind*III having glyceraldehyde 3 phosphate dehydrogenase (*gpdA*) promoter, end filled and cloned at *EcoRV* site (present in between the *MoALR2* gene). The whole disruption cassette (~6kb) was moved from pBluescript KS (+) and cloned into a binary vector pGKO2 at *Kpn*I and *Spe*I site. The *A. tumefaciens* strain LBA4404/pSB1 was first transformed with pGKO2-*MoALR2*-HPT via triparental mating (Helper plasmid pRK2013). The transformed *Agrobacterium* was then used to carry out *A. tumefaciens* mediated transformation of *M. oryzae* as described [53]. The transformants were selected on Hygromycin (200 $\mu$ g ml<sup>-1</sup>) and 5-fluoro-2'-deoxyuridine (5 $\mu$ M). We attempted several rounds of transformation to disrupt *MoALR2* using ATMT. Protoplast transformation was also carried out with the full disruption cassette and by split marker technique (two different overlap regions). Further, supplementation of different Mg<sup>2</sup> concentrations during selection was done to overcome the selective disadvantage facing slow growing mutants. A smaller disruption cassette of *MoALR2*(~4kb) was also made in the vector pBluescript KS (+) where KS-*MoALR2* was digested with *EcoRV* (site present in between the gene) and HPT cassette of 2kb was PCR amplified from pSilent and cloned at *EcoRV* site in KS-*MoALR2* to give pBSKS-*MoALR2*-HPT. This cassette was used to carry out transformation of the  $\Delta$ *ku80* strain. Targeted deletion of *MoMNR2* was carried out by transforming WT protoplast with a knockout construct which was obtained by double-joint PCR [54], where ~1kb flanking sequence of *MoMNR2* was amplified and fused to Zeocin resistance cassette. Transformants were selected on Zeocin (300 $\mu$ g ml<sup>-1</sup>). They were screened with PCR using different sets of primer combinations and confirmed for target gene replacement by Southern blot analysis using both the flanking sequences as probes.

For knockdown of *MoALR2* a ~110 bp fragment of *MoALR2*, which spans the siRNA matching to the 5' UTR, was amplified and cloned in pSilent-Dual 2 vector [5] at *Sma*I site. For simultaneous silencing of *MoALR2* and *MoMNR2*, the full length gene of *MoALR2* cloned in pBluescript KS (+) was digested with *Kpn*I and *Bam*HI to give a fragment of 1.4kb (having a portion of the CorA domain) and was cloned in anti-sense orientation in pSilent-1 [55] at *Kpn*I and *Bgl*II site. For RNAi approach, the full length gene of *MoALR2* cloned in pBluescript KS (+) was digested with *Hind*III and 525bp fragment (spanning CorA domain) was cloned in pSilent-Dual 2 vector at *Hind*III site. The knockdown constructs were used for protoplast transformation of WT as described [31]. Putative knockdown transformants were selected on Hygromycin (200 $\mu$ g ml<sup>-1</sup>) and Geneticin (1mg ml<sup>-1</sup>). Untransformed WT was kept as a control which did not grow on either Hygromycin or Geneticin medium. Vector transformation (pSD2) was also done as a control. The transformants were maintained as monoconidial isolates to obtain pure cultures. The knockdown transformants were screened by PCR and confirmed by Southern hybridization.

## Nucleic acid manipulation and Southern Blotting

Fungal genomic DNA was extracted as described by Dellaporta et al. [56]. Southern blot analysis was carried out as previously described Sambrook et al. [57]. In case of  $\Delta$ *mnr2* and WT, genomic DNA was digested with *Hind*III, *Eco*RI and *Eco*RV and the blot was probed first with a 1kb upstream fragment of *MoMNR2* and then re-probed with a 1kb downstream fragment of *MoMNR2*. The knockdown transformants for *MoALR2* were digested with *Eco*RI and probed with 1.2kb upstream fragment of *MoALR2*. The simultaneously silenced transformants, A2 and A15 was digested with *Sal*I and the blot was probed with TrpC promoter (~400bp). The probes were labeled and hybridizing bands were detected using Gene Images AlkPhos Direct Labeling and Detection system as per manufacturer's instructions (Amersham, Buckinghamshire, England).

## Quantitative Real Time PCR analysis for gene expression

Fungus was grown in Complete Medium (CM) for 72 hours (when no treatment was given to the biomass), else it was grown in CM for 48 hours, followed by two washes of the biomass with sterile milliQ water. The fungus was then transferred into Minimal Medium for 24 hours after which it was given treatments of  $Mg^{2+}$  or  $Ca^{2+}$  for the given time period. Fungal biomass was harvested and frozen in liquid nitrogen. Total RNA was isolated using TRIzol reagent (Invitrogen Life Technologies, California, USA). 2  $\mu$ g of total RNA was reverse transcribed into first strand cDNA using oligo (dT) primer and M-MuLV Reverse transcriptase (NEB, Massachusetts, USA). Quantitative PCR was performed by monitoring in real time the increase in fluorescence of the SYBR Green dye either on a Light Cycler system for real-time PCR (Roche Applied Science, Mannheim, Germany) or ABI 7900 HT real time PCR (Applied Biosystems, California, USA), according to the manufacturer's instructions. Thermal cycling conditions consisted of 10 minutes at 95°C 1 cycle, followed by 40 cycles of 10 seconds at 95°C, 10 seconds at 55°C and 15 seconds at 72°C for SYBR chemistry. Also Taqman Probes (Applied Biosystems, California, USA) specific for gene(s) were used to validate and study expression profile quantitatively. Reaction conditions were according to manufacturer's instructions. Thermal cycling conditions consisted of 2 minutes at 50°C 1 cycle, 10 minutes at 95°C 1 cycle, 15 seconds at 95°C and 1 minute at 60°C 40 cycles. Each qRT-PCR quantification was carried out in triplicate and every biological repeat was kept in duplicate. To compare the relative abundance of target gene transcripts, the average threshold cycle (Ct) was normalized to that of GPDH gene for each of the treated samples as  $2^{-\Delta Ct}$ , where  $\Delta Ct = (Ct_{\text{gene of interest}} - Ct_{\text{GPDH}})$  and fold changes were calculated by  $2^{-\Delta\Delta Ct}$ , where  $\Delta\Delta Ct = (Ct_{\text{gene of interest}} - Ct_{\text{GPDH}})_{\text{test condition}} - (Ct_{\text{gene of interest}} - Ct_{\text{GPDH}})_{\text{control}}$ . The transcript levels were expressed as relative values, with 1 corresponding to the Wild type (WT).

**Statistical Analyses.** One-way ANOVA and non-parametric test was performed for all the statistical analyses wherein the mean of each column was compared with the mean of control column, followed by Fisher's LSD test at 95% confidence interval. \*\* means P value at <0.0001 and \* means significant at P value <0.05.

## X-Ray Fluorescence (XRF) for element analysis

For determining the levels of elements (mainly  $Mg^{2+}$  and  $Ca^{2+}$ ) in the knockout and knock-down transformants X-ray Fluorescence Analysis (XRF) [58] was performed. WT, knockout and knockdown transformants were grown in CM for 48 hours. The fungal biomass was washed twice with sterile milliQ water and the biomass was transferred into Minimal media for 24 hours. Then the biomass was grown under different concentrations of  $Mg^{2+}$  (4mM, 50mM and 250mM) for another 6 hours. The fungal biomass was harvested, frozen in liquid nitrogen and ground to fine powder. The biomass was dried completely at 37°C for 3–4 days, after which the element analysis was done using Energy dispersive X-ray Fluorescence Spectrometer EDX-720/800HS (Shimadzu, Singapore).

## Phenotypic Characterization of transformants

Vegetative growth of the knockdown and knockout transformants was measured on OMA and YEGA 5 days post inoculation. The experiments were performed with replicates in three independent experiments.

The ability to produce conidia was measured by counting the numbers of conidia for the knockdown and knockout transformants isolated from the surface. Quantification of conidia was done using a hemacytometer (Marienfeld Superior, Lauda-Konigshofen, Germany).

For appressorium formation, equal number of spores were inoculated on hydrophobic surface, Gelbond film (Amersham Pharmacia Biotech AB, Uppsala, Sweden) and incubated under

moist conditions for 6 and 12 hours. For non-sporulating knockdown transformants, mycelial plugs from actively growing transformants (5<sup>th</sup> day plate) were inoculated and incubated under moist conditions for 48 hours. Appressorium formation in the knockdown and knock-out transformants was checked at 40X magnification (Olympus, Tokyo, Japan). The relative percentage of appressoria formed was calculated for each time interval.

For assaying the sensitivity of the knockdown and knockout transformants towards CorA specific inhibitor (Cobalt(III) hexaammine(Co(III)Hex), a concentration ranging from 300 $\mu$ M to 400 $\mu$ M of Cobalt(III) hexaammine was added to YEG medium. The sensitivity was assessed 5 days post inoculation and radial growth was measured for these transformants.

### Surface hydrophobicity assay

The knockout and knockdown transformants were tested for defects in surface hydrophobicity with water and detergent solution (0.02% SDS+5mM EDTA). 5 day old fungal culture grown on YEGA was inoculated with water and detergent solutions. The wettability of the transformants was checked by the extent to which water or detergent was retained on mycelia compared to WT.

### Western blotting

Total protein was extracted from WT and knockdown transformants grown in CM for 72 h (when no treatment was given to the biomass); else the fungus was grown in CM for 48 hours, which was followed by two washes of the biomass with sterile milliQ water. The fungus was then transferred into Minimal medium for 24 hours after which the fungus was given treatments of Mg<sup>2+</sup> or Ca<sup>2+</sup> in the present study for the given time period. Fungal biomass was harvested and frozen in liquid nitrogen. Protein was extracted in Urea Buffer (9.5M urea, 2% v/v NP40, 5%  $\beta$ ME) for 1 hour at RT. The concentration of the protein was estimated by Bradford method. The protein samples were electrophoresed on 10% SDS-polyacrylamide gel, followed by electro transfer to PVDF membrane (Hybond ECL, Amersham, Buckinghamshire, England). The immunoblots were developed with 1<sup>o</sup> antibody against MoMnr2 CorA domain and 2<sup>o</sup> antibody conjugated with HRP using 3'-3'-diamino Benzidine tetrahydrochloride dehydrate (Fluka, Washington DC, USA) detection method (Bangalore Genei, Bangalore, India) and Super Signal West Pico Chemiluminescent substrate (Thermo Scientific, Rockford, USA) as per the manufacturer's instructions.

### Cation sensitivity assay

For cation sensitivity assays, the knockout, knockdown transformants and WT were inoculated on YEGA having Zinc (Zn<sup>2+</sup> 500 $\mu$ M), Cobalt (Co<sup>2+</sup> 150 $\mu$ M), Manganese (Mn<sup>2+</sup> 3mM), Iron (Fe<sup>3+</sup> 2mM), Copper (Cu<sup>2+</sup> 750 $\mu$ M), Aluminium (Al<sup>3+</sup> 800 $\mu$ M), Nickel (Ni<sup>2+</sup> 200 $\mu$ M). The sensitivity to different cations was studied by comparing the growth of transformants 5 days post inoculation with respect to WT. For all the sensitivity assays the minimum inhibitory concentration (MIC) was determined with respect to WT.

### Infection assay and cell wall integrity assay

Leaves of 21 day old rice seedlings of HR-12 cultivar were used for inoculating spores or mycelial plugs (for non-sporulating transformants) of knockout and knockdown transformants and were placed on water agar with kinetin (2 mg l<sup>-1</sup>). Disease symptoms were recorded after 3–4 days.

For the cell wall integrity assay, WT, knockout and knockdown transformants were inoculated on YEGA containing Congo Red (1.5mg ml<sup>-1</sup> and 2mg ml<sup>-1</sup>) or Caffeine (2.5mM and

3mM). Sensitivity to these cell wall stress molecules was studied by comparison of growth to that of WT 5 days post inoculation.

## Quantification of intracellular cAMP levels

WT, knockout and knockdown transformants were grown in CM for 48 hours. The fungal biomass was washed twice with sterile milliQ water and then the biomass was transferred into Minimal media containing 4mM  $Mg^{2+}$  for 24 hours. The biomass was harvested and frozen. The fungal biomass was ground to fine powder in liquid nitrogen and after the liquid nitrogen was evaporated, equal weight of frozen biomass (0.1gm) was taken and homogenized in 300 $\mu$ l of 0.1N HCl. The sample was vortexed for 30 minutes, followed by centrifugation at 5000 x g for 15 minutes at room temperature. The supernatant was collected and 100 $\mu$ l of sample in each case was taken. Quantification of intracellular cAMP levels was carried out by cAMP Direct Immunoassay Kit as per manufacturer's instructions (Calbiochem, Darmstadt, Germany).

## Supporting Information

**S1 Fig. Southern blot analysis of  $\Delta mnr2$  and WT.** (A) Schematic representation of *MoMNR2* locus and *MoMNR2* knockout cassette. (B) Wild type (WT) and three independent transformants (T1, T2, T3) for  $\Delta mnr2$  were digested with three different restriction enzymes and the blot was probed with two different probes to confirm targeted replacement of *MoMNR2* (L-1Kb ladder, P- Positive control).

(TIF)

**S2 Fig. Southern blot and Western blot analysis of knockdown transformants.** (A) WT, pSD2 transformants and knockdown transformants both in the background of WT and  $\Delta mnr2$  were digested with *EcoRI* and probed with 1.2Kb fragment upstream to *MoALR2* to confirm integration of the silencing cassette. WT and simultaneously silenced transformants, A2 and A15, were digested with *SalI* and probed with TrpCP to confirm integration of silencing construct. (B) Western blot showing levels of MoAlr2 and MoMnr2 proteins in WT and knockdown transformants using polyclonal antibodies raised against the CorA domain of MoMnr2. 30 $\mu$ g of protein was run on 10% SDS-PAGE and the blot was developed using luminal/enhancer + peroxide solution.

(TIF)

**S3 Fig. Element analysis and colony growth of knockdown transformants.** (A) Intracellular levels of  $Zn^{2+}$  in WT, A2 and A15 were estimated by XRF. The values are expressed as relative values, with 1 corresponding to the WT at 4mM  $Mg^{2+}$ . (B) Colony growth and melanization of WT,  $\Delta mnr2$  and knockdown transformants on OMA. Photographs were taken 9 days post inoculation.

(TIF)

**S4 Fig. Growth of WT under  $Mg^{2+}$  limiting conditions (EDTA).** (A) Growth of WT in presence of different concentrations of EDTA. 3x3 mm mycelial plugs were inoculated on OMA with and without EDTA and growth was assessed 5 days post inoculation. (B) Restoration of growth on  $Mg^{2+}$  supplements in presence of EDTA (top). Growth of sectorized colonies obtained under stress conditions (EDTA) (bottom). Growth of different sectors was assessed on OMA.

(TIF)

**S5 Fig. Sporulation and Appressorium formation in WT under  $Mg^{2+}$  limiting conditions (EDTA).** (A) The ability of WT to sporulate was checked on OMA with different

concentrations of EDTA 8 days post inoculation and quantified. (B) The ability to form appressoria in water, 0.25mM EDTA and 0.25mM EDTA+50mM  $Mg^{2+}$  was observed at different time intervals in WT and percentages of spores (ungerminated), germ tubes and appressoria formed were calculated for each time interval and for each condition.  
(TIF)

**S6 Fig. Recovery of growth on  $Mg^{2+}$  supplements in double knockdown transformants.** YEG and YEG with Congo Red (1.5mg/ml) and Caffeine (2.5mM) were supplemented with different concentrations of Magnesium. 2X2 mm mycelial plugs of WT and knockdown transformants A2 and A15 were inoculated. Recovery in growth was assessed 5 days post inoculation.  
(TIF)

**S7 Fig. Growth of WT and  $\Delta mnr2$  on media supplemented with EDTA.** WT and  $\Delta mnr2$  were grown on OMA and YEGA supplemented with 0.5mM EDTA. Growth was assessed 5dpi.  $\Delta mnr2$  shows more growth inhibition than WT.  
(TIF)

**S1 Table. Disruption of *MoALR2* by different approaches.** Table shows number of transformants obtained from ATMT and protoplast transformation (with full cassette and split marker using two different lengths of overlaps) and by using F2DU, different concentrations of  $MgSO_4$  and Co(III)Hex. for selection.  
(DOCX)

**S2 Table. Relative Expression of CorA  $Mg^{2+}$  transporters, *MoALR2* and *MoMNR2*, in knockdown transformants.**  
(DOCX)

**S3 Table. Vegetative Growth of WT,  $\Delta mnr2$  and knockdown transformants.** Vegetative growth was measured on OMA 5 days post inoculation. Data are presented as mean $\pm$ SD from three independent experiments.  
(DOCX)

**S4 Table. List of primers used in the present study.**  
(DOCX)

## Acknowledgments

The authors would like to thank Richard Gardner (University of Auckland, New Zealand) who kindly provided *S. cerevisiae*  $\Delta alr1\Delta alr2$  mutant (CM66) and the strain CM52 from which it was derived.

## Author Contributions

Conceived and designed the experiments: MHR JM BBC. Performed the experiments: MHR HS. Analyzed the data: MHR JM BBC. Contributed reagents/materials/analysis tools: JM BBC. Wrote the paper: MHR HS JM BBC.

## References

1. De Jong JC, McCormack BJ, Smirnov N, Talbot NJ. Glycerol generates turgor in rice blast. *Nature*. 1997; 389:471–483.
2. Talbot NJ. On the trail of a cereal killer: exploring the biology of *Magnaporthe grisea*. *Annu Rev Microbiol*. 2003; 57:177–202. PMID: [14527276](https://pubmed.ncbi.nlm.nih.gov/14527276/)

3. Ribot C, Hirsch J, Balzergue S, Tharreau D, Notteghem JL, Lebrun MH et al. Susceptibility of rice to the blast fungus, *Magnaporthe grisea*. *J Plant Physiol*. 2008; 165:114–124. PMID: [17905473](#)
4. Wilson RA, Talbot NJ. Under pressure: investigating the biology of plant infection by *Magnaporthe oryzae*. *Nat Rev*. 2009; 7:185–195.
5. Nguyen QB, Kadotani N, Kasahara S, Tosa Y, Mayama S, Nakayashiki H. Systematic functional analysis of calcium-signalling proteins in the genome of the rice-blast fungus, *Magnaporthe oryzae*, using a high throughput RNA-silencing system. *Mol Microbiol*. 2008; 68:1348–1365. doi: [10.1111/j.1365-2958.2008.06242.x](#) PMID: [18433453](#)
6. Zhang HF, Liu KY, Zhang X, Tang W, Wang JS. Two phosphodiesterase genes, PDEL and PDEH, regulate development and pathogenicity by modulating intracellular cyclic AMP levels in *Magnaporthe oryzae*. *PLoS One*. 2010; 6:e17241.
7. Lee YH, Dean RA. cAMP regulates infection structure formation in the plant pathogenic fungus *Magnaporthe grisea*. *Plant Cell*. 1993; 5(6):693–700. PMID: [12271080](#)
8. Andreini C, Bertini I, Cavallaro G, Holliday GL, Thornton JM. Metal ions in biological catalysis: from enzyme databases to general principles. *J Biol Inorg Chem*. 2008; 13(8):1205–1218. doi: [10.1007/s00775-008-0404-5](#) PMID: [18604568](#)
9. Asbell MA, Eagon RG. Role of multivalent cations in the organization, structure and assembly of the Cell Wall of *Pseudomonas aeruginosa*. *J Bacteriol*. 1996; 92(2):380–387.
10. Zimelis VM, Jackson GG. Activity of aminoglycoside antibiotics against *Pseudomonas aeruginosa*: specificity and site of Calcium and Magnesium antagonism. *J Infect Dis*. 1973; 127(6):663–669. PMID: [4196445](#)
11. Prescott AR, Comerford JG, Magrath R, Lamb NJ, Warn RM. Effects of elevated intracellular magnesium on cytoskeletal integrity. *J Cell Sci*. 1988; 89(3):321–329.
12. Trofimova Y, Walker G, Rapoport A. Anhydrobiosis in yeast: influence of calcium and magnesium ions on yeast resistance to dehydration rehydration. *FEMS Microbiol Lett*. 2010; 308(1): 55–61. doi: [10.1111/j.1574-6968.2010.01989.x](#) PMID: [20487021](#)
13. Wolf FI, Cittadini A. Chemistry and biochemistry of magnesium. *Mol Asp Med*. 2003; 24(1–3):3–9.
14. Pasternak K, Kocot J, Horecka A. Biochemistry of Magnesium. *J Elementol*. 2010; 15(3):601–616.
15. Walker GM, Duffus JH. Magnesium ions and the control of the cell cycle in yeast. *J Cell Sci*. 1980; 42:329–356. PMID: [6772655](#)
16. Walker GM, Sullivan PA, Shepherd MG. Magnesium and the regulation of germ-tube formation in *Candida albicans*. *J Gen Microbiol*. 1984; 130(8):1941–1945. PMID: [6432954](#)
17. Lim PH, Pisat NP, Gadhia N, Pandey A, Donovan FX, Stein L, et al. Regulation of Alr1 Mg transporter activity by intracellular Magnesium. *PLoS One*. 2011; 6(6):e20896. doi: [10.1371/journal.pone.0020896](#) PMID: [21738593](#)
18. Graschopf A, Stadler JA, Hoellerer MK, Eder S, Sieghardt M, Kohlwein SD et al. The yeast plasma membrane protein Alr1 controls Mg<sup>2+</sup> homeostasis and is subject to Mg<sup>2+</sup> dependent control of its synthesis and degradation. *J Biol Chem*. 2001; 276(19):16216–16222. PMID: [11279208](#)
19. Pfeiffer J, Guhl J, Waidner B, Kist M, Bereswill S. Magnesium uptake by CorA is essential for viability of the gastric pathogen *Helicobacter pylori*. *Infect Immun*. 2002; 70(7):3930–3934. PMID: [12065537](#)
20. MacDiarmid CW, Gardner RC. Overexpression of the *Saccharomyces cerevisiae* magnesium transport system confers resistance to aluminum ion. *J Biol Chem*. 1998; 273(3):1727–1732. PMID: [9430719](#)
21. Knoop V, Groth-Malonek M, Gebert M, Eifler K, Weyand K. Transport of magnesium and other divalent cations: evolution of the 2-TM-GxN proteins in the MIT superfamily. *Mol Genet Genomics*. 2005; 274(3):205–216. PMID: [16179994](#)
22. Schindl R, Weghuber J, Romanin C, Schweyen RJ. Mrs2p forms a high conductance Mg<sup>2+</sup> selective channel in mitochondria. *Biophys J*. 2007; 93(11):3872–3883. PMID: [17827224](#)
23. Li L, Tutone AF, Drummond RS, Gardner RC, Luan S. A novel family of magnesium transport genes in *Arabidopsis*. *Plant Cell*. 2001; 13(12):2761–2775. PMID: [11752386](#)
24. Raman V, Simon SA, Romag A, Demirci F, Mathioni SM, Zhai J, et al. Physiological stressors and invasive plant infections alter the small RNA transcriptome of the rice blast fungus, *Magnaporthe oryzae*. *BMC Genomics*. 2013; 14:326. doi: [10.1186/1471-2164-14-326](#) PMID: [23663523](#)
25. Kucharski LM, Lubbe WJ, Maguire ME. Cation hexaammines are selective and potent inhibitors of the CorA magnesium transport system. *J Biol Chem*. 2000; 275(22):16767–16773. PMID: [10748031](#)
26. Harding MM. The architecture of metal coordination groups in proteins. *Acta Crystallogr D Biol Crystallogr*. 2004; 60(5):849–859.

27. Punt PJ, Oliver RP, Dingemanse MA, Pouwels PH, van den Hondel CA. Transformation of *Aspergillus* based on the hygromycin B resistance marker from *Escherichia coli*. *Gene*. 1987; 56(1):117–124. PMID: [2824287](#)
28. Pham CL, Rey A, Lo V, Soules M, Ren Q, Meisl G, et al. Self assembly of MPG1, a hydrophobin protein from the rice blast fungus that forms functional amyloid coatings, occurs by a surface driven mechanism. *Sci Rep*. 2016; 6:25288. doi: [10.1038/srep25288](#) PMID: [27142249](#)
29. Bell-Pedersen D, Dunlap JC, Loros JJ. The *Neurospora* circadian clock-controlled gene, Ccg-2, is allelic to Eas and encodes a fungal hydrophobin required for formation of the conidial rodlet layer. *Genes Dev*. 1992; 6(12A):2382–2394. PMID: [1459460](#)
30. Inoue K, Kitaoka H, Park P, Ikeda K. Novel aspects of hydrophobins in wheat isolate of *Magnaporthe oryzae*: Mpg1, but not Mhp1, is essential for adhesion and pathogenicity. *J Gen Plant Pathol*. 2016; 82(1):18–28.
31. Van Wetter MA, Schuren FHJ, Schuurs TA, Wessels JGH. Targeted mutation of the SC3 hydrophobin gene of *Schizophyllum commune* affects formation of aerial hyphae. *FEMS Microbiol Lett*. 1996; 140(2–3):265–269.
32. Talbot NJ, Ebbole DJ, Hamer JE. Identification and characterization of MPG1, a gene involved in pathogenicity from the rice blast fungus *Magnaporthe grisea*. *Plant Cell*. 1993; 5(11):1575–1590. PMID: [8312740](#)
33. Talbot NJ, Kershaw MJ, Wakley GE, De Vries O, Wessels J, Hamer JE. MPG1 encodes a fungal hydrophobin involved in surface interactions during infection related development of *Magnaporthe grisea*. *Plant Cell*. 1996; 8(6):985–999. PMID: [12239409](#)
34. Kim S, Ahn IP, Rho HS, Lee YH. MHP1, a *Magnaporthe grisea* hydrophobin gene, is required for fungal development and plant colonization. *Mol Microbiol*. 2005; 57:1224–1237. PMID: [16101997](#)
35. Choi W, Dean RA. The adenylate cyclase gene MAC1 of *Magnaporthe grisea* controls appressorium formation and other aspects of growth and development. *Plant Cell*. 1997; 9(11):1973–1983. PMID: [9401122](#)
36. Zimmermann G, Zhou D, Taussig R. Mutations uncover a role for two Magnesium ions in the catalytic mechanism of adenylate cyclase. *J Biol Chem*. 1998; 273(31):19650–19655. PMID: [9677392](#)
37. Wiesenberger G, Steinleitner K, Malli R, Graier WF, Vormann J, Schweyen RJ, et al. Mg<sup>2+</sup> deprivation elicits rapid Ca<sup>2+</sup> uptake and activates Ca<sup>2+</sup>/Calcineurin signaling in *Saccharomyces cerevisiae*. *Eukaryot Cell*. 2007; 6(4):592–599. PMID: [17337637](#)
38. Ram AF, Klis FM. Identification of fungal cell wall mutants using susceptibility assays based on Calcofluor white and Congo red. *Nat Protoc*. 2006; 1(5):2253–2256. PMID: [17406464](#)
39. Martin H, Rodriguez-Pachon JM, Ruiz C, Nombela C, Molina M. Regulatory mechanisms for modulation of signaling through the cell integrity Sit2-mediated pathway in *Saccharomyces cerevisiae*. *J Biol Chem*. 2000; 275(2):1511–1519. PMID: [10625705](#)
40. Calvo IA, Gabrielli N, Iglesias-Baena I, Santamarina SG, Hoe KL, Kim DU, et al. Genome-wide screen of genes required for Caffeine tolerance in Fission Yeast. *PLoS One*. 2009; 4(8):e6619. doi: [10.1371/journal.pone.0006619](#) PMID: [19672306](#)
41. Munro CA, Selvaggini S, de Bruijn I, Walker L, Lenardon MD, Gerssen B, et al. The PKC, HOG and Ca<sup>2+</sup> signalling pathways co-ordinately regulate chitin synthesis in *Candida albicans*. *Mol Microbiol*. 2007; 63(5):1399–1413. PMID: [17302816](#)
42. Mathioni SM, Belo A, Rizzo CJ, Dean RA, Donofrio NM. Transcriptome profiling of the rice blast fungus during invasive plant infection and in vitro stresses. *BMC Genomics*. 2011; 12(49).
43. Lee JM, Gardner RC. Residues of the yeast ALR1 protein that are critical for Magnesium uptake. *Curr Genet*. 2006; 49(1):7–20. PMID: [16328501](#)
44. Walker GM. Metals in yeast fermentation processes. *Adv Appl Microbiol*. 2004; 54:197–229. PMID: [15251282](#)
45. Pisat NP, Pandey A, Macdiarmid CW. MNR2 regulates intracellular Magnesium storage in *Saccharomyces cerevisiae*. *Genetics*. 2009; 183(3):873–884. doi: [10.1534/genetics.109.106419](#) PMID: [19720860](#)
46. Filippi MC, Prabhu AS. Relationship between panicle blast severity and mineral nutrient content of plant tissue in upland rice. *J Plant Nutr*. 1998; 21(8):1577–1587.
47. Soanes DM, Kershaw MJ, Cooley RN, Talbot NJ. Regulation of the MPG1 hydrophobin gene in the rice blast fungus *Magnaporthe grisea*. *Mol Plant Microbe Interact*. 2002; 15(12):1253–1267. PMID: [12481998](#)
48. Smit G, Straver MH, Lugtenberg BJ, Kijne JW. Flocculence of *Saccharomyces cerevisiae* cells is induced by nutrient limitation, with cell surface hydrophobicity as a major determinant. *Appl Environ Microbiol*. 1992; 58(11):3709–3714. PMID: [1482191](#)

49. Levin DE. Cell wall integrity signaling in *Saccharomyces cerevisiae*. *Microbiol Mol Biol Rev.* 2005; 69(2):262–291. PMID: [15944456](#)
50. Dean RA, Talbot NJ, Ebbole DJ, Farman ML, Mitchell TK, Orbach MJ, et al. The genome sequence of the rice blast fungus *Magnaporthe grisea*. *Nature.* 2005; 434:980–986. PMID: [15846337](#)
51. Kachroo P, Leong SA, Chattoo BB. Pot2, an inverted repeat transposon from the rice blast fungus *Magnaporthe grisea*. *Mol Gen Genet.* 1994; 245(3):339–348. PMID: [7816044](#)
52. Patkar RN, Chattoo BB. Transgenic indica rice expressing ns-LTP-like protein shows enhanced resistance to both fungal and bacterial pathogens. *Mol Breed.* 2006; 17:159–171.
53. Mullins ED, Chen X, Romaine P, Raina R, Geiser DM, Kang S. Agrobacterium-mediated transformation of *Fusarium oxysporum*: an efficient tool for insertional mutagenesis and gene transfer. *Phytopathol.* 2001; 91(2):173–180.
54. Yu JH, Hamari Z, Han KH, Seo JA, Reyes-Dominguez Y, Scazzocchio C. Double-joint PCR: a PCR-based molecular tool for gene manipulations in filamentous fungi. *Fungal Genet Biol.* 2004; 41(11):973–981. PMID: [15465386](#)
55. Nakayashiki H, Hanada S, Quoc NB, Kadotani N, Tosa Y, Mayama S. RNA silencing as a tool for exploring gene function in ascomycete fungi. *Fungal Genet Biol.* 2005; 42(4):275–283. PMID: [15749047](#)
56. Dellaporta SL, Wood J, Hicks JB. A plant DNA miniprep: version 2. *Plant Mol Biol Rep.* 1983; 1(4):19–22.
57. Sambrook J, Fritsch EF, Maniatis T. *Molecular Cloning: A Laboratory Manual*, second ed. Cold Spring Harbour Laboratory Press; 1989.
58. Reidinger S, Ramsey MH, Hartley SE. Rapid and accurate analyses of silicon and phosphorus in plants using a portable X-ray fluorescence spectrometer. *New Phytol.* 2012; 195(3):699–706. doi: [10.1111/j.1469-8137.2012.04179.x](#) PMID: [22671981](#)